



CHALMERS
UNIVERSITY OF TECHNOLOGY



Virtual Verification of Complete Vehicle Requirements for Heavy Vehicles for the Development of Brake Systems

Master's Thesis in Automotive Engineering

Adpita Laha
Ramesh Kumar Adhikarla

Department of Mechanics and Maritime Sciences
CHALMERS UNIVERSITY OF TECHNOLOGY
Gothenburg, Sweden 2020

MASTER'S THESIS IN AUTOMOTIVE ENGINEERING

**Virtual Verification of Complete Vehicle
Requirements for Heavy Vehicles for
Development of Brake Systems**

ADIPTA LAHA
RAMESH KUMAR ADHIKARLA



CHALMERS
UNIVERSITY OF TECHNOLOGY

Department of Mechanics and Maritime Sciences
Division of Vehicle Engineering and Autonomous system
CHALMERS UNIVERSITY OF TECHNOLOGY
Gothenburg, Sweden 2020

Virtual Verification of Complete Vehicle Requirements for Heavy Vehicles for Development of Brake Systems

Adipta Laha

Ramesh kumar Adhikarla

© ADIPTA LAHA, 2020.

© RAMESH KUMAR ADHIKARLA, 2020.

Examiner and Academic Supervisor

Bengt Jacobson

Professor and group leader Vehicle Dynamics,

Division of Vehicle Engineering and Autonomous Systems,

Mechanics and Maritime sciences, Chalmers University of Technology

Academic Supervisor

Ingemar Johansson

Professor of the Practice,

Vehicle Engineering and Autonomous Systems

Mechanics and Maritime sciences, Chalmers University of Technology

Master's Thesis 2020:72

Department of Mechanics and Maritime Science

Division of Vehicle Engineering and Autonomous Systems

Chalmers University of Technology

SE-412 96 Gothenburg

Telephone +46 31 772 1000

Cover: Volvo FH 2012 - Truck Model used in the simulations. [Image Source: [23]].

Typeset in L^AT_EX

Printed by Chalmers Reproservice

Gothenburg, Sweden 2020

Virtual Verification of Complete Vehicle Requirements for Heavy Vehicles for Development of Brake Systems

ADIPTA LAHA

RAMESH KUMAR ADHIKARLA

Department of Mechanics and Maritime Science

Chalmers University of Technology

Abstract

Heavy vehicles mainly have electronic controlled pneumatically actuated braking systems or the EBS systems. Developments are carried out in this sector to improve the braking performances of these vehicles as well as costs and their ability to be integrated with other vehicle functions. Subsystem manufactures which mainly works on the braking systems, came up with the idea of fast actuators or advanced actuation system, which substantially reduces the braking distances of heavy vehicles. The main aim of this thesis is to develop simulation tools and methods for the development of control system and actuation system of brake systems.

Vehicles as a whole is a complex product. Different subsystem manufacturers and vehicle manufacturers have to collaborate to develop a vehicle. Traditionally, prototypes were built for development and testing of technical solutions. With the advancement of technology, CAE tools are used for development of technical solutions before the testing can start. This virtual testing has reduced the time for development and also cost. This thesis focuses on the development process for control system of the brake system which comprises of simulation tools that can be used both by the truck manufacturers and also by the subsystem manufacturers to improve the communication between them and hence reduces the development time.

IPG TruckMaker is selected as the software to be used for this thesis. A Volvo FH semi-truck was set up which was used for all the simulations. Vehicle maneuvers considered are straight-line braking . Different road frictions are used along with split-mu conditions to get a wide range of results. Basic actuator system and advanced actuator system are types of brakes control system which have been implemented on this heavy vehicle and hence results were obtained.

Stakeholder in the project

IPG Automotive Sweden AB has been a stakeholder in the project. IPG Automotive Sweden and the team here has been a source of constant support for our work with TruckMaker.

Keywords: Braking systems, simulations, virtual verification, Fast Actuators, heavy vehicles

Acknowledgements

To begin with, we would like to thank our supervisor Ingemar Johansson at Chalmers for his tireless support throughout this thesis support. It was only because of his constant optimism and guidance that we have been able to steer our thesis in the right direction and retain its course. Throughout the course of this thesis work, he has helped us with difficult decisions and taught us some valuable lessons that we would never forget.

We would also like to thank our examiner, Bengt Jacobson, who has been a constant source of help with respect to vehicle dynamics and making sure we have all the tools at our disposal to carry out this thesis work. His impeccable quality of providing us with instant technical solutions helped us in getting unstuck at multiple situations.

Furthermore, we would like to extend our gratitude to David Andersson and Aditya Mukherjee at IPG Automotive, Sweden for making sure we have the optimum quality of support from their end. They have helped us at every point in providing solutions to all of our queries; be it with respect to setting up TruckMaker or queries regarding the simulation setup.

We would also like to thank Pontus Fyhr and Alireza Marzbanrad. We're highly indebted to them for the level of support they've provided us in understanding the braking systems and dynamics involved. Their extensive knowledge about the minute details of the systems involved helped us setup the required simulations.

Adipta Laha, Gothenburg, September 2020
Ramesh Kumar Adhikarla, Gothenburg, September 2020

Contribution from Individual Authors

Most of the tasks performed in this thesis were divided equally among both the authors including the literature survey.

Adipta was involved with the task of simulation setup of basic actuation system and obtaining the results, whereas Ramesh was assigned with the complicated task of handling of the FMU and also the simulation of the Advanced Actuation system.

The report writing was also divided equally between both the authors.



Contents

1	Introduction	1
1.1	Background	1
1.2	Problem Motivating the Project	1
1.3	Envisioned Solution	2
1.4	Objectives	2
1.5	Deliverables	3
1.6	Limitations	3
2	Theory	5
2.1	Braking -Theory	5
2.2	Braking configurations in Heavy Vehicles	5
2.2.1	Electronically controlled Braking System[EBS]	7
2.3	Brake Control System	8
2.3.1	Basic Actuator System with ABS Control - Mechanics	8
2.3.2	Advanced Actuator System	10
2.3.2.1	Force Observer	12
2.3.2.2	Sliding Mode Slip Controller	12
2.3.2.3	Pressure Controller	13
2.4	Functional Mock-up Units	16
3	Methodology	17
3.1	Vehicle Model	19
3.2	Tire Model	21
3.3	Manoeuvres Description	23
3.3.1	Maximum Straight Line Braking	23
3.3.1.1	With Different Friction Coefficients	23
3.4	Step Response Test	24
3.5	Basic Actuator Control Implementation	27
3.6	Advanced Actuator Control Implementation	28
3.7	Solver time step	31
4	Results and Discussions	33
4.1	Tools and Methods of Development	33
4.2	Results with Basic Actuator-Controller	33
4.2.1	Straight Line Braking - Constant μ Surfaces	35

4.2.2	Straight Line Braking - Split μ Surfaces	44
4.3	Results with Advanced Actuator-Controller	52
4.3.1	Results with FMU	52
4.3.2	Results with Actual Reference Models	55
5	Conclusion	69
6	Future Work	71
	Bibliography	73
A	Appendix	I
A.1	Results with Basic Actuator	I
A.1.1	Straight Line Braking - Constant μ Surface	I
A.1.2	Straight Line Braking - Split- μ Surface	IV
A.2	Results with Advanced Actuator	VI
A.2.1	Straight Line Braking - Constant- μ Surface	VI

1

Introduction

1.1 Background

Brakes used in a vehicle are mechanical devices that are used to reduce the speed of the vehicle or to stop the vehicle by means of friction and convert the energy of the moving vehicle into heat. The brakes must dissipate this heat. Since these heavy vehicles such as Trucks or Buses have a significantly higher mass when compared to passenger vehicles, consequently, it increases the kinetic energy of the vehicle while in motion. This, in turn, implies that greater forces are required to bring the vehicle to rest especially from high speeds. Therefore, the force exerted by the driver's foot at the brake pedal becomes insufficient. So, to rectify this issue a servo system is required to increase the load on the actuator of the brakes. In heavy vehicles, compressed air is used as the working fluid for brake actuation.

Heavy vehicles make use of the pneumatically actuated braking systems. This is because these brakes are capable of transmitting higher mechanical forces over great distances using simple components and connections. These systems make use of compressed air to produce the force that applies the brakes at each wheel. Special valves are used to make sure that the air moves through the system as quickly as possible. There is a split-second delay in brake reaction from the moment the brake pedal is pushed. This delay can be observed in most conventional pneumatic brake systems.

The truck brake system are usually electronically controlled and pneumatically actuated. This type of braking system is known as Electronic Braking System (EBS). Technological advancement in this sector has led to the development of advanced actuator system that reduces the stopping distance in low friction surfaces.[2] It essentially consists of an advanced actuator with a reduced delay and an ECU which has the brake control algorithm. This braking system acts considerably faster than the conventional modular systems. These brake valves not only reduces the time delays as observed in a conventional air brake system but also consume lesser air.

1.2 Problem Motivating the Project

The problem arises during the development stage, when a subsystem supplier is developing these braking systems, since this require vehicle's performance data at the wheel end. Usually, only selected data of the wheel end performance is shared by

the vehicle manufacturer. Therefore, both the subsystem supplier and the vehicle manufacturer have to cooperate to develop new technical solution of the system. This eventually increases the development time of the braking systems. Therefore, it becomes necessary to look for alternatives that would not only reduce the development times but also improve the quality of these systems. In this thesis, we are mainly focused on the development of the brake control system so that the communication between both subsystem suppliers and the vehicle manufacturers improves which in turn decreases the time for development and testing of brake systems. The development of foundation brakes is not in the scope of this thesis.

The problem being investigated here is whether modeling and simulation techniques can be implemented to facilitate the development of new technical solution and also to substantially reduce the development time of brake systems. Since the modern braking systems involve a complex interaction with different vehicular subsystems, simulation results would be a good way for subsystem suppliers to interact with the truck manufacturer.

1.3 Envisioned Solution

One way to solve the problem of long development time and issues with communication between the subsystem suppliers and vehicle manufacturers, is by virtual verification i.e. by using modeling and simulation techniques in that way improving the communication between the subsystem suppliers. This would involve development and sharing of simulation models to understand how these can be used both at the vehicle manufacturer's end as well as at the brake supplier's end. This integration can be achieved by using Functional Mock-up Units (FMUs [17]) and a vehicle simulation software, e.g. IPG TruckMaker to gain a better perspective about the exchanging of models. IPG provides a good interface for implementing different FMU's or external models.

1.4 Objectives

The objectives of this thesis work involves answering the following research questions: [2]

- How should vehicle manufacturer and brake system supplier utilize simulation models to improve quality and speed of development?
- Is there a possibility to develop good test scripts for the selected manoeuvres to perform an assessment of the complete vehicle?

In order to perform an assessment on the complete vehicle, it also becomes important to use good tire models in the simulations as well as friction.

1.5 Deliverables

The thesis has the following deliverables:

- Tools and method to simulate and develop the control and actuation system of brake systems for heavy vehicles.
- A reference truck model equipped with a basic actuator system.
- The same truck model as above but replaced with an Advanced Actuator system and brake actuator controls.
- Test Scripts for the selected complete vehicle maneuvers (around 3 maneuvers).
- Conducting a detailed study about basic and advanced actuation system.
- Test and verify the step responses of the actuation systems that are being used.
- An integration environment which supports the simulation tools of both the vehicle manufacturer and the subsystem supplier. In this case, IPG Truck-Maker with Simulink will be the only tools required.
- Results obtained from the reference models with basic actuator system and also with the advanced Actuators will be studied and analysed for the development of simulation tools and methods.

1.6 Limitations

- Since modeling the parts is not the main objective of this thesis, the truck model being used for simulations is a pre-built model available within the simulation software. This is taken as the reference model.
- For maneuver evaluation and result validation, only maximum straight line braking would be evaluated with multiple variations of speed and friction within these two would be considered.
- Foundation brakes are selected based on the selection of the truck model. Foundation brakes are not developed in this thesis.
- There are no pre-existing Simulink example models for application of ABS brake control system nor advanced brake controllers on trailer wheel ends. Therefore a truck with a trailer was replaced with 2 axle truck for final simulations.

2

Theory

2.1 Braking -Theory

Brake system of a vehicle is used to either reduce the speed of the vehicle or to make it stop. The Braking system converts the kinetic energy of the vehicle in form on momentum to heat energy with the application of friction. Traditionally, drum brakes were used in a braking system. In a drum brake, when the brake pedal is pressed, the brake pads are applied to the drum which generated the required frictional force to reduce the speed of the vehicle. However, the drum brakes have less capability to dissipate the heat energy effectively in heavy braking conditions. The disc brakes were developed to overcome the problem faced by drum brakes. As the name suggests, the disc brakes consists of disc which are mounted on the wheels bearing. The caliper consists of brake pads and are in turn mounted on the suspension uprights. During a braking operation, the caliper applies the brake pads to the disc and a braking torque is applied which reduces the speed of the vehicle.

This thesis mainly emphasizes on the development of a method and scripts for the development of the control system for the actuation system of brake system for heavy vehicles. For the development of the method, we are mainly focusing on only two types of brake system namely basic actuation system and advanced actuation system. The different types of actuation and controls systems for the brake systems are explained in the following section.

2.2 Braking configurations in Heavy Vehicles

Heavy vehicles mainly have Pneumatic actuation system for braking applications due to its advantages over the hydraulic braking system. The pneumatic braking system is explained below.

Pneumatic braking system uses air as a working fluid. The main components of a pneumatic braking system are:

- Actuation system
 - Air filter
 - Air dryer
 - Air compressor
 - Storage reservoir and pressure control valve
 - Brake valve

2. Theory

- Brake chamber
- Foundation brakes
 - Disc brakes or Drum Brakes

Air from the atmosphere is taken in and it is then filtered and dried to remove any impurities and moisture from the air. This air is then passed to the air compressor. The compressor is driven by the engine either by belt drives or by gears. The compressor compresses the air and it is stored in the reservoirs. The storage reservoir along with the pressure control valves stores the compressed air within the limits which the reservoirs can sustain. These are the basic components of a pneumatic braking system.

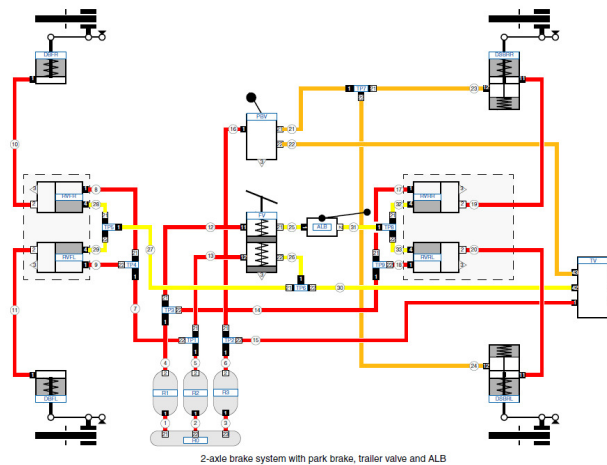


Figure 2.1. Pneumatic Braking System[22]

This is the schematic view of the pneumatic braking system. There are three reservoirs present, two of which are connected to the front axle and the rear axle of the truck. The third tank is specifically for operating the parking brakes. There are different kinds of valves present in the system which will be explained in the later part of the report. When the pedal valve is pressed and the main valve is actuated, the information is sent to the relay valves present in all the four wheels. The relay valves allow the high-pressure fluid to pass through it and actuate the braking of the wheels. When the foot valve is released the relay valve stops the fluid to pass through it and hence the braking stops.

The valves present in the pneumatic braking system are explained here:

- Foot valve- The foot valve present in our system is a dual foot valve. The foot valve or the treadle valve is used to apply the service brakes to the heavy vehicles. Depending upon the amount of pressure applied by the driver on the foot valve, the vehicle's brakes are actuated accordingly.
- Relay valve- Relay valves are used to reduce the delay in the application and the release of the brakes of the rear axle. As the rear axle is situated far from

the reservoir or the foot valve, there comes a delay between the depression of the foot valve and the actual application and release of the brakes. This delay can substantially reduce the performance of the brakes. So, a relay valve is set up near the rear axle. The relay valve senses the signal as soon as the brake valve is depressed or when it is released and accordingly allows the braking fluid to pass through it and reach the braking chamber for the application of the brakes. This kind of valves reduces the time delay in the braking system.

2.2.1 Electronically controlled Braking System[EBS]

Electronically controlled Braking systems was developed during the mid 1990s. The modular design of this system helps to incorporate this system to wide variety of vehicle types. The programming control of the main or the central Electronic Control Unit (ECU) is changed depending upon the type of the vehicle. Schematic diagram for an EBS system is shown below.

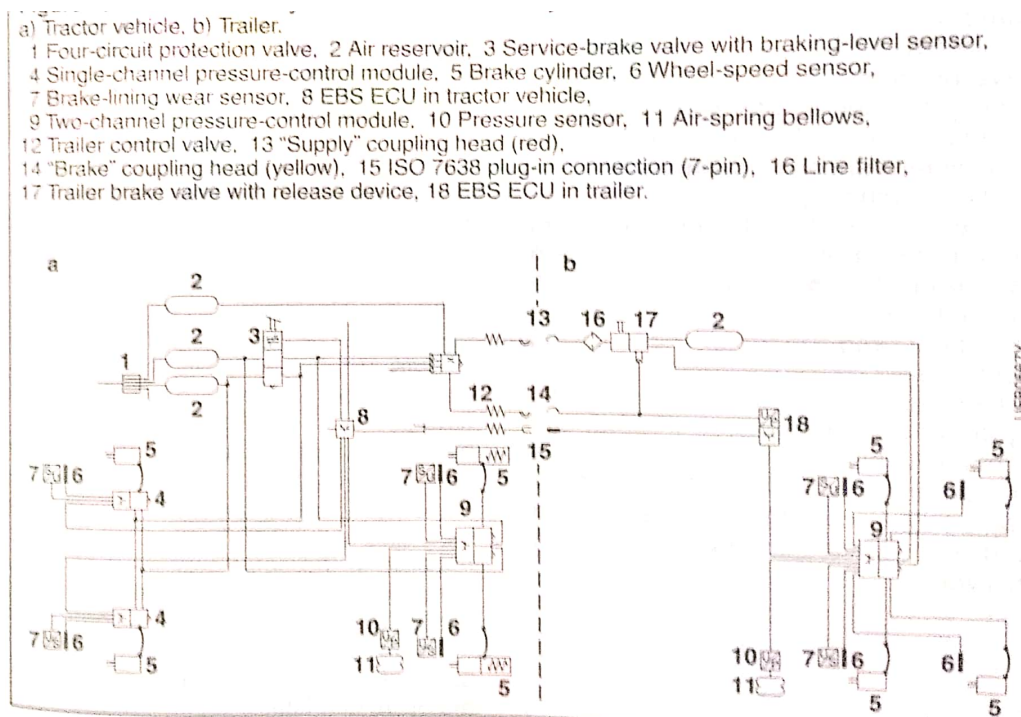


Figure 2.2. Electronically Controlled Braking System[5]

The operation of an EBS system is similar to that of an pneumatic braking system with ABS. The compressed air is stored in the storage reservoirs. When a feed is supplied to the service brake valve, it sends electrical signals to the central ECU. The ECU in turn sends signal to the pressure control modules of the front and the rear axle, so that the required brake pressure can be evaluated and can be sent to the brake cylinder and hence by the actuation system, the vehicle is braked. A trailer can also be incorporated in this system due to its modular design.

Many types of sensors are present in a EBS system which performs different types of function. A wheel speed sensor senses the speed of the rotating wheel and when

the wheel is about to lock, the ECU sends signal to the pressure control module to release the pressure for a very small instance of time. This helps the driver to be in control of the vehicle all the time and also improves the braking distance of the vehicle. Pneumatic circuits present in the system are used to brake the vehicle if in case there is a failure in the electrical circuit.

2.3 Brake Control System

In this section, two brake actuators, namely; Basic Actuator and Advanced Actuator; will be described. These two actuators will later be used as a case study for comparing how the complete vehicle functions. Parameter such as braking distance will be used to evaluate the two types of actuators.

The method of implementation of these two types of actuators will be described in the Methodology section. The basic actuator's implementation methodology will be described in Section 3.5 whereas the advanced actuator's implementation will be described in Section 3.6.

2.3.1 Basic Actuator System with ABS Control - Mechanics

Basic Actuator system with an ABS control system which prevents locking of the wheels of the vehicle during braking. When the brake pedal is pressed during emergency situation, the wheels of the vehicle do not lock up. The basic actuator assist the driver to be in full control of the vehicle during all instances. When the brakes are pressed with high force, the basic control system prevents the wheel lock-up by releasing the pressure at the wheels for a very small instant of time. The wheel speed sensor notifies the ECU that the lock-up is evident, the Pneumatic Actuation unit reduces the pressure at the wheels to prevent the lock-up. A schematic diagram of the basic actuator system is shown below.

The main subsystems of a basic actuator system are as follows.

- Wheel Speed Sensor[21]- As the name suggest, the wheel speed sensors detects the speed of individual wheels of a vehicle. This sensor comprises of a magnet, a coil and a tooth wheel. When the wheel rotates, a magnetic flux is induced into the coil, which in turn generates a voltage. The voltage induced is directly proportion to the speed of the wheel.
- Electronic Control Unit- the electronic control unit is considered as the brain of the basic actuator system. It receives the signal from the wheel speed sensor and determines what action to be taken next. If the wheel is very close to locking, then the ECU sends signal to the pneumatic actuation unit to release the pressure of the brakes and vice versa. ECU in a vehicle also performs various other tasks as well.
- Pneumatic Actuation Unit- It is an device used to hold or release the pressure at the wheels. During hard braking, the pneumatic actuation unit hold and releases the brakes of the vehicle depending on the situation. The pneumatic

actuation unit directly receives its command from the ECU present in the system.

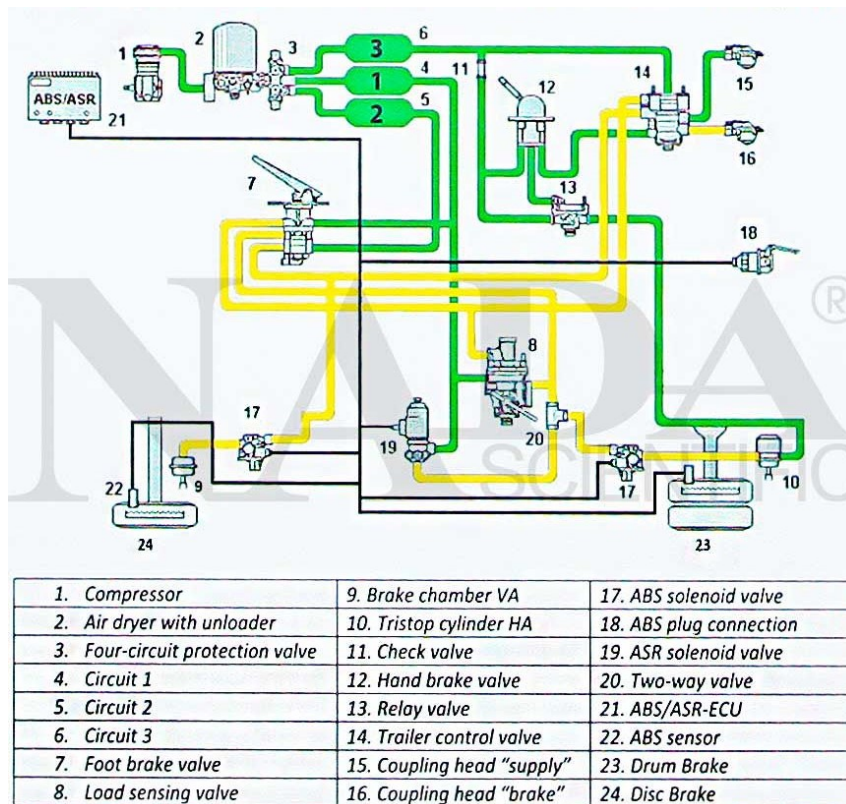


Figure 2.3. Basic Actuation system [4]

2.3.2 Advanced Actuator System

Please note that the advanced actuator will be further described in Section 3.6.

One of the major limitations of using ‘Slip Control’ in a way that the longitudinal slip is retained around its peak point, is the amount of time delay introduced by the brake system. This delay is nothing but the time difference between the requested brake torque and the applied brake torque. As stated in [10], this time delay in the brake system should be maintained at around 5ms for a relevant tracking of the longitudinal slip around its peak point in braking force-slip curve by the respective controller. In real world scenarios, this optimum time delay of 5ms is difficult to achieve and the delay values are much higher than this. For e.g, the pneumatic valves being used by most ABS controllers possessing an orifice diameter of about 8mm present time delays in the range of 20-40ms which is as much as 4-8 times the optimum values of 5ms needed to track the slip around its optimal point [10],[11]. In order to achieve values of time delays that are closed to or less than 5ms optimum time, it becomes essential that we use fast acting pneumatic valves of the same orifice diameter of 8mm which present a time delay as low as 3ms and reduce the stopping distances by a great extent. [10],[11]

To achieve an actuation which are similar in magnitude or faster than the one stated above, one of the suggested ways is by replacing the pneumatic and hydraulic actuators altogether by electrical actuators. One of implementation techniques of these type of brakes was proposed by Siemens which refer to these electronic brakes as Electronic Wedge Brakes. These run on 12V power to spin two small motors attached to a caliper in each wheel. It does not use any hydraulic systems. Here, the piston and fluid ducts used in a hydraulic system are replaced with a double plate. Each plate is slick on one side and contains wedge shaped teeth on the other side. The teathed side of the two plates face each other with a set of cylindrical rollers in between them. The brake pad is assembled in the same way as they would have been on a regular disc brake i.e. on the inner fixed plate of the caliper whereas the outer brake pad is set against the floating plate of the caliper. When the brake pedal is engaged, the two electric motors move the wedges connected to them against each other. These wedges push the double plates, in turn, push the brake pads against the discs. The cylindrical roller between the double plates allows the vertical movement of one plate when the two of them are pressed against each other.

The main advantage of using the electronic wedge braking, is its ability to apply maximum brake force with minimum amount of energy being spent during its operation. As there are no hydraulic brake lines between the pedal and the actual brake system, Siemens claims the amount of energy spent in the operation is as low as one tenth of that spent in a hydraulic system. [12].

Another way of achieving this fast actuation in heavy vehicles was a version of Electromechanical Brakes (EMB) introduced by Haldex Brake Products. It is a system that is electrically controlled wherein, electric brake actuators are used which actuated the electromechanical disc brakes. These disc brakes make use of an electric motor to control the amount of clamp forces corresponding to the requested brake

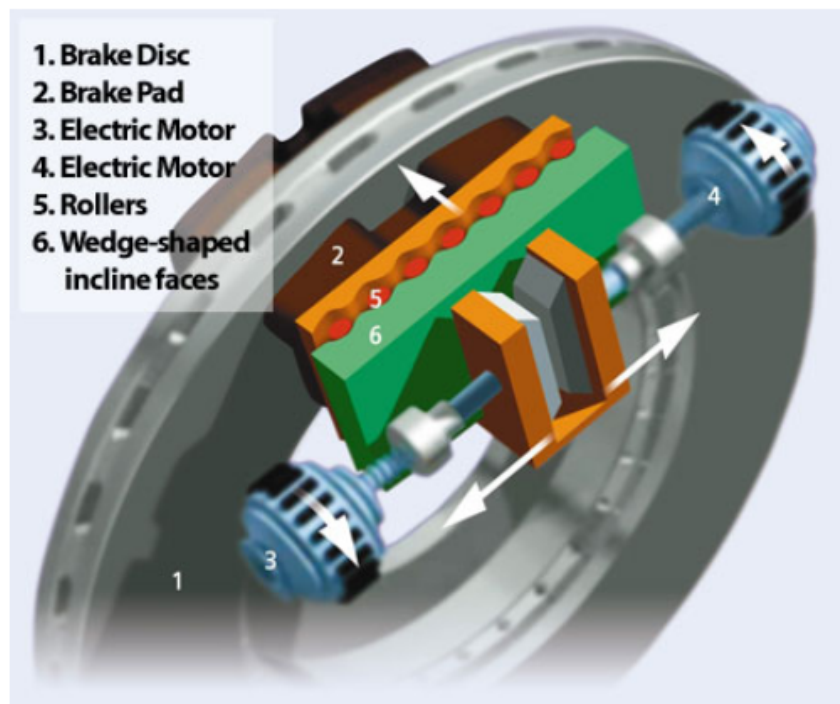


Figure 2.4. Siemens Electronic Wedge Braking [13]

torque. An optimized slip controller is used to control the braking torque in a way that the wheel slip is extracted from the peak slip point on braking force-slip curve. This combination of the optimized slip controller and the new Brake-by-Wire system making use of electromechanical brakes (EMB) resulted in a reduction in stopping distances of about 24% [10] when compared to vehicles with a pneumatic brake system (i.e. EBS) which makes use of ABS control. These results were achieved for straight line braking tests performed on a tractor plus trailer unit fitted with EMB-Slip Control combination.

As mentioned earlier, the reason for the braking performance in HGVs in emergency situations can partly be attributed to the slow performance of the pneumatic brake actuators which restrict the bandwidth of the ABS systems and partly to the control algorithms used to achieve the maximum braking force throughout the braking maneuver. To counter this issue, the Cambridge Vehicle Dynamics Consortium (CVDC) developed a new system wherein the conventional brake actuators used in an electro-pneumatic braking system which uses slow solenoid valves, are replaced with high bandwidth, binary-actuated valve system that are placed directly at the brake chambers. These bi-stable valves operate at an order of magnitude faster than the ones being used on heavy vehicles with the conventional modulator valves used for the ABS system. Since this valve system can operate in a bi-stable manner, the permanent magnets inside the valve can hold it in a particular state i.e. either in fully-open state or fully-closed state. The binary valves used in here, shown in Figure 2.5.a, changes state with the help of a mechanical spring when an electrical pulse is sent across the coil to switch the magnetic field. This mechanical spring which stores the potential energy gained during the switching of states, to reduce the

impact of landing and enables it to endure a huge number of switching cycles. Since the already available pneumatic valves have proven to be too restrictive in terms of their design (particularly their orifice diameter which is restricted to 3.5mm) [6], a novel bi-stable valve was designed by CVDC as the formerly available valves resulted in slow response to brake chamber pressure demands. The new architecture proposed, seemed to fulfill the design requirements of a comparatively large orifice diameter along with high switching speed requirements and high pressure demand differential. This novel binary valve had an orifice diameter of 8mm and included a low moving mass steel flexure mounted between two magnets which used to switch states, on passing a short electric pulse across the coils, in approximately 3ms [7]. These high bandwidth modulator valves are comparable in performance with the electromechanical brake setups described previously in this section. This improved prototype architecture of the actuator was controlled using a sliding mode slip controller. This setup consisting of HGV disc brake assembly fitted with prototype bi-stable valves and controlled using the sliding mode slip controller presented results which showed a reduction in braking distance of up to 25% [7] when compared to conventional ABS setup in HGVs.

The forces and torques applied on each wheel are calculated with the help of a series of controllers and observers. They're discussed in the sections below since they're a major part of their complete integration with the vehicle model.

2.3.2.1 Force Observer

The wheel slip controller developed by Miller [11] includes a real-time force observer that is used to estimate the braking force at the wheel-road contact patch. This observer estimates the longitudinal braking force by constantly monitoring the wheel acceleration along with monitoring the brake pressure. The data from these two measured variables are then used to estimate the instantaneous longitudinal braking force at the contact patch between the tire and road surface. This information about the instantaneous longitudinal tire force is needed for the slip controller to adapt to the varying road conditions. Since it is expensive to obtain the exact contact patch force between the tires and the road for every scenario, therefore an observer is used to estimate its values in real-time.

2.3.2.2 Sliding Mode Slip Controller

As stated earlier, the actuator valves are controlled using a sliding mode slip controller developed by Miller. In the current thesis, a peak seeker (using extremum seeking algorithm) is not included within this slip control function and is considered a separate function. These are non-linear, high speed switched feedback controllers which are robust to uncertainties and disturbances introduced by road surfaces. Here, the sliding mode slip controller is used to calculate the Pressure demand P_d to be sent to the Pressure controller. In order to calculate the pressure demand, a first order sliding surface is defined which is given as:

$$s_x = \lambda - \lambda_d \quad (2.1)$$

where λ_d is the demanded slip level and λ is the longitudinal slip calculated using the information about the vehicle speed. The sliding surface is set up in such a way that the controller seeks the limiting value of slip within the slip-friction curve. This equation combined with a equations of motion for a single wheel which is subjected to a braking torque and following procedure outlined by Miller, the equation for the pressure demand is given as:

$$P_d = \frac{r_r r_b F_x - (1 - \lambda) a_x J_\omega}{K_{bg} r_r} - k_s \left(\frac{s_x}{|s_x| + \delta_s} \right) - \phi_s s_x \quad (2.2)$$

where r_r is the rolling radius of the wheel, r_b is the radius at which the braking force acts, F_x is the longitudinal force at the contact patch between the tire and the road, J_ω represents the polar moments of inertia of the wheel whereas k_s , δ_s and ϕ_s are tuneable gains that represent sliding gain, width of boundary layer and a positive design constant. These gains are added so as to reduce the amount of ‘chattering’ or high frequency disturbances in the system. These high frequency disturbances or oscillations may arise due to reasons such as actuator time delays, imperfect control switching etc. [11] and may lead to undesired effects such as high consumption of air during the low speed phase in the braking maneuver.

2.3.2.3 Pressure Controller

The pressure demand estimated by the sliding mode controller above is passed onto the pressure controller which is a simple proportional controller that calculates the mark-space ratio demand for the inlet and outlet valves connected to the brake chamber. At each wheel, the valve enclosure consists of two hi-speed bi-stable valves are used to modulate the brake pressure demand. The two valves act as inlet and outlet of the configuration (shown in Figure 2.5.a). The modulation of brake pressure is obtained by controlling the amount of air flowing in and out of the enclosure through each of these two valves. This control of air flow is achieved through a Pulse Width Modulation (PWM) method which is a method to reduce the average power of an electrical signal by discretizing it into rectangular waves. The proportional controller is thus used to define this modulation with the help a PWM mark-space ratio R_{MS} for the two valves which are connected to the brake chamber and is calculated using the relation:

$$R_{MS} = k_{pr} (P_d - P_c) \quad (2.3)$$

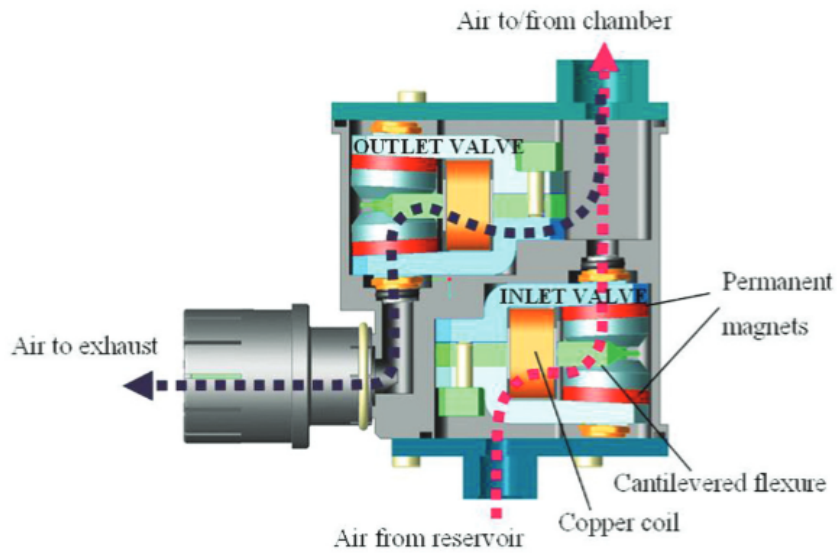
where a positive R_{MS} value would correspond to a demand at the inlet valve and a negative value would correspond to an outlet valve demand. P_d is the pressure demand calculated by the limiting slip controller and P_c corresponds to a pressure value inside the chamber which would either be measured or estimated with the help of a pressure observer. This R_{MS} value is further sent into the valve plant

wherein this value is converted into brake torque with the help of brake gain which is calculated as:

$$T_B = K_{bg}P_c \quad (2.4)$$

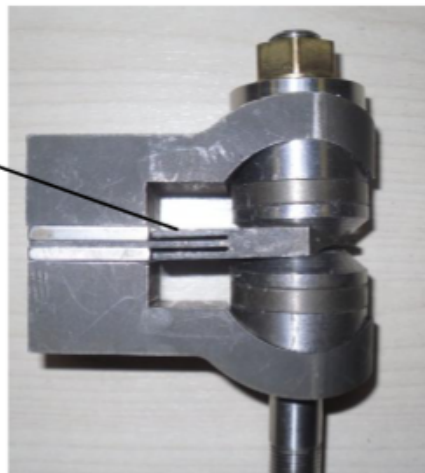
where P_c is the chamber pressure. Since the valves used here are high speed bi-stable valves, a delay is introduced into the system to simulated the 3ms switching time of the valves.

For this thesis, the whole of the local controller consisting of the force observer, sliding mode slip controller, pressure controller and the valve plant has been packed inside a Functional Mock-up Unit as Co-simulation FMU. The method in which the components of the FMU communicate with each other along with the implementation of the FMU within the simulations will be described in Section 3.6.



2.5.a. Valve cross section showing the two Bi-Stable Valves

Flexure modifications for improved magnetic performance



2.5.b. The Valve Assembly

Figure 2.5. The advanced actuator's Valve Assembly[10]. [The actuator will be further described in Section 3.6.]

2.4 Functional Mock-up Units

A Functional Mock-up Unit (FMU) is a black-box which packs within it a simulation model that adheres to a standard known as Functional Mock-up Interface (FMI). The Functional Mock-up Interface is a standard which is independent of any tool that provides a common interface. This common standardized interface plays an important role when it comes to both model exchange as well as for co-simulation. Therefore, FMIs provide a standard platform so that simulation models developed in various tools and platforms can be used with each other in the form of FMUs. The main aim of providing this type of a platform is to allow easy exchange of simulation models between OEMs and suppliers wherein intellectual property rights is a major confidential concern for both parties. It allows for an open import and export to a common standard irrespective of the tool being used for simulating or analyzing the dynamic models. This also helps in reusing the models and repurposing them for future use without worrying about the steps needed to import them.

Every FMU file comes with an extension ".fmu" and is shared between tools as a zip file. This zip file when unpacked usually consists of a set of equations contained within the model in the form of C-functions, an XML file which contains the definition of variables to be used by the FMU when it is deployed in the target system and also parameters and documentation to be used by the FMU.

There are two kinds of FMUs specified by the FMI standards. They are:

- FMI for Model Exchange: Here, the FMUs containing the models, represent dynamic systems that are characterized by algebraic or differential equations. These Model Exchange FMIs do not have a numerical solver of their own. Therefore, once they're deployed within the target system, the external solver employing the FMU sets the state and its derivatives. The goal for the numerical solver here is to solve the required set of discrete algebraic and differential equations and also determine the state at the next time step. The model generated is in the form of input-output blocks so that it can be easily utilized by the other simulation tools.
- FMI for Co-Simulation: These FMUs usually contain their own solver. The primary goal here is to enable the coupling of two or more simulation tools to be used simultaneously. These FMUs contain a communication time step which determines the time between the two solve their set of equations independently of each other.

As mentioned earlier, for the current thesis, the different components of the advanced actuator are packed in an FMU. The kind of FMU being used currently is Co-Simulation FMU which is defined above. There are a number of different parameters governing the behavior of the FMU. These can be varied within the current FMU. The behavior of the FMU to the variation of these parameters defined within the FMU will be out of scope of this thesis and hence will not be discussed. Rather, a predefined set of parameters (described further in Section 4.3.1) will be used to assess the results.

3

Methodology

This chapter deals with the development of tools and methods. When the tools and methods were in place, simulations with basic control system and advanced actuator system were carried out. An outline of the basic steps being followed to setup and analyze the behaviour of the two brake actuator and controller models is shown here. Further details about the setup is explained in the consequent sections.

An outline of the steps being followed to setup and analyze the brake control models are:

1. The first step was to select simulation tools, create maneuvers and then have a method to simulate the control system and actuation system for the brakes.
2. Initially the plan was to study a truck and a trailer system. However, after carrying out initial simulations, it was clear that IPG TruckMaker requires co-simulation functions to make the ABS system work on the trailer and that was not possible to develop in this project. Therefore, the following simulations were run with 4x2 semi-truck.
3. The simulation in IPG TruckMaker is setup with establishing a reference truck model with the relevant parameters. The truck being used in this thesis is Volvo FH 2012 (4x2) semi-truck.
4. After this, the relevant tire models and the brake system for the tractor setup are used. The brake system model used here is the pneumatic brake model for a 2 axle tractor defined within IPG TruckMaker.
5. Once all the relevant models are setup and/or implemented, road section for the manoeuvre is created. The road section is built with relevant friction coefficient which can be modified depending on the type of manoeuvre being simulated.
6. Next, the manoeuvres to be simulated are listed. The manoeuvre used in this thesis work is:
 - Maximum Straight Line Braking: This manoeuvre is developed with the following variations:
 - With different Friction Coefficients and also with split-mu conditions [Ice, Snow, Dry Asphalt]
7. Once everything has been selected as listed in the steps above, for the baseline simulation setup, a Basic Actuator controller (described in Section section 3.5 on page 27) is used.
8. After the simulations with the baseline setup has been carried out, the next set of simulations will evaluate the same truck model (i.e. the model stated in (2))

but this time the basic brake actuator-controller model will be replaced with the advanced actuator-controller model (described in section 3.6 on page 28).

9. The results obtained from steps (7) and (8) will be analyzed individually.

The next sections outline the models being used in detail.

3.1 Vehicle Model

The vehicle model chosen for the simulations in this thesis is a 2 axle semi-truck with 2 wheels on each axle. Initially, the aforementioned semi-truck along with a single axle trailer was chosen. However, after carrying out the initial set of simulations, it was realized that the brakes on the trailer could not be included in the brake control systems and therefore require co-simulation functions that was not available in this project. Therefore, it was decided to execute the simulations hereafter with only the semi-truck.

The vehicle model is a multibody system comprising of different bodies. Defining the degrees of freedom of the complete vehicle would be quite difficult as it is the complete vehicle that is being simulated inside the tool. Since this thesis work deals with the analysis of the braking maneuver, for the most part, longitudinal dynamics of the complete tractor is modelled and analyzed. This would also include the longitudinal load transfer due to pitching motion of the tractor during the braking maneuver. The road surface is chosen such that its vertical profile is smooth. Since no extra load has been added to the existing tractor model within the current setup, and also since the road surface being simulated is smooth, no extra traction is assumed to be required. Hence, the twin wheels setup on each axle was avoided. The advantage of this type of setup was that the vehicle model was kept as simple as possible which resulted in least amount of variability in terms of simulation parameters.

The equation of motion of the complete vehicle in the longitudinal direction can be described as:

$$\sum F_x = m_{veh} \dot{v}_x \quad (3.1)$$

where $m_{veh} = m_s + m_{us}$ is the total mass of the vehicle (i.e. equal to the sum of sprung and un-sprung masses), in kg and \dot{v}_x is the acceleration or deceleration of the vehicle. $\sum F_x$ is the summation of all the longitudinal forces acting on the vehicle, in N, which can be given as:

$$\sum F_x = F_{x,propulsion} + F_{x,brake} + F_{x,aero} + F_{x,rollingresis} \quad (3.2)$$

The forces acting on the vehicle, are generated during braking or accelerating, where the torque on the tire gets transferred to the road through the contact patch. The normal force on each wheel and the friction of each wheel determines the maximum amount of torque that can be transferred. If the dynamics of one wheel during braking is considered, the equation resulting from taking the moments about the center of the wheel can be depicted by:

$$J\dot{\omega} - r_b F_x + T_b = 0 \quad (3.3)$$

where, T_b is braking torque, r_b is the radius of the tire at which the braking force acts, J is the rotational moment of inertia of the wheel, and ω is the rotational speed of the wheel, F_x is the braking force which is related to the friction between the tire and the road by:

$$F_x = \mu F_z \quad (3.4)$$

3. Methodology

where μ is the coefficient of friction and F_z is the vertical load on the wheel. Here, μ not only depends on the surface type but is also a function of the longitudinal slip λ which is given by:

$$\lambda = \frac{(v_x - R\omega)}{v_x} \quad (3.5)$$

The F_x in Equation 3.3 is the braking force which is obtained by Magic Formula described in Equation 3.6 (described in the next Section 'Tyre Model'), which, along with its dependence on other parameters, also depends on the coefficient of friction μ_x . The parameter D used in the Magic Formula, which represents the peak value of the curve, is given by the relation $D_x = \mu_x F_z$ for the case when longitudinal braking force during pure braking is being considered. Therefore, F_x is dependent on μ and hence μ is one of the variables. In TruckMaker test run simulations, a value of μ is set here for each scenario which helps TruckMaker decide the type of tire-road interaction and subsequently calculate F_x .

The free body diagram depicting the forces and torques which leads Equation 3.3 acting on the single wheel after taking moments about center of the wheel is shown in Figure 3.1.

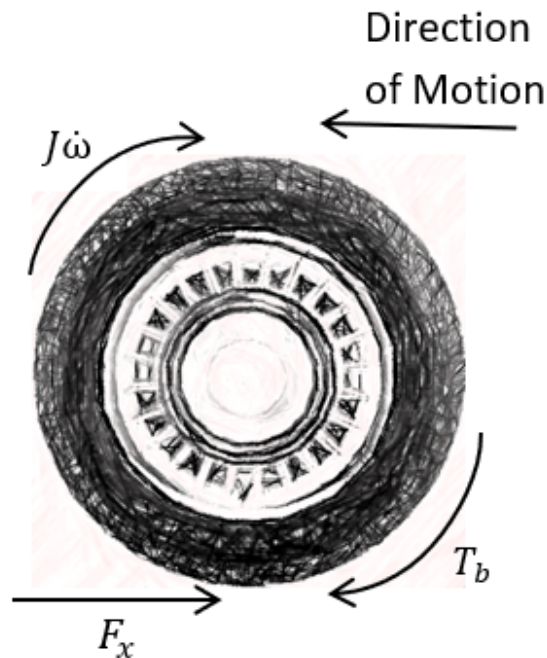


Figure 3.1. Free body diagram of a wheel under braking

3.2 Tire Model

The tire model being used in the simulations is a tire based on Pacejka's Magic Formula MF-Tire/MF-Swift 6.2 tire model developed by TNO Automotive (an organisation that played a leading role in developing the tire model for a number of simulation tools). This tire model is used because of its ability to provide a close and accurate correlation to the characteristics measured experimentally. It is used extensively in the automotive industry due to its wide availability and ease of use. Here, the tire dynamics are introduced with the help of a tire belt that is modeled in the form of a rigid ring [14]. This type of tire model developed by TNO is well-suited to be used in scenarios wherein an analysis of a controller of some sort is being carried out within a simulation tool.

Within the software, this tire model makes use of the Standard Tire Interface (STI) which provides a standardized way to integrate the tire models with the vehicle models. The model, which makes use of this interface, calculates the necessary parameters such as slip angle, slip ratio, etc. which are required for updating the local suspension variables. Unlike the Contact Point Interface (CPI), this describes the entire tire behavior including the vertical and horizontal tire characteristics. The interface is essentially needed to calculate the required tire forces and moments at the wheel center along with the calculation of slip, slip angle, normal forces, inclination angle, etc at the tire road contact point. It first obtains the tire-road contact point using the road model used and calculates the variables such as slip, slip angle, inclination angle and normal force at the tire-road contact point. It also calculates the required tire forces and torques at this contact point and then transforms these tire forces and torques to the wheel center. The inputs (such as co-ordinates of the wheel center, velocity and wheel rotational speed at the wheel center, etc.) to the tire model implementing type of interface is given by the vehicle model. The tire model with this type of interface makes use of these inputs along with general tire parameters such as mass of the wheel, its inertia tensor, details about the inflation pressure, etc. The flow of information within the tool, is shown in Figure 3.3.

The required tire forces and/or torques are calculated using the Magic Formula, the general form of which is given by:

$$y(x) = D \sin[\text{Catan}[Bx - E(Bx - \text{atan}Bx)]]$$

$$Y(x) = y(x) + S_V; \quad x = X + S_H \quad (3.6)$$

where $Y(x)$ is the force (F_x or F_y or M_z), x here is the Slip, B is the stiffness parameter, C is the shape parameter, D is the peak value parameter and E is the curvature parameter of the curve. Here, S_V and S_H represent the vertical and horizontal shift parameters respectively that are introduced in order to account for the errors introduced in the measured data for tire radius and rolling resistance. Both vertical and horizontal shift parameters shift the curve in way that it passes through the origin which might not be possible when the measure data is plotted directly.

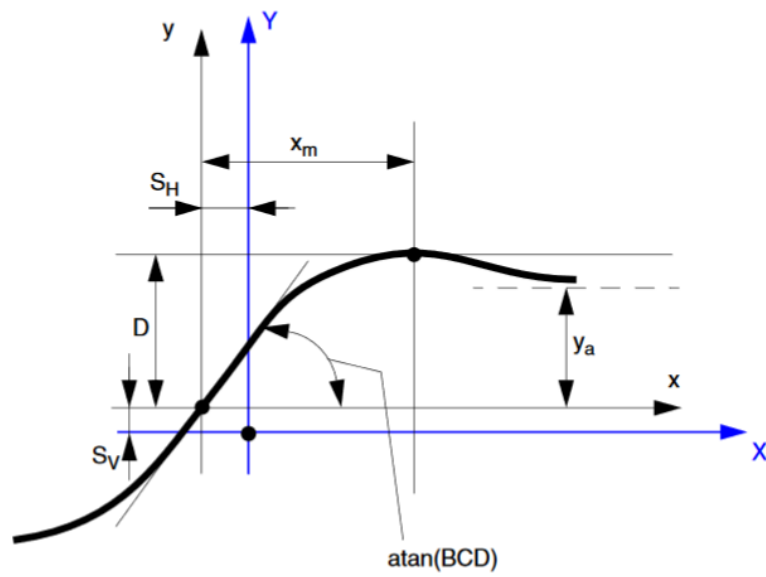


Figure 3.2. Magic Formula [20]

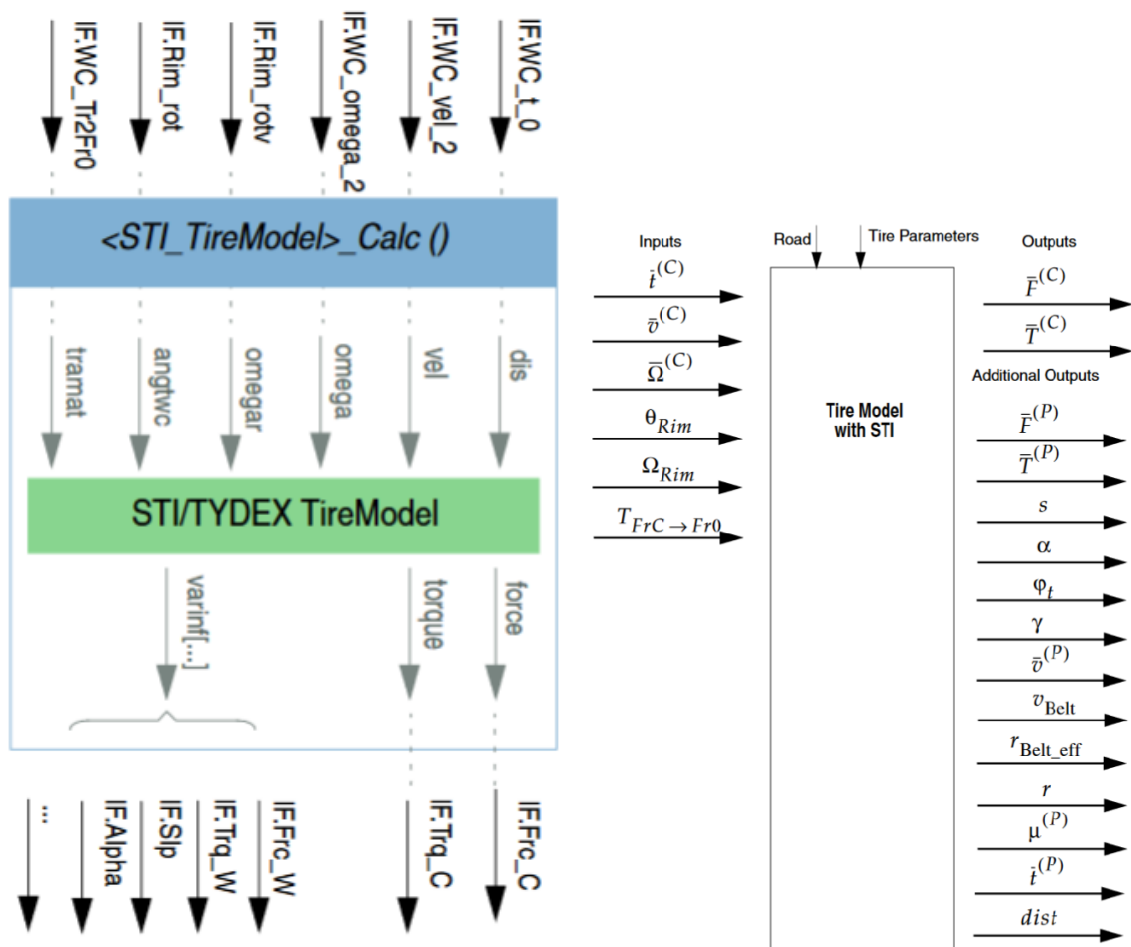


Figure 3.3. TruckMaker Standard Tire Interface (STI) Block Evaluation [20]

3.3 Manoeuvres Description

In this section, the selected driving manoeuvres are described in detail, to present the different aspects that the manoeuvres cover.

In general, for all the simulations, the braking manoeuvre within the tool is designed using a set of commands or instructions. These commands written within the mini-manoevr command section instruct the tool the instant when it should engage the brake pedal and bring the vehicle to a standstill. The braking manoeuvre in the simulations is triggered after the vehicle fulfills the initial condition of reaching a vehicle speed of 70 km/h. The simulations are setup in such a way that once the vehicle accelerates to a speed of 70 km/h and coasts to a distance of 400m, the brake pedal is instructed to be fully engaged till the point the vehicle speed is as low as 0.001 km/h. Since this complete scenario is performed in simulations, the driver model embedded within the tool performs the corrective steering actions on low friction road surfaces where it might become difficult to keep the vehicle on a desired straight ahead path. The braking system is instructed to be engaged till the vehicle's velocity is close to a standstill.

The different types of braking scenarios being evaluated for comparison are as explained below.

3.3.1 Maximum Straight Line Braking

As the name suggests, the desired path for carrying out the braking manoeuvre is built as a straight line along the center of a lane which has a total length of 1500m. The vehicle velocity at the beginning of the braking is taken as 70km/h. The length of the road before braking trigger point is 400m and 100m after this point. The width of the lane is maintained as 3m throughout the entirety of the road.

3.3.1.1 With Different Friction Coefficients

In order to ensure that both the brake controllers produce reliable results when compared to real world experimental results, the straight line braking manoeuvres are tested on different road surfaces. Here split-mu surfaces are also taken in to consideration when testing the braking systems within the simulations.

The different road friction coefficients taken in this test are:

- Dry Asphalt : $\mu = 0.8$
- Snow : $\mu = 0.3$
- Ice : $\mu = 0.1$
- Split-Mu 1 [R/L] : 0.5/0.8
- Split-Mu 2 [R/L] : 0.3/0.8
- Split-Mu 3 [R/L] : 0.1/0.8

3.4 Step Response Test

Step response of a system refers to the way a system behaves over time when the inputs of the system suddenly change from zero to one in a very short period. The step response test is a time domain test used for determining the dynamic output of the system when the input is a step signal. Determining this type of response gives information about the system on the time required to reach a steady state when starting from another steady state. The reason for knowing this behavior is that the system is unable to act until and unless the response of the system becomes stable and reaching this final settled state takes time. Thus, delaying the system response. This delay should be as low as possible.

In case of brake control for HGVs, the step response test has been performed for two reasons:

1. To separate the validation of the pneumatic actuator used within the EBS system in TruckMaker from the Basic Actuator control algorithm.
2. To determine the time delay and time constant and compare them with the standard values of time constants determined experimentally. These are then used within the as parameters within the controller for basic actuator to control the response of the system.

In order to carry out this test for the actuator model used in the in-built system, the following procedure is employed:

1. The control algorithm for the basic actuator model (described in Section 3.5) is disconnected from the system so that the pneumatic system can be evaluated alone without any external influences on the actuator's variables.
2. Once this is done, the required vehicle model with the actuator model (which is essentially a time delay modeled in series with a first order brake system) is simulated statically i.e. the simulation is carried out with just engaging the brake pedal from position 0 (No engagement) to 1 (Full engagement) in time of 0.2 seconds. It should be noted that no motion is given to the vehicle i.e. brake engagement is done on a stationary vehicle so that other parameters do not affect the time constant of the valve.
3. The value of 0.2 seconds determines the 'aggressiveness' with which the driver applies the ramp or gives the step input in the form of application of brake pedals.
4. The static evaluation method helps in determining the reaction time difference between the target pressure set by the demand for complete engagement of the pedal and time in which the actual change in pressure within the chamber is visible. This time difference between the two also helps in determining the time delay or lag and time constant required to be used in the controller for this basic actuator.
5. There are two different kinds of time-based variables which are essential to be defined for the actuator model at this instant:
 - (a) Time Delay: This defines the time difference between the instants when an electrical signal is given to the solenoid in the valve to change state and instant when an initial change in pressure is seen in the brake chamber. In reality, this can be evaluated as the time required for the pressure response

to reach at least 1% of the total demanded pressure. In other words, the first instance when a pressure rise is observed within the chamber.

- (b) Time Constant: For a first order system, the time constant represents the time required for the pressure response to reach 63.2% [19] of the maximum pressure at which the pedal is completely engaged i.e. the when the state is changed from 0 to 1. Alternatively, this can also be stated as the time required to reach 36.8% of the peak pressure when the pedal is completely disengaged i.e. when the state is changed from 1 to 0.
6. The time constant obtained from the above calculations would help determine the time constant to be used in the controller for the basic actuator. Within the controller, it would be the time difference between the required clamping force (calculated by making use of the brake torque request) and the clamping force that is observed at the calipers. Therefore, it defines the rate which the caliper would apply the clamping force and a corresponding change in pressure is observed. It is the most essential parameter defining the response of a first order system to a step input.
 7. The time delay defined for the actuator valves in the basic actuator brakes is 50 milliseconds which is gradually increased or decreased (depending on whether the pressure is decreased or increased respectively) to track the peak of the mu-slip curve.
 8. The time constant is calculated as shown in step 5b i.e. when the pressure response reaches 63.2%. The time constant obtained through this method is 0.350 seconds.

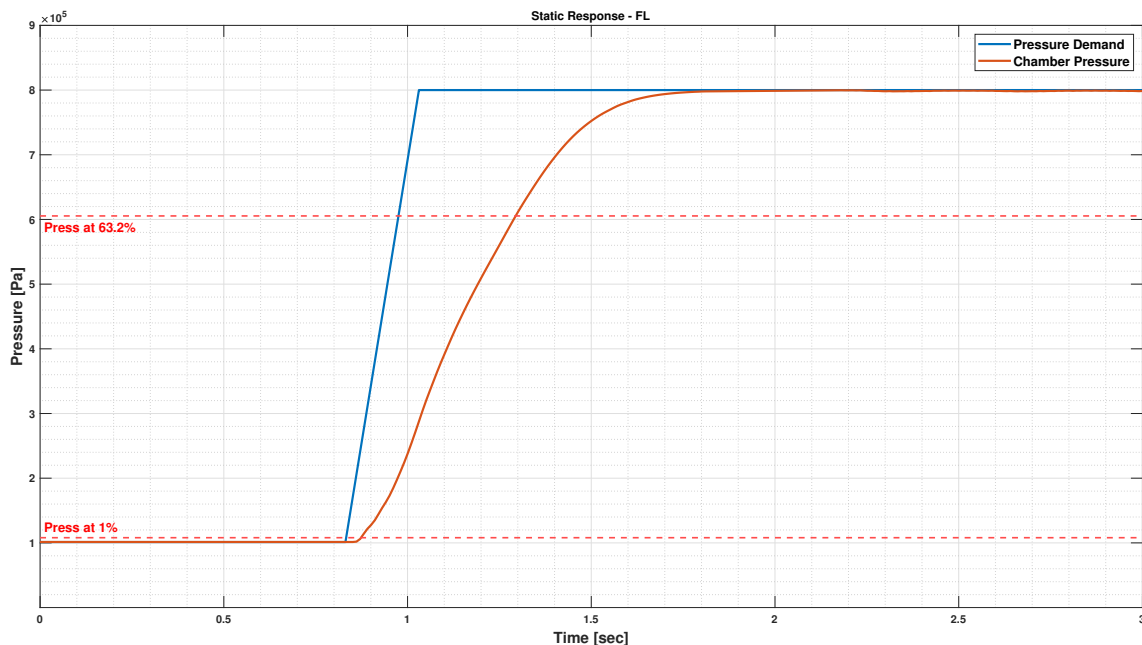


Figure 3.4. Step Response of the generic actuator in TruckMaker

The plot shown below depicts the response of the actuator system within TruckMaker to a step input supplied to the system in form of brake pedal engagement

from an initial steady to a final state.

1. Since this is complete engagement of the brake pedal from an initial steady state to a final state, therefore the pressure demands remain high at 8 bar which is reflected at the foot valve and hence it creates a pressure target.
2. It becomes important to define the flow through the valve chamber in this part. The flow here becomes choked or restricted during the charging process i.e. the velocity of the flow through the valve becomes so high that it reaches a speed of sound. This is when the flow is said to be choked. When the velocity is below the speed of sound, the flow is said to be un-choked.
3. Here, the flow of air through the valves becomes choked during charging the brake chamber when the pressure is seen to be increasing during the brake pedal engagement phase to reach a fully engaged state. Once the pressure reaches a target value of 8 bar, it remains at that particular point until the pedal is kept engaged. Here, only the engagement phase is shown. Once the pedal is disengaged after the vehicle comes to rest, the discharge of air starts due to which the flow again tends to become choked. It becomes unchoked just before the discharging process is complete.
4. Thus, the pressure response within the chamber shows a linear behavior due to the fact that the flows get choked during the build-up phase of the pressure, as can be seen here.
5. The engagement of brake pedal can be seen as gradual here and not as 'aggressive'. If it were to be aggressive, the pressure demands would rise and drop steeply during the engagement or disengagement phases, respectively. This steep behavior can be achieved either by modifying the behavior of the driver within the software or by modifying the rise or drop time as defined in item 3.
6. As per the definitions, it is possible to calculate the instant at which the pressure reaches 1% & 63.2% of the target pressure. The time delay and time constant obtained through this method is 53 milliseconds and 350 milliseconds.

3.5 Basic Actuator Control Implementation

The basic actuator which has been used in this thesis was provided to us by Chalmers University of technology. It works as a slip control model. The basic actuator model is shown here.

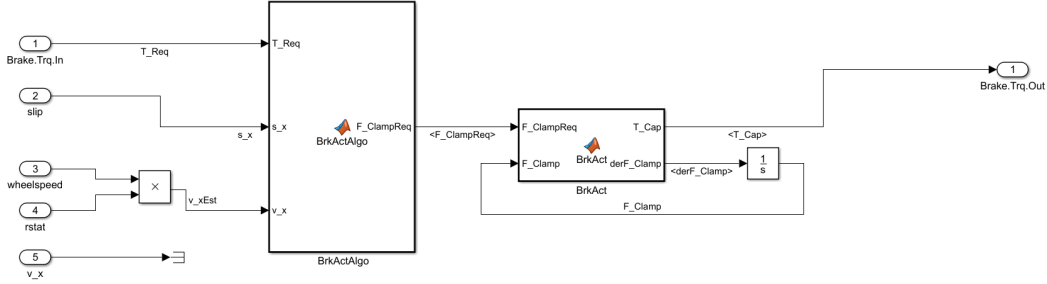


Figure 3.5. Controller for Basic Actuator

The above model is divided into two parts namely "BrkActAlgo" which contains the algorithm for calculating the clamping force required at each wheel and "BrkAct" which generates the clamping force at each instance of time. This brake controller is in form of a bang bang controller which means it has only two states, on and off.

The block "BrkActAlgo" calculates the required clamping force at the disc. The limiting slip value for this block is set to 0.2. This means the clamping is calculated when the longitudinal slip value is greater than 0.2 and in the rest of time, the clamping force remains zero in all other values of slip. The inputs fed to this block are brake torque input, longitudinal slip and the speed of the vehicle. the formulae used to calculating the required clamping force is shown below:

$$F_{ClampReq} = \begin{cases} Gain * T_{b,in}, & \text{if } -s_x < s_{sLim} \\ 0, & \text{Otherwise} \end{cases} \quad (3.7)$$

The output brake torque is generated by the block "BrkAct". This block takes the output from the "BrkActAlgo" which is the clamping force required and generates the output brake torque. A non linear clamping force is required at each time instant so as to prevent the wheels from locking up. This is done by dividing the clamping force output from the previous block by a time constant. The output of this block is then integrated and then fed as an input to reduce the error in the clamping force required at each time instant. The nonlinear clamping force is then multiplied by the friction coefficient and the radius of the disc to get the output brake torque at each wheel. The formulae used is as shown below:

$$dF_{clamp} = \frac{(F_{ClampReq} - F_{Clamp})}{t_{const}} \quad (3.8)$$

$$T_{b,out} = \frac{\mu_{disc} F_{clamp}}{R_{disc}} \quad (3.9)$$

3.6 Advanced Actuator Control Implementation

As discussed earlier, the primary aim of this thesis is the development of a methodology so that the brake models can be verified virtually with the help of different tools used in co-simulation. This is achieved by making use of a Functional Mockup Interface which contains all the necessary parameters required to replicate the behavior of the actual models without revealing the proprietary details about the models. This section deals with the development of this methodology.

Therefore, the primary aim here is to integrate the FMU containing the advanced actuator-controller described in Section 2.3. To do this, the basic actuator-controller is detached from the loop and instead an advanced actuator and controller within an FMU replaces it. Thus, the FMU used here becomes the ‘heart’ of the advanced actuator.

To perform this integration, the following methodology is implemented:

1. To begin with, it is important that tools used in this process are described in brief. The tool used is IPG TruckMaker which is used with another tool, Simulink, in co-simulation. This co-simulation is an important aspect of integration of the FMU with the vehicle model.
2. In order to integrate this, it is essential that the FMU is imported at the right location within Simulink. IPG TruckMaker4Simulink contains a detailed architecture of the complete vehicle which provides a greater independence to manipulate certain aspects of the vehicle. The FMU is imported within the ‘Brake’ module of the vehicle.
3. Since this advanced actuator has to be implemented on all the four wheel ends of the truck, it is necessary that four different copies of the FMU be imported and integrated within this block.
4. But before importing the FMU, it is essential that the required vehicle, tire and brake models be selected within the main Graphical User Interface or GUI of TruckMaker. As mentioned earlier, the vehicle model used here is 2-axle semi-truck Volvo FH 2012. The tire model used here is based on Pacejka’s Magic Formula and is called MF-Tire/MF-Swift 6.2. It was developed by TNO.
5. At this point, it is necessary to parameterize certain aspects of the vehicle model such as the polar moment of inertia, the unloaded radius and the mass of the wheel carrier. The information on these parameters can be obtained by extracting the parameters of the selected tire. This is done so as to increase the accuracy of the results and to avoid any unwanted influence of parameters such as addition of mass and moment of inertia of the wheel. Also, the vehicle’s mass and inertia properties may be modified. In this case, it is kept as it is without addition of any extra weights or modification of the default mass of the semi-truck as changing these would not only increase the variability within the model but might also introduce any unwanted oscillations in the results.
6. Once these are selected, it is now necessary to choose the required brake models. Since this work involves verification of complete vehicle using a pneumatic brake system, an in-built 2-axle pneumatic brake model that comes bundled

with a basic pneumatic controller is chosen.

7. Once this is chosen, it is now necessary to validate the actuator within this system. This validation is carried out with the help of a step response test which has been shown in Section 3.4 so as to be ensure that the vehicle gives a response that is expected of it. For e.g: the pressure demands reach a peak when the brake pedals are fully engaged on giving a step input to the system and that the time constants and delays also match the standard values obtained experimentally.
8. After this initial validation, the required advanced actuator's FMU can be imported within the brake module of the TruckMaker's vehicle architecture. This is done in Simulink.
9. Since the FMU is now going to act as a local brake controller, it is necessary to import the controller in the correct module within TruckMaker so that it replaces the default controller of the pneumatic actuator. In this case, it is the 'Brake' module within the module 'IPG Vehicle'. This is done because this module provides us with the required flexibility of manipulating the input brake torque signals.
10. Since the FMU is now the local brake controller, it is important to define the input and output signals which would lead to the final optimized brake torque signal demand for improved braking control. These can be summarised as follows:

- Inputs: Most of the input signals that are required to be fed to the FMU, can be obtained directly through the 'User Accessible Quantities' within TruckMaker. Others have to be manipulated before sending them as inputs.

For e.g., the input brake torque and the rolling radius. During braking, since the rolling radius varies continuously depending on the brake torque requested by the driver. To model this, brake pedal's position is used as a reference. The rolling radius is calculated by making use of the tire's belt velocity which would be a more accurate quantity to use instead of 'Current wheel radius' (available directly as a User Accessible Quantity) which measures the distance between the road and the wheel center. When this belt velocity is divided by the wheel rotational speed (for which the quantity is directly available), the resulting quantity is the effective rolling radius. But this would depend on the brake pedal's relative position i.e. if the pedal is engaged, the rolling radius of the previous step is utilized.

It should also be noted that for all the variable input quantities, the sampling rates of the TruckMaker signals coming into the FMU should match with the communication step size of the models defined inside the FMU in order to avoid an introduction of additional signal delays into system which might effect the final results. Therefore, a zero order hold is added to every input at this stage so that the input is held for a specific time period set in the block that matches with the one specified for the FMUs.

- FMU: After defining the inputs, it is now essential to give a brief summary of what happens inside the FMU now that it acts as the local brake

controller. The FMU, here includes the Valve Plant hardware modeled into it along with other controllers and observers. Therefore, the elements inside the loop are: Force Observer, Sliding Mode Slip Controller, Pressure Controller and the Valve Plant.

- The force observer estimates the braking force (F_{xEst}) by making use of rotational velocity (ω) and the applied brake pressure (P_c) from the Valve Plant as described in Section 2.3.2.1.
- This estimated braking force from the force observer is sent as an input to the sliding mode slip controller (described in Section 2.3.2.2) along with other inputs such as vehicle speed (v_x), longitudinal slip (λ), etc. The slip controller then calculates the Pressure Demand (P_d) using Equation 2.2.
- The pressure demand calculated above is sent to the pressure controller which makes use of a proportional controller to calculate the mark space ratio (R_{MS}) using Equation 2.3.
- The mark space ratio (R_{MS}) is then used by the Valve Plant to help switch states. The Valve Plant, then calculates the Brake Torque ($T_{b,out}$) to be applied at the wheel ends along with the pressure that is to be applied at the wheel ends (P_c). This applied pressure (P_c) is then feedback into the force observer and the pressure controller to close the loop.

This interaction between the 4 components within the FMU can be shown in Figure 3.6.

- Output The output of the FMU is the brake torque capacity ($T_{b,out}$) which is sent to the wheel end to apply the required brake torque.
11. Once the the FMU block setup, the simulation is ready to run on a smooth road where different friction coefficients can be used to observe the changes in behaviour of the required parameters such wheel speed, longitudinal slip, etc. This behaviour can then be verified with the experimental results (shown in [10]) for validation.

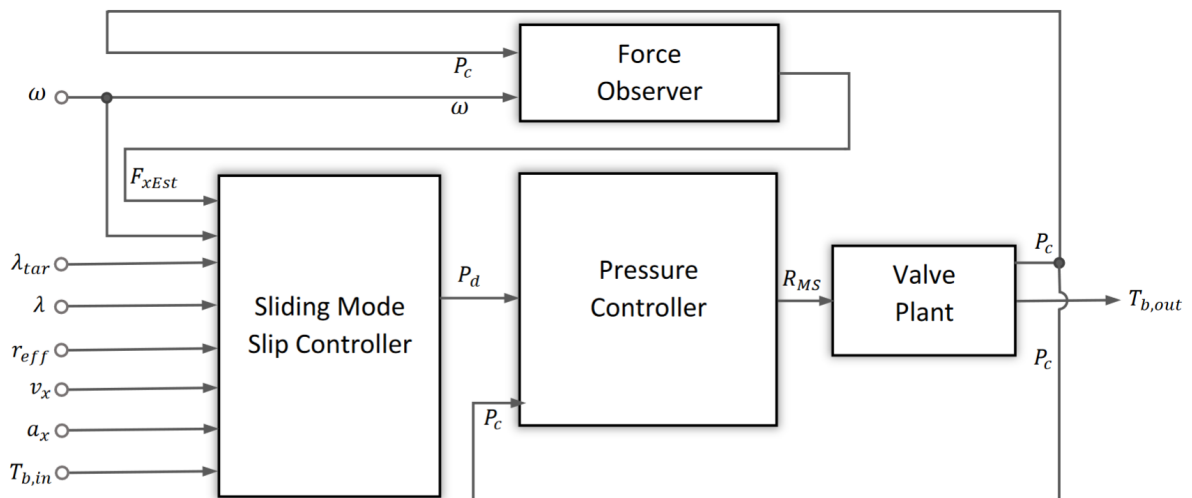


Figure 3.6. Block Diagram of components inside the FMU.

3.7 Solver time step

Most of the systems present in a vehicle are characterised by constant change. If these systems are to be analyzed, a proper solver is required with definite time steps. Solver time step signifies that the computation of the system occurs at definite time intervals. These time intervals should be specified by the user along with other details about the complex model. The model which is to be computed is represented in form of differential equations which is then solved by the solver.

Based on the above criterion, two different numerical integration techniques has been developed. They are:

- Fixed Step Solvers- The fixed step solvers have fixed step sizes throughout the whole simulation. The accuracy of the results varies inversely with increase of the step size.
- Variable Step Solvers- The step sizes in this solvers are not fixed during the simulation. Depending on the requirements, the step sizes increases to reduce the time for the simulation and the step also decreases during certain instances to increase the accuracy.

All the above mentioned solvers are incorporated in MATLAB for computation of complex dynamic models.

4

Results and Discussions

4.1 Tools and Methods of Development

The main aim of the thesis is to develop tools and methods for the development of the brake control system for heavy vehicles. IPG TruckMaker was selected as the simulation tool to carry out the simulations as it has a user friendly interface and capability to allow for quick and easy change in vehicle parameters. Two sets of braking controllers were used to assess the tools and methods, namely basic actuation system and advanced actuation system to develop as a method for the development of brake control system.

This chapter entails the results that have been obtained via simulations for the two types of brake controllers. The results follow a pattern in which, first, the baseline results i.e. results obtained through simulations of the basic actuator are presented and then the results with the advanced actuator system will be presented.

The general parameters of the vehicle used in the simulation is shown in Table 4.1. These parameters remain the same while simulating with the two different actuators being used in this thesis.

4.2 Results with Basic Actuator-Controller

This section deals with the results obtained through simulations with the Basic Actuator and its controller in loop. The results presented here are for simulation runs on a road surface which has the same μ on both the lanes (referred here as 'Constant μ ') as well as for surface with different coefficient of friction on the two lanes (referred here as 'Split μ '). The braking distance at the end of each simulation run is measured and is reported in Table 4.2 shown towards the ends of this section.

There are multiple results for each wheel end and each wheel end's results are related to a particular scenario defined by the different coefficients of friction between the road and the tires. Therefore, this section is dedicated to analysing the results of all four wheel ends for different surfaces.

In the case of basic actuator, it should be noted that at present, the basic actuator being used is an ideal actuator. At this point, it can be said that this might not be completely representative of a real brake actuator which might involve a complex model comprising of valves. This is discussed further in the subsections describing the results with the basic actuator in different scenarios.

Parameters	Values	Units
Total Mass	6800	kg
Sprung Mass	5800	kg
Unsprung Mass	1000	kg
Axle Load Front	4806	kg
Axle Load Rear	1995	kg
Vehicle Overall CoG [x/y/z]	3.473/0.00/0.934	m
Drag Coefficient	0.41	-
Frontal Area	8.33	m ²
WheelBase	3.57	m
TrackWidth	2.1	m
Tyres Front & Rear	315/80R22.5	-
Free Radius (Unloaded Radius)	0.548	m
Tyre Diamterical Moment of Inertia I_{XX}	10.5	kg-m ²
Tyre Polar Moment of Inertia I_{YY}	16.8	kg-m ²
Tyre Vertical Stiffness	1000	kN/m
Tyre Vertical Damping	5	kNs/m

Table 4.1: Vehicle Parameters

Longitudinal Speed v_x [kph]	Friction μ [-]	Braking Distance [m]		
		$t_c = 150ms$	$t_c = 350ms$	$t_c = 450ms$
70	0.8	35.28	35.54	38.18
70	0.3	108.55	112.42	115.69
70	0.1	362.07	368.91	373.03
70	0.5/0.8	49.35	50.45	51.76
70	0.3/0.8	80.61	80.64	82.68
70	0.1/0.8	106.34	113.55	114.87

Table 4.2: Braking Distance Results with Basic Actuator

4.2.1 Straight Line Braking - Constant μ Surfaces

The simulation results for braking on a constant friction road surface are shown in the figures below. As mentioned earlier, each figure shown in this section pertains to a simulation run with a specific friction coefficient road surface. The friction coefficient for the three different simulation runs shown here are 0.1, 0.3 and 0.8. The vehicle is brought to rest from a speed of 70km/h. The slip target set out is 12% on the front and 10% on the rear axles.

For the plots shown in Figure 4.1 (also in Figures 4.2 and 4.3) below, the variation can be understood as follows. The first steep drop in the wheel rotation speed is observed due to three main factors, namely: time constant in the pneumatic system, inertia of the wheel and the slip target set. Once the wheel reaches a deceleration threshold, the controller re-evaluates the input torque which, in turn, reduces the clamping force. This can be understood with the help of the following equation:

$$J\dot{\omega} = r_b F_x - T_b \quad (4.1)$$

where, T_b is braking torque, r_b is the radius of the tire at which the braking force acts, J_ω is the rotational moment of inertia of the wheel, and ω is the rotational speed of the wheel. F_x is the braking frictional force applied to the tire by the road. As the braking starts, the angular acceleration of the wheel would be negative because initially the brake torque is higher than the braking force. There is also a decrease in the wheel rotational speed due to this. This causes an increase in the term $r_b F_x$. Further application of brakes increases the brake torque further due to which the angular acceleration decreases rapidly and vehicle goes into deep slip i.e. when the wheel speed is zero. This rapid decrease in angular acceleration is detected by the controller. At this point, $r_b F_x$ reaches a peak value. Once this peak value is reached, the braking force reduces as the brake chamber pressure is reduced to reduce the amount of brake torque applied. At this point the braking torque T_b is lower than $r_b F_x$ and therefore, the angular acceleration becomes positive again and starts increasing. It increases till a particular point after which the controller detects the rapid acceleration and aims to increase the brake torque.

It should be noted that no peak seeker is added in the loop to estimate the peak slip in every scenario. Rather, a slip target of 12% on the front and 10% on the rear are set as constants.

The first subplots in Figures 4.1.a, 4.2.a and 4.3.a show the variation in wheel speeds for low ($\mu=0.1$), mid ($\mu=0.3$) and high ($\mu=0.8$) friction surfaces, respectively. For low and mid friction surfaces, the current controller for the basic actuator can be observed to show oscillations in the frequency range of approximately 5-7Hz which is very high for a HGV when compared to experimental results. Usually the pneumatic systems are much slower with a frequency of oscillations around 1-2Hz. For the high- μ surface, the variation of wheel rotational speeds on the front wheel ends is depicted in the first subplots of the Figures 4.3.a and 4.3.b. It can be observed that, for the high friction surface, the amplitude of oscillations are very low and the frequency is very high. This is due to the reason that the actuator used is ideal and suggesting

that the controller in this particular case can be observed to work perfectly well for the front wheel ends. In reality, it might not be possible to achieve such high frequency results given the hardware restrictions. Therefore, the results, in this case, needs to be further analyzed and verified.

The second subplot within the Figures 4.1.a and 4.2.a shows the variation of longitudinal slip with respect to a constant slip target. For the low and mid friction scenarios, the longitudinal slip variation seems to be beyond the target value set here and that it just reaches the slip target before going into deeper slip . This means that the actuator here reacts really fast to the extent that there appears to be no effect of the time constant set because through these results it can be inferred that the moment the longitudinal slip reaches the slip target, the required pressure gets applied and it goes into a deeper slip. But when there is a time constant actually acting on the system, the variation is expected to be in a way that it goes above the slip target for a short period due to the lag introduced by the time constant and then go below the slip target.

For the high friction scenario represented in Figure 4.3, the longitudinal slip for front wheel ends (i.e. in the second subplots in Figures 4.3.a and 4.3.b) shows small variation in longitudinal slip compared to the slip target set. The drop in longitudinal slip very close to the constant slip target depicts that the slip control's tracking is close to the slip target set which is close to the peak of the longitudinal force-slip curve. Thus implying that the controller works well for the target value set in this high friction scenario.

The third subplots in each of the Figures for a constant- μ scenario, represent the variation of the longitudinal force F_x at the tire contact patch. On comparing the results of F_x between either of the front and the rear wheel ends (for e.g. Figures 4.1.a and 4.1.c), it can be observed that $F_{x,rear} < F_{x,front}$ for all the case which is because of the longitudinal load transfer from the rear to the front during braking. Specifically for the high- μ case, it can be observed that $F_{x,rear} \approx \frac{1}{10}^{th}$ of $F_{x,front}$ (as it can be observed that $F_{x,rear} \approx 2kN$ whereas $F_{x,front} \approx 20kN$). This huge difference in magnitude can be a bit concerning given the axle load of the front is approximately 2.5 times the axle load of the rear (as seen in Table 4.1). This should be investigated further to validate the values of F_x in the high- μ case specifically.

These results also point towards a possibility that the current setup needs to be further looked into because the actuator here appears to work really fast to the extent that it seems to ignore or over-ride all of the actuator dynamics designed within TruckMaker and instead, may be applying the brake torque calculated directly at the wheel. This needs to be evaluated further.

The time constant obtained from the step response tests (described in Section 3.4) is 0.350s. This value of time constant is close to the value achieved through experimental results in [15], though a more detailed controller was implemented in the latter. A value lower than this can be used to obtain shorter stopping distances. For eg., when a time constant of around 0.150 seconds is used instead of 0.350s. This reduces the stopping distance from around 369m (in the scenario when time constant was 350ms) to 362m (in the scenario when the time constant was reduced

to 150ms) while retaining the same slip targets as before, i.e. 12% on the front and 10% on the rear axles and simulating on the same low friction surface i.e. for $\mu = 0.1$. This lower value of time constant cannot be validated since in reality, the valve plant used might not be able to change states within this significantly reduced time due to the existing hardware limitations for this type of setup.

On increasing the slip target to 20% while retaining the same time constant value of 0.350s, the braking distance increases to 386m. The reason for this can be attributed to the fact that the value chosen here may be further away from where the peak of the longitudinal force-slip curve occurs.

From the plots of results with 150ms as the time constant shown in Figure A.1 in the Appendix section (A), the longitudinal slip variation can still be observed to be going beyond the target value set here pointing to the fact that the inbuilt TruckMaker actuator's dynamics appear to be ignored or over-ridden and instead the brake torque, calculated within the Simulink model representing the ideal actuator-slip control, seem to be applied directly at the wheel.

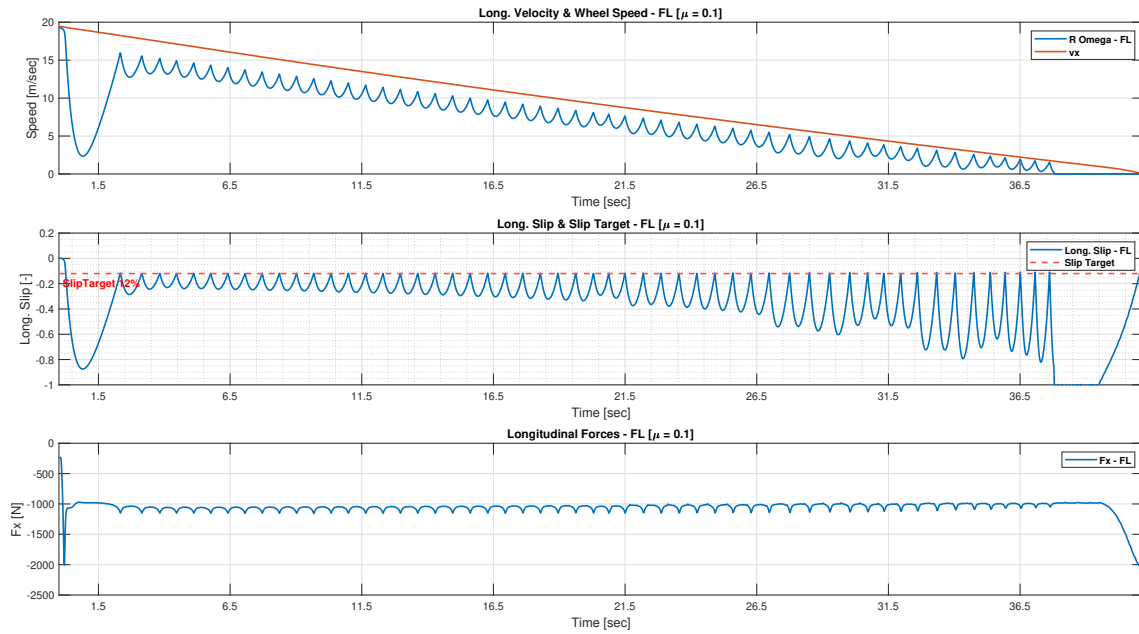
From these results, it can be said that at present, the basic actuator acts as an ideal actuator i.e. an actuator on which there is little to no effect of a time constant. Therefore, it acts as if it has infinite bandwidth wherein the slip reaches the slip target and continues perfectly along the target which can be observed in the results of a high- μ case. Also, it can be said that the current setup with the basic actuator is not using the built-in plant model in TruckMaker. Rather, it is using the pant model within the basic actuator's logic which is essentially just a time constant and at present, with the current setup, the effect of that time constant is little to none. This means that there is little to no delay between the torque applied and torque requested. Thus, it can be said that with the current setup the torque is getting applied directly at the wheels. This needs to be evaluated further to reach a more concrete conclusion.

From Table 4.2, it is quite evident that there are huge differences between the braking distances in moving from a high μ case to a low μ case. This difference can be explained through simple dynamics equation. For a high μ case, the maximum braking distance that we can get can be given by:

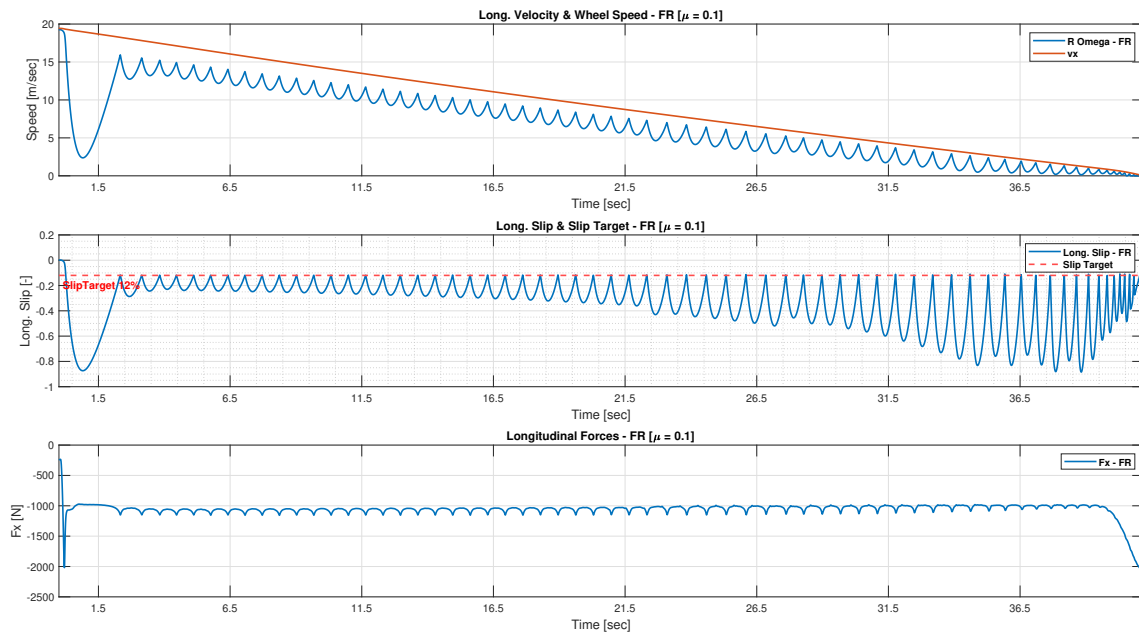
$$F_{x,max} = \mu_{max} F_z \quad (4.2)$$

where, $F_{x,max}$ is the maximum braking force, μ_{max} is the maximum coefficient of friction available and N is the normal force from the ground. For a high- μ case, the maximum braking force obtained would be 0.8 times the weight of the vehicle. Whereas, for a low- μ surface, the maximum braking force available would be 0.1 times the weight. Therefore, theoretically, for a high- μ case, 8 times more braking force should be available than for a low- μ case. But the braking distance is also affected by the value of slip target used here. Since the slip target is not necessarily the peak of the slip-friction curve and since the utilized friction is comparatively lower than the surface friction, therefore, the available friction force and the braking distance of a particular friction scenario may be affected accordingly.

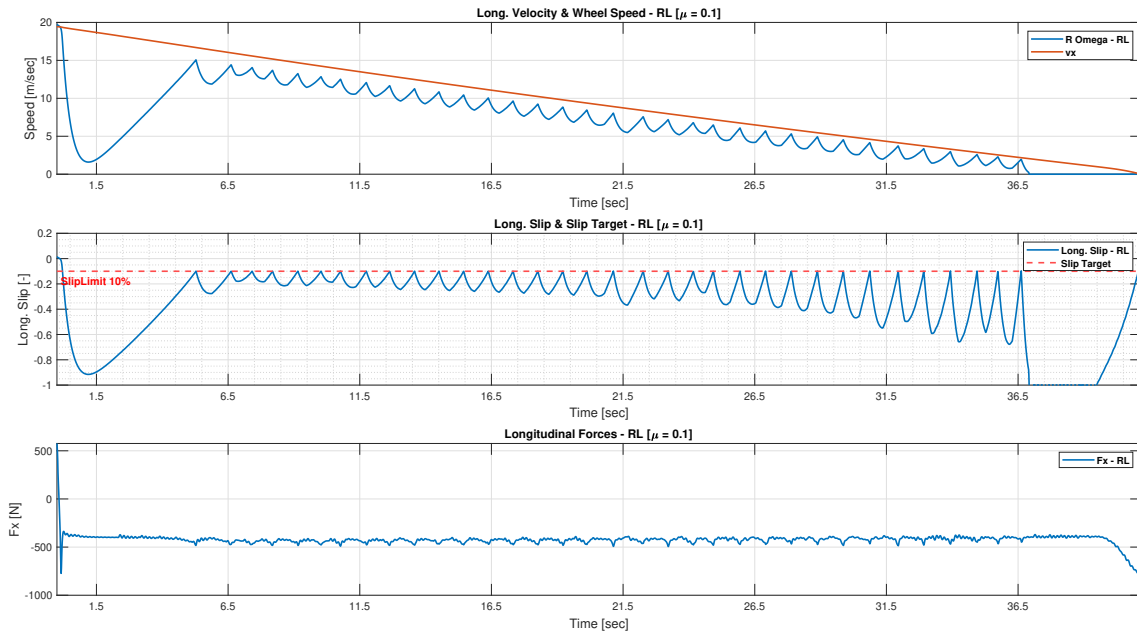
4. Results and Discussions



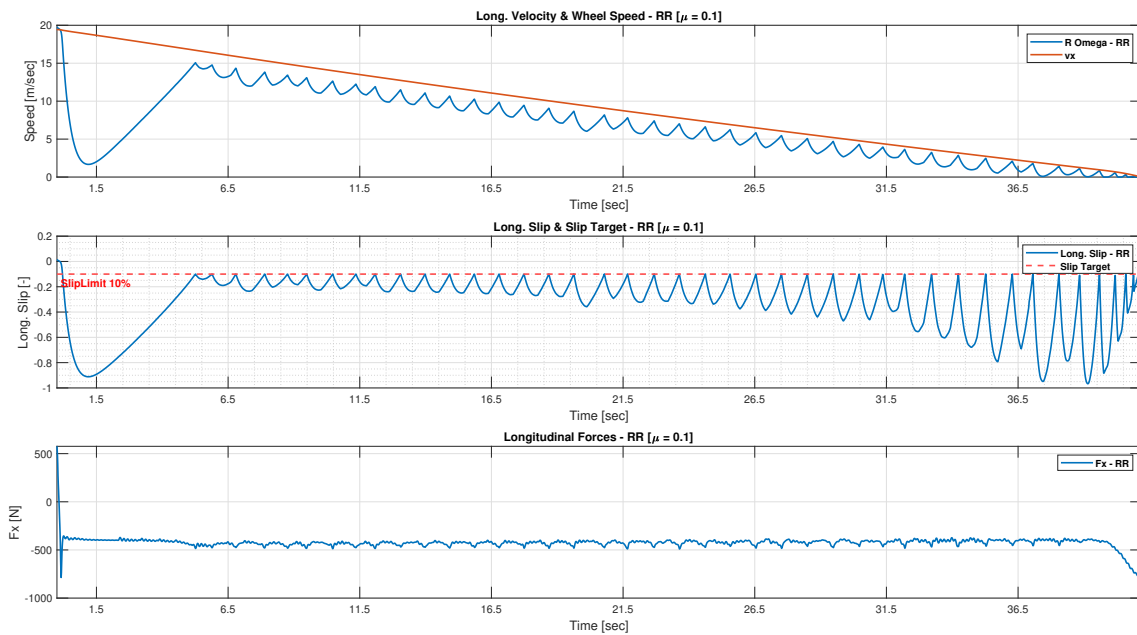
4.1.a. Front Left



4.1.b. Front Right



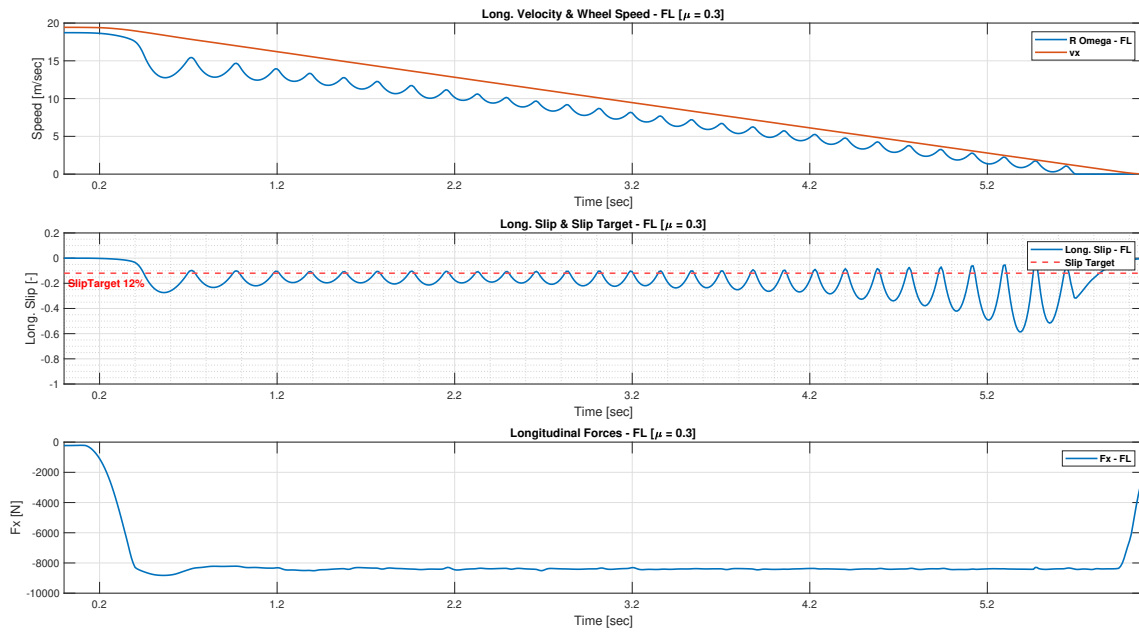
4.1.c. Rear Left



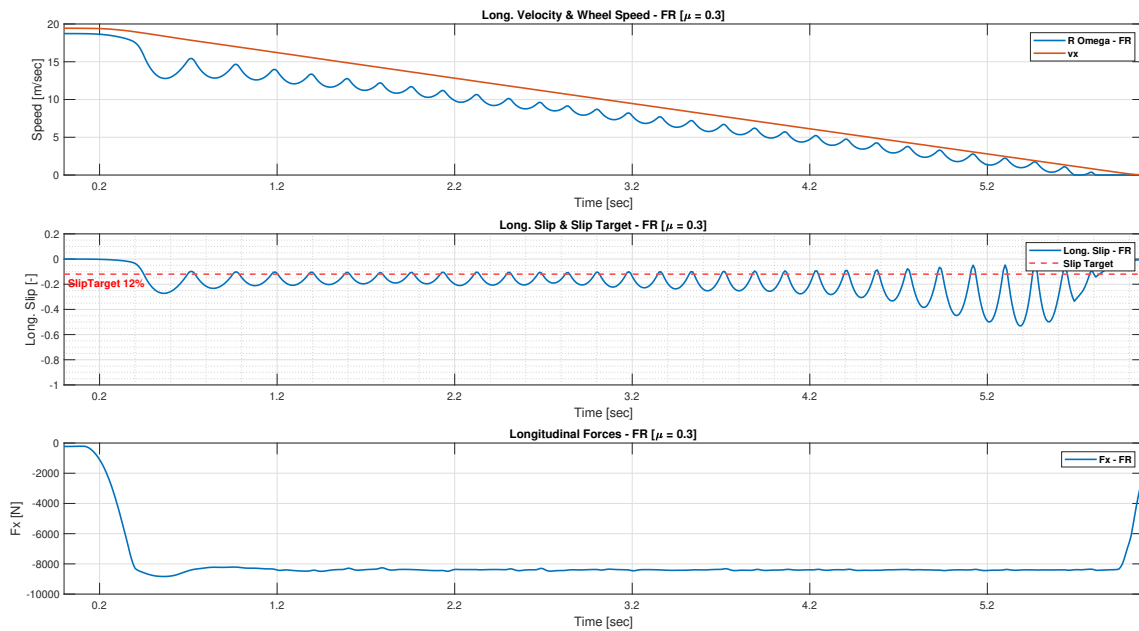
4.1.d. Rear Right

Figure 4.1. Results with Basic Actuator - Speed Variation, Longitudinal Slip Variation and Long. Force Variation for a Low μ Surface ($\mu = 0.1$), Time Constant - 350ms and Slip Target - 12% Front and 10% Rear

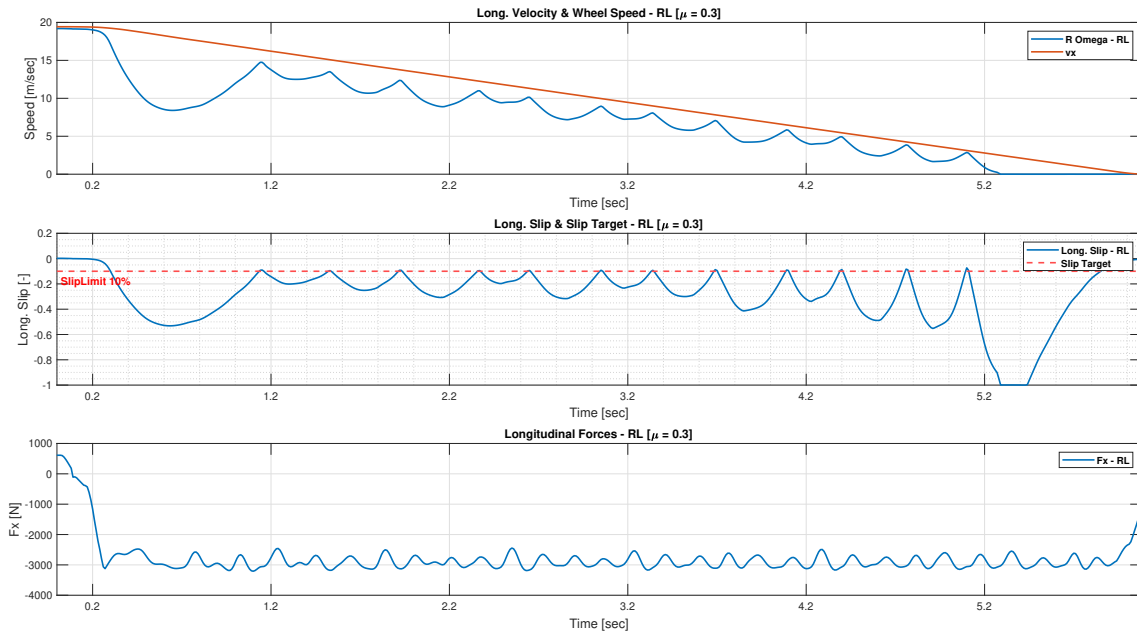
4. Results and Discussions



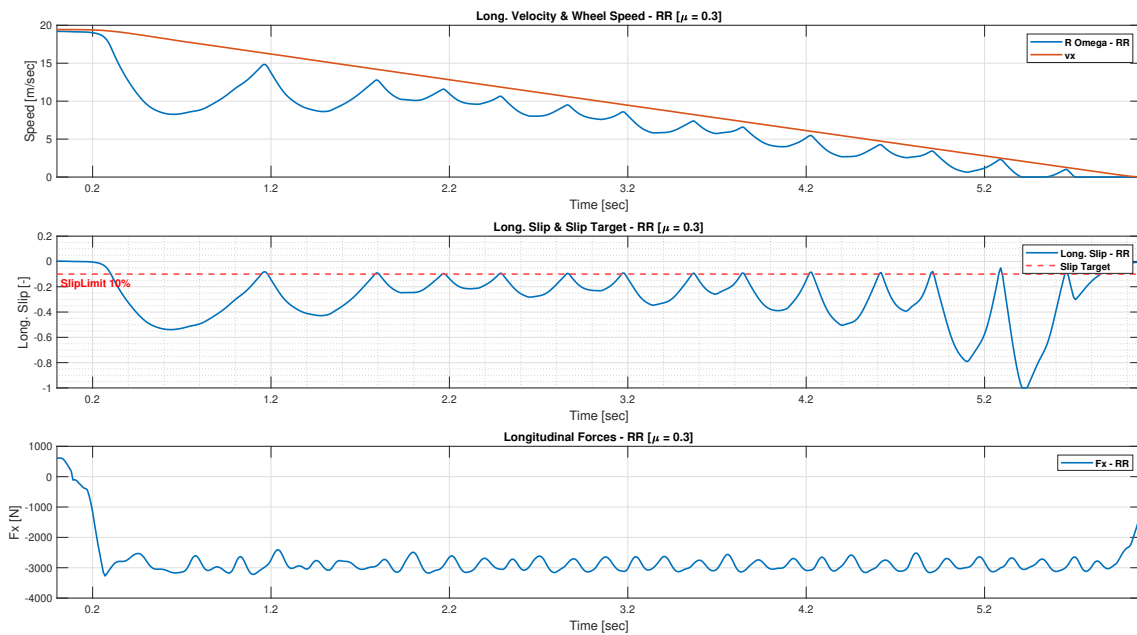
4.2.a. Front Left



4.2.b. Front Right



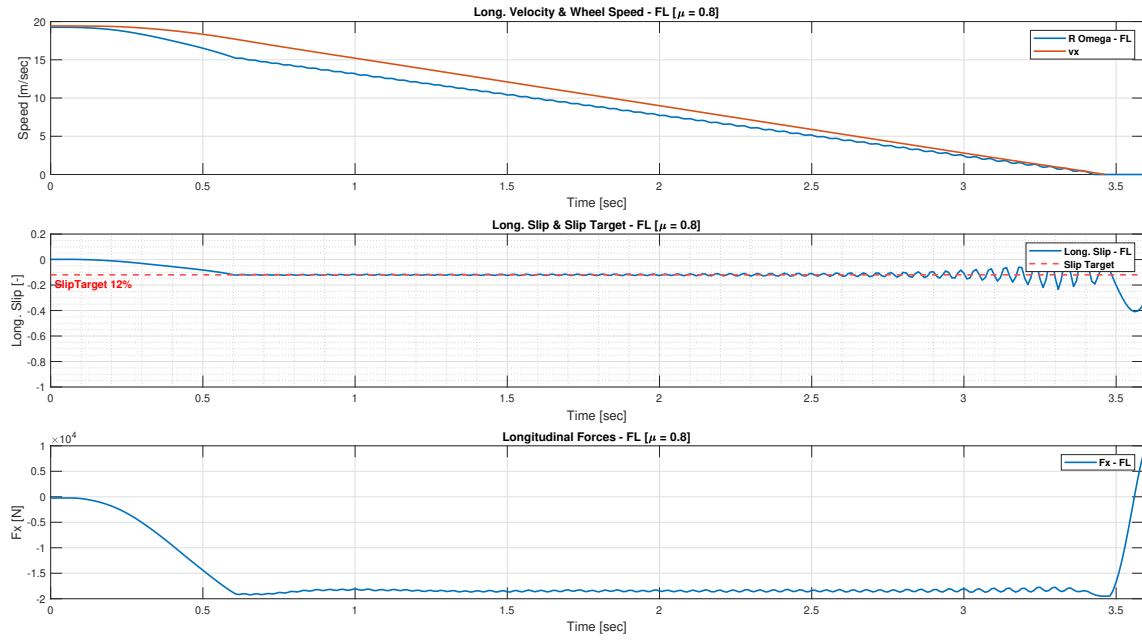
4.2.c. Rear Left



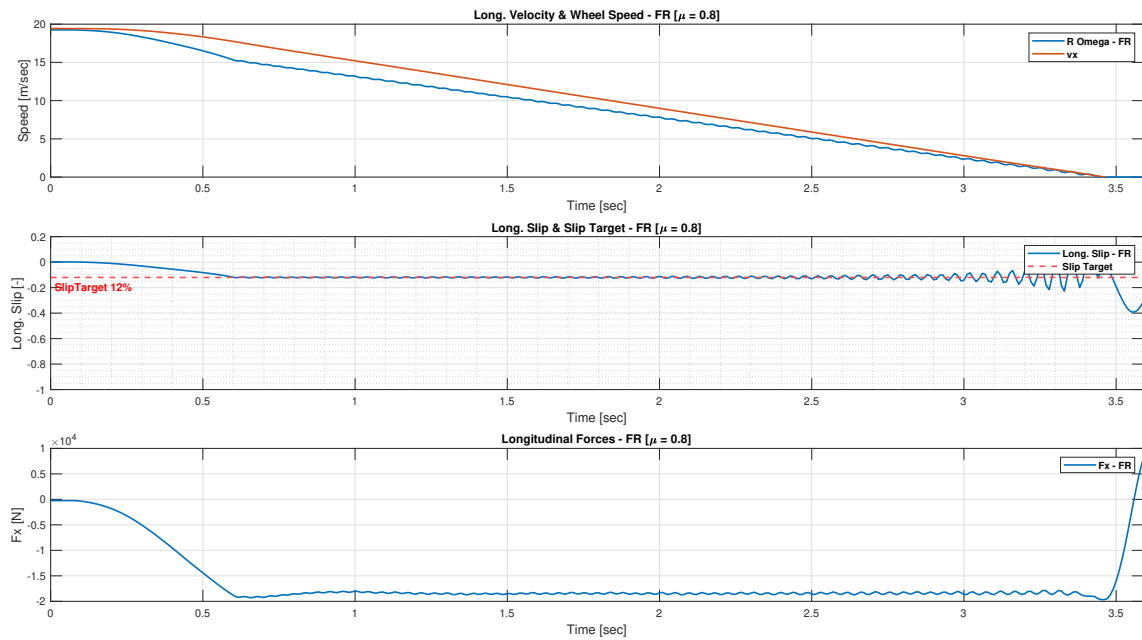
4.2.d. Rear Right

Figure 4.2. Results with Basic Actuator - Speed Variation, Longitudinal Slip Variation and Long. Force Variation for a Mid μ Surface ($\mu = 0.3$), Time Constant = 350ms and Slip Target - 12% Front and 10% Rear

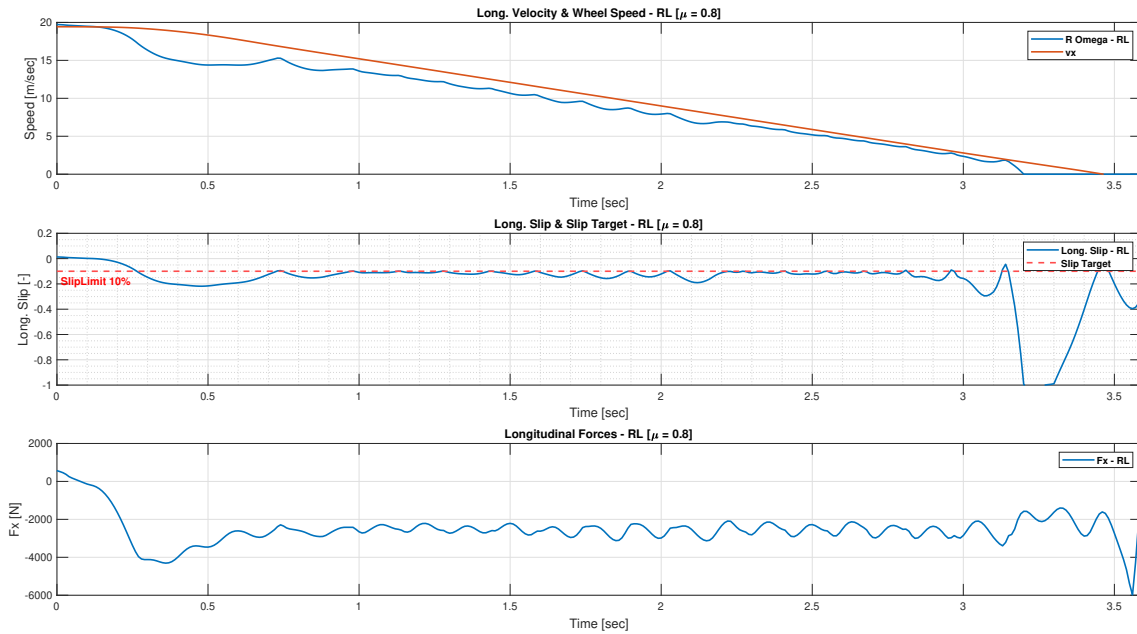
4. Results and Discussions



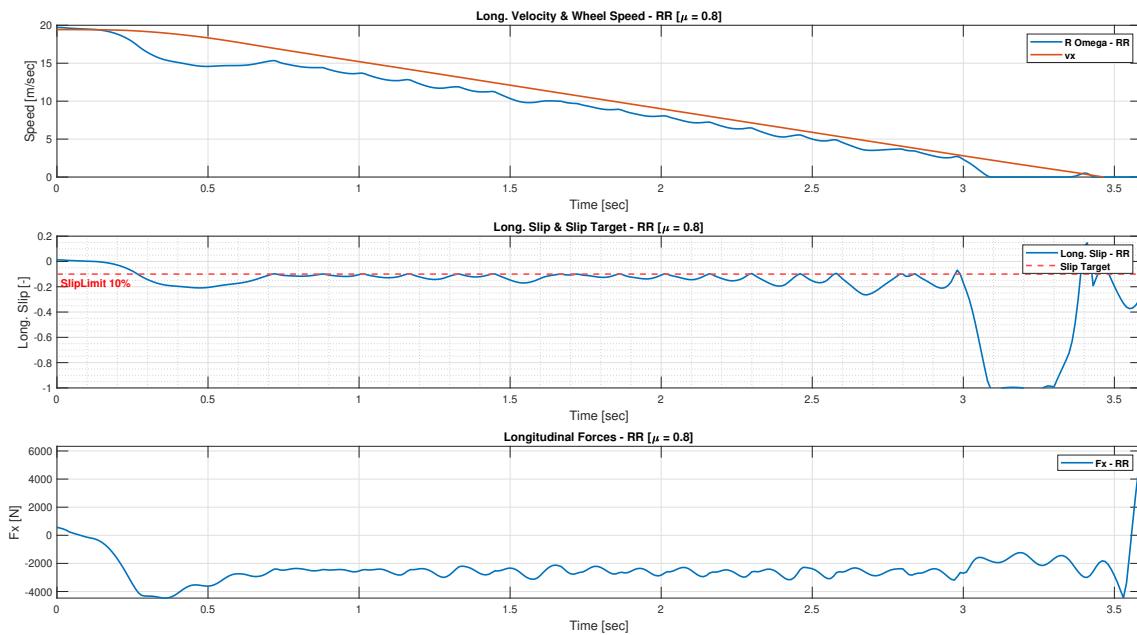
4.3.a. Front Left



4.3.b. Front Right



4.3.c. Rear Left



4.3.d. Rear Right

Figure 4.3. Results with Basic Actuator - Speed Variation, Longitudinal Slip Variation and Long. Force Variation for a High μ Surface ($\mu = 0.8$), Time Constant = 350ms and Slip Target - 12% Front and 10% Rear

4.2.2 Straight Line Braking - Split μ Surfaces

In this section, the results have been presented for the basic brake actuator and controller for a scenario wherein the vehicle is moving on a road surface which has 2 different friction coefficients. The differences observed on left and right wheel ends would help in understanding if these conform to the reasoning mentioned above for a single wheel in the scenario of constant μ . Again, the results presented here represent three different the split- μ scenarios. Figure 4.4 shows for a scenario with split- $\mu = 0.5/0.8$; meaning, both left wheel ends (i.e. Front and Rear Left) are subjected to a friction coefficient of 0.5 whereas right wheel ends (i.e. Front and Rear Right) face a road surface with a friction coefficient of 0.8. The slip targets for the front and the rear wheels ends remain the same as before, i.e. 12% and 10% respectively.

The first plot in Figures 4.4.a and 4.6.a, shows the variation of slip and wheel speed over time of the front left wheel end. The front left wheel end which is on a lower friction surface (in both the scenarios), shows a comparatively higher amplitude of oscillations during the entire braking manoeuvre than the ones shown in the front right wheel ends. This difference between the left and right wheels can be understood again by considering the fact that for the same torque request (as in the Constant- μ case), the difference in the friction coefficients of the road surface contributes to different longitudinal force magnitudes at the two wheel ends. This can also be observed from the third subplots in Figures 4.4.a and 4.4.b, which represents the tire force interaction with the road.

The maximum longitudinal force in the split- μ scenario on the front right wheel end is around 25kN (observed in Fig. 4.4.b) whereas in the constant- μ scenario, the value of this is 20kN (observed in Fig. 4.3.b); both of which are on a high- μ surface. The difference in the values of longitudinal forces may be attributed to the fact that, in the split- μ case, during braking, the vehicle does not move exactly in a straight path. This can be observed from the Figure A.2 which shows the deviation of the vehicle from the straight ahead path. This means that a steer angle correction of 15° is applied to keep the vehicle on the straight ahead path and prevent it from losing control. This causes an additional lateral load transfer on the front right wheel end (on a high- μ surface) which is why we see the difference of almost 5kN in the values of F_x between the front right wheel end in the two cases (i.e. between constant- μ and split- μ). This path deviation can also be observed in the 0.3/0.8 split- μ case (observed in the Figure A.3 but the steer angle correction at the wheels in this case significantly small ($\approx 0.2^\circ$) which is significantly less and hence we do not see a huge change in the values of F_x when compared to the constant- μ case. This should also be analysed further by looking into the values of F_z .

Again, following Equation 4.1, this variation in the longitudinal forces causes a consequent variation in $\dot{\omega}$ and hence the wheel rotational speeds are affected. This, in turn, causes a subsequent variation in longitudinal slips in both the front right and front left. This difference can be observed from the second subplots in the Figures 4.4.a and 4.4.b.

The same can be observed when comparing the results of the rear left and rear right wheel ends (shown in Figures 4.4.c and 4.4.d). Again, the rear left takes a longer

time to recover and also shows a deeper spike when the first instance of high brake torque request is encountered. The deeper spike on the rear left can be attributed to the fact that in this case $\dot{\omega}$ is comparatively lower due to lower F_x than in the case of rear right wheel end. Thus frequency of oscillations is comparatively higher in the lower $-\mu$ wheel end.

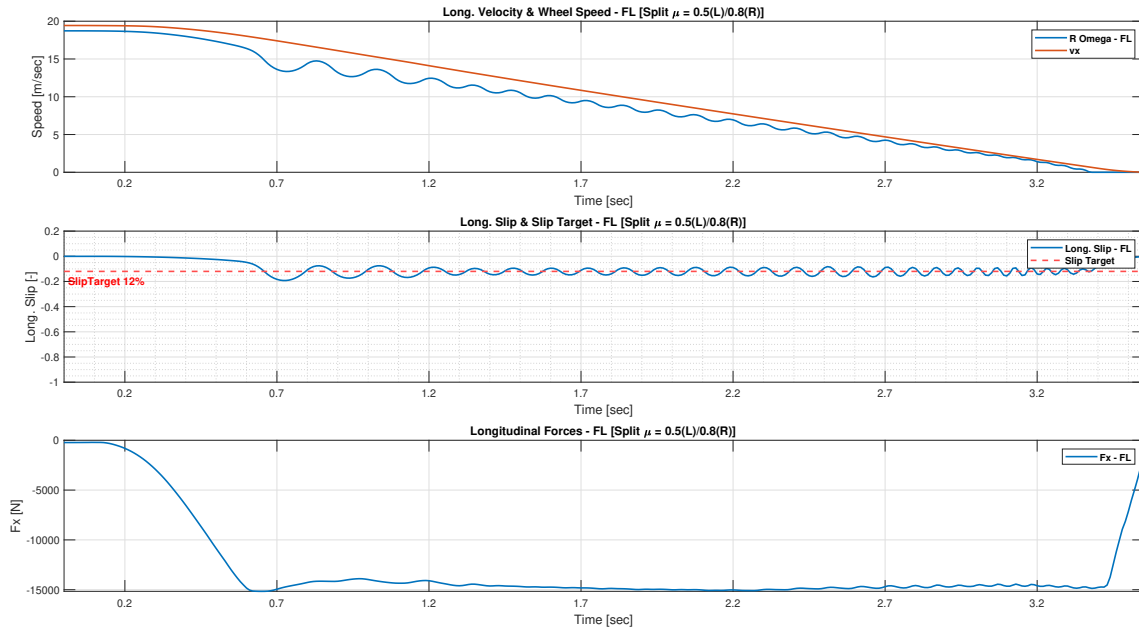
Also, the F_x for rear right wheel shown in Figure 4.4.d shows a peculiar behaviour wherein it becomes 0 after almost 1.4 seconds meaning that this wheel gets lifted from the ground. But this is not possible in the case of straight line braking and needs to be analysed further to reach a conclusion.

On observing the case shown in Figures 4.5.b and 4.6.b, it can be seen that even though the slip does not change from zero, a F_x of magnitude 10kN is applied at this wheel end. This seems to be a strange result suggesting that either slip control does not act on this wheel end or that there is a problem with the way the brakes are applied here. Again, this needs to be evaluated further.

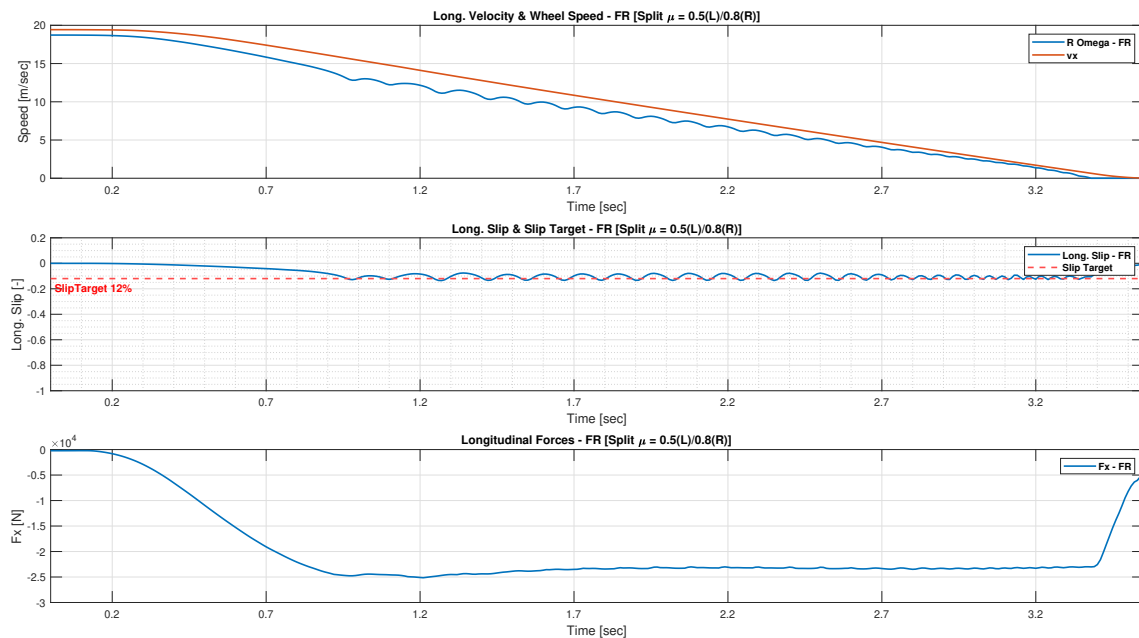
On comparing the results shown in Figures 4.6.a and 4.6.c with the ones shown in Figures 4.1.a and 4.1.c (both pertain to cases wherein these wheel ends are on low- μ surface), it can be observed that the value of F_x in the split- μ scenario is almost double that of F_x in the constant- μ case. Again, in the split- μ case, the vehicle deviates from a straight ahead path and a steering correction of approximately 5° - 7° has to be applied to keep it on the straight ahead path. Since the vehicle moves towards the high- μ , therefore there is a lateral load transfer on the left wheel ends. Hence, a higher value of F_x is observed.

On comparing the results of the front left wheel ends between the cases of Constant μ and Split μ for a surface with friction coefficient of 0.3 (depicted in the Figures 4.2.a) and 4.5.a, it can be observed that the wheel end in the constant μ case starts with a deeper slip and continues with a higher frequency of oscillations whereas, the split μ case goes through the braking manoeuvre with a lower amplitude and frequency of oscillations. From the third subplots in each of the wheel ends, it can be observed that magnitude of braking force remains the same in both the cases; which is expected in this case since both are subjected to the same friction coefficient. But since the right side is subjected to a higher friction coefficient surface, therefore higher friction is available in the longitudinal force-slip curve and hence the stopping distance is comparatively lower in the case of split- μ .

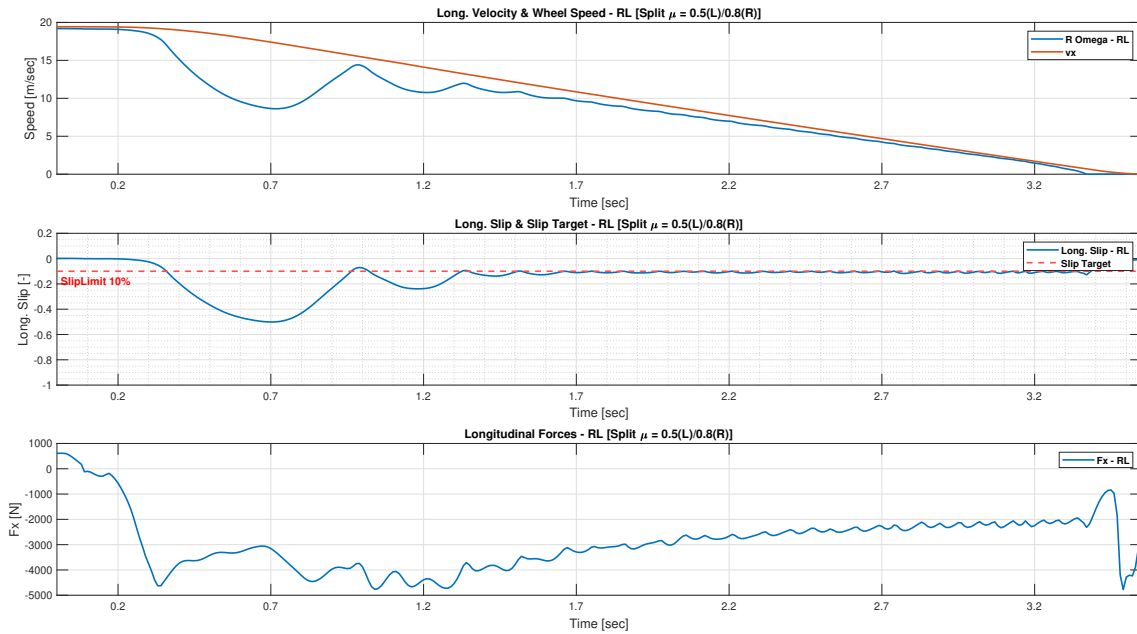
4. Results and Discussions



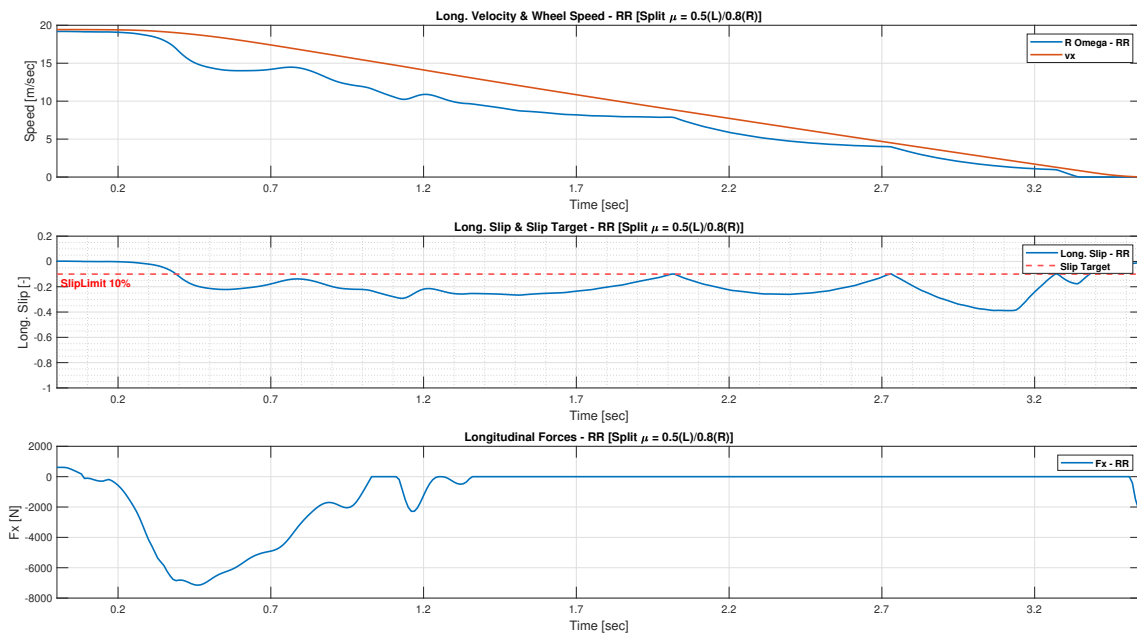
4.4.a. Front Left



4.4.b. Front Right



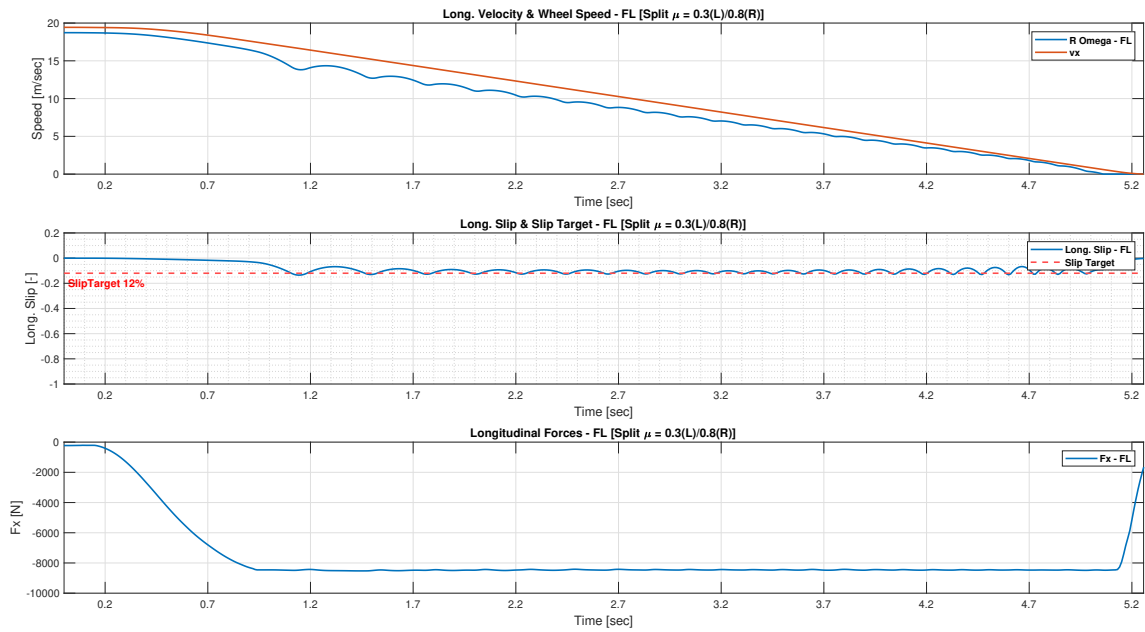
4.4.c. Rear Left



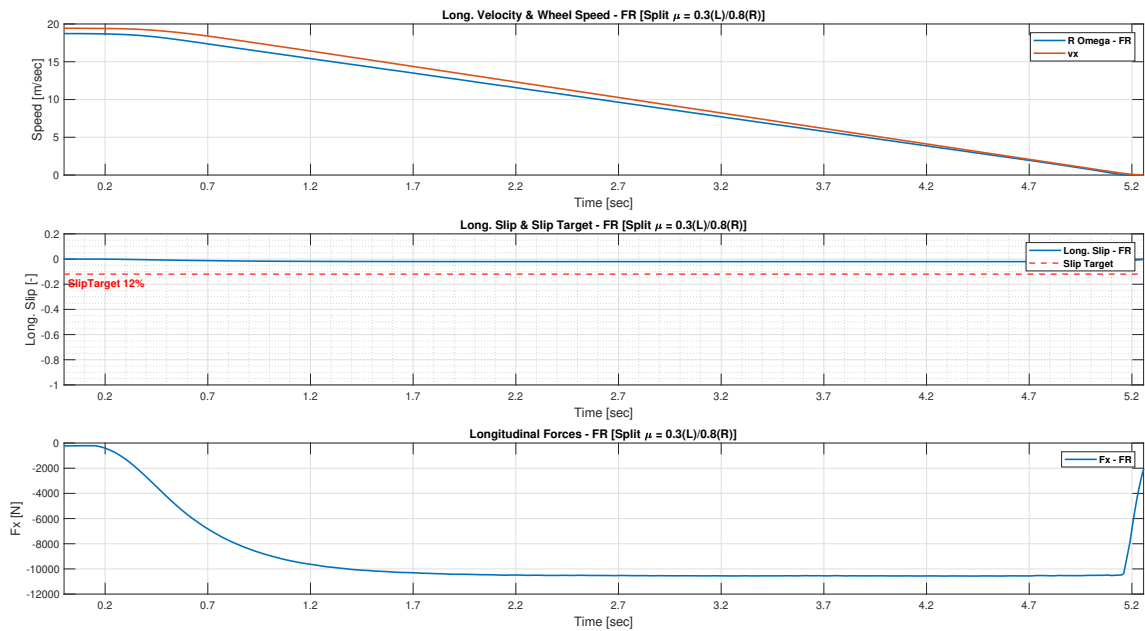
4.4.d. Rear Right

Figure 4.4. Results with Basic Actuator - Speed Variation, Long. Slip Variation and Long. Force Variation for a Split μ Surface ($\mu = 0.5(\text{Left})/0.8(\text{Right})$), Time Constant = 350ms and Slip Target of 12% Front and 10% Rear

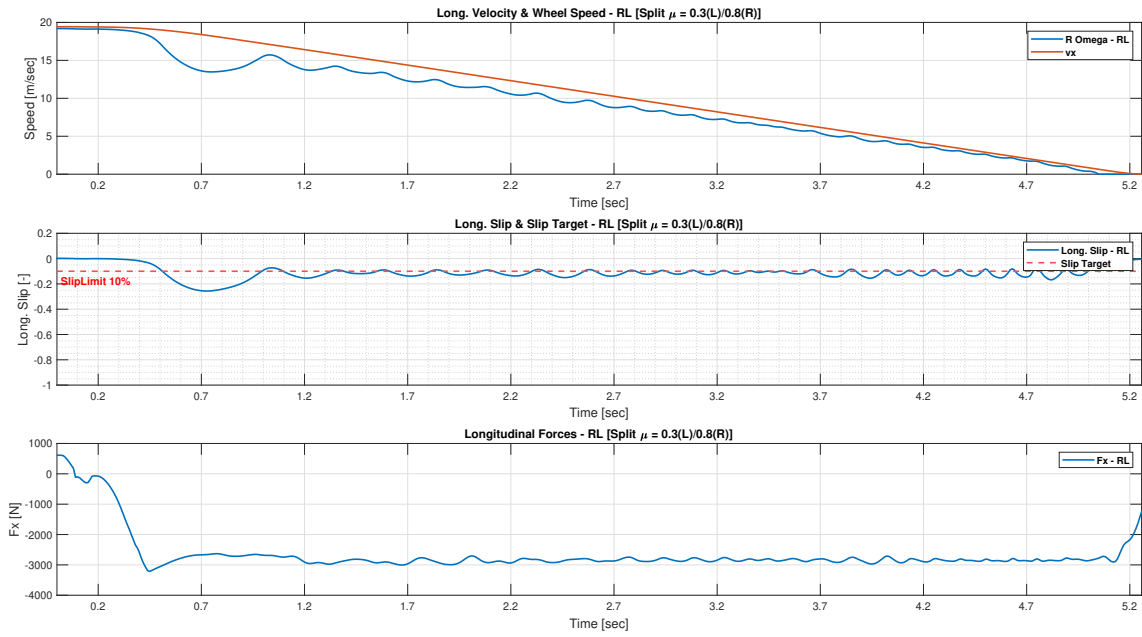
4. Results and Discussions



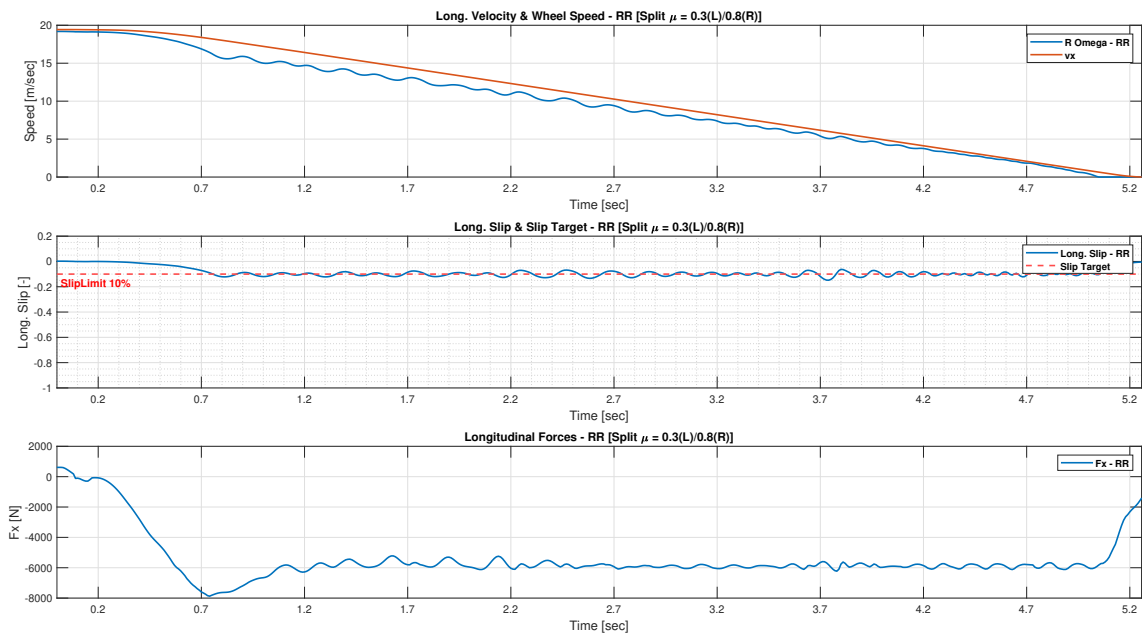
4.5.a. Front Left



4.5.b. Front Right



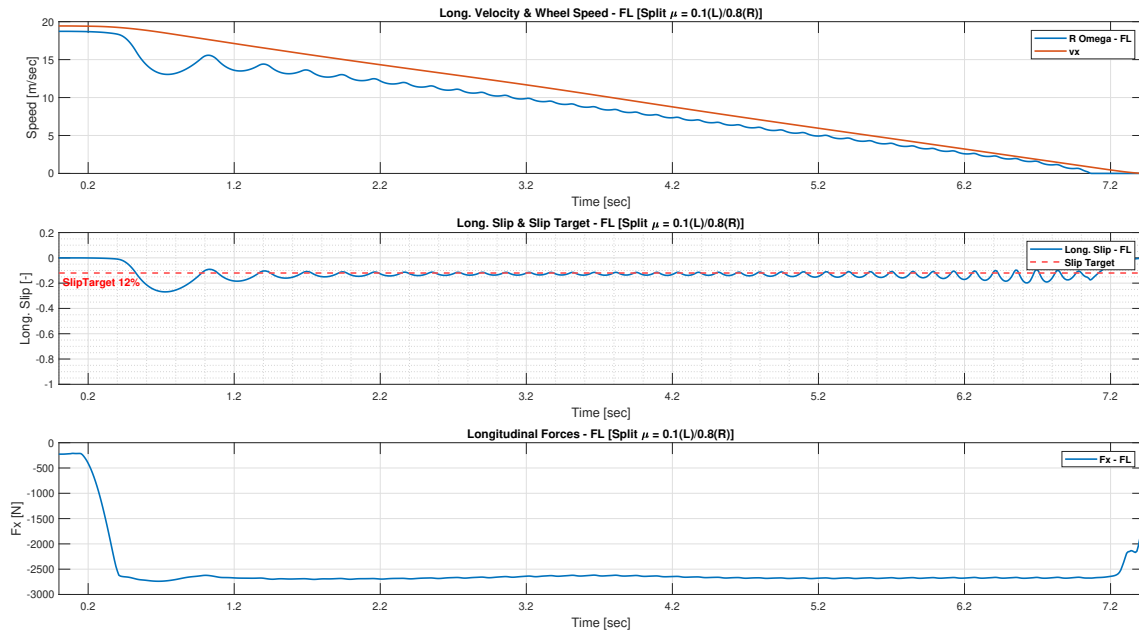
4.5.c. Rear Left



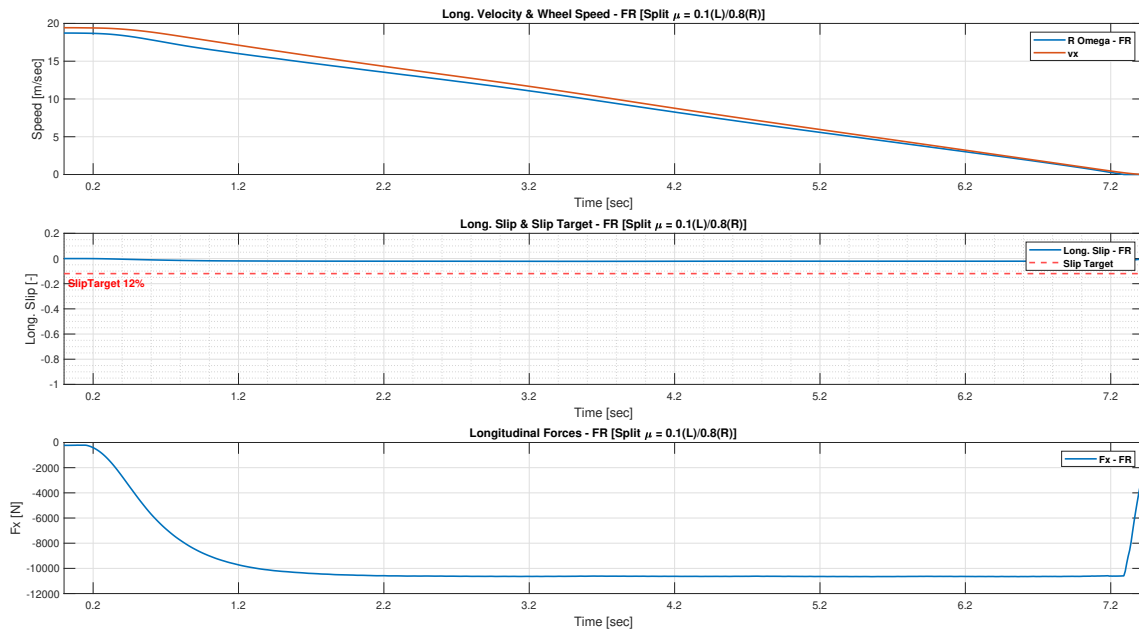
4.5.d. Rear Right

Figure 4.5. Results with Basic Actuator - Speed Variation, Long. Slip Variation and Long. Force Variation for a Split μ Surface ($\mu = 0.3(\text{Left})/0.8(\text{Right})$), Time Constant = 350ms and Slip Target of 12% Front and 10% Rear

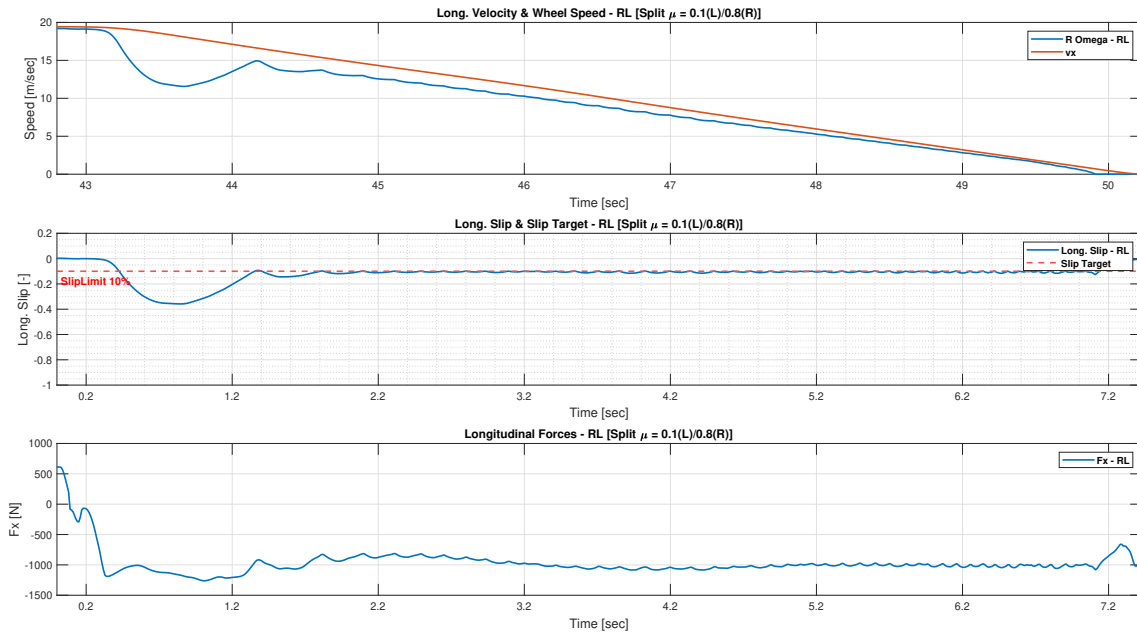
4. Results and Discussions



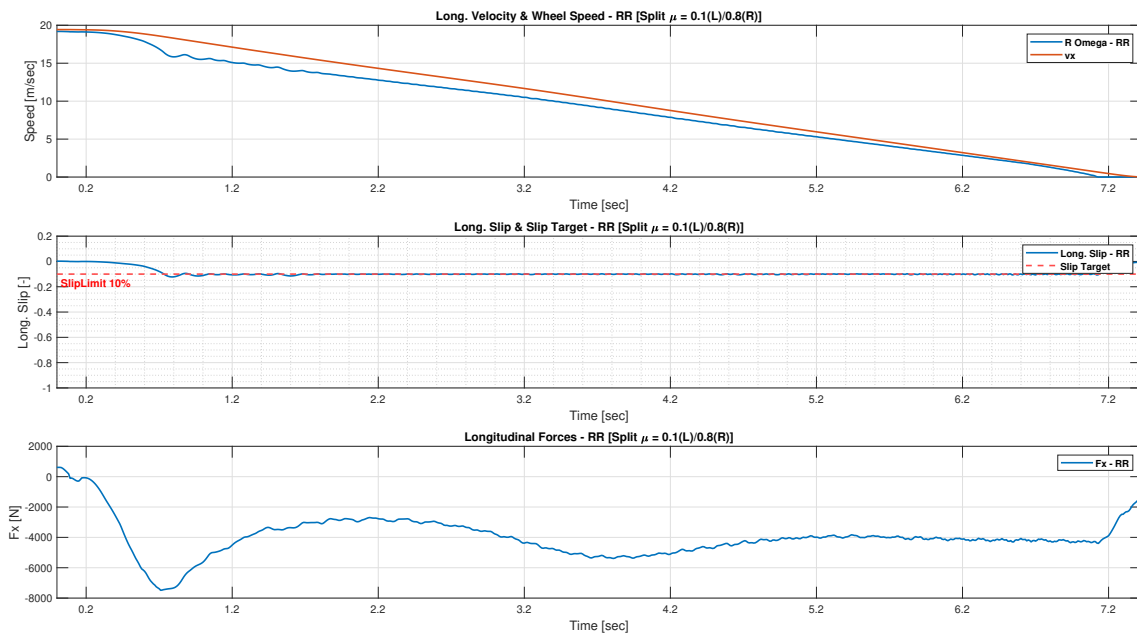
4.6.a. Front Left



4.6.b. Front Right



4.6.c. Rear Left



4.6.d. Rear Right

Figure 4.6. Results with Basic Actuator - Speed Variation, Long. Slip Variation and Long. Force Variation for a Split μ Surface ($\mu = 0.1(\text{Left})/0.8(\text{Right})$), Time Constant = 350ms and Slip Target of 12% Front and 10% Rear

4.3 Results with Advanced Actuator-Controller

The following section describes the results for the scenario when the simulation setup includes the advanced actuator-controller instead of the basic actuator-controller. The two setups have already been outlined in Sections 3.5 and 3.6 under the chapter Methodology. In this section, the results for all four wheels-ends have been included so as to understand the basic differences in the way the vehicle reacts to the components of the advanced actuator being used in the 4 wheel ends.

The results in this section is divided into two subsections. The first subsection, namely 'Results with the FMU', contains results for the case when the simulations are carried out with the advanced actuator packed in a FMU. The second subsection, namely 'Results with Actual Models', shows results for the case when the simulations are carried out with the actual reference models of the advanced actuator.

4.3.1 Results with FMU

As stated earlier, the FMU here contains four different components i.e. slip controller, force observer, pressure controller and the valve plant hardware. The main difference between the advanced actuator and the basic actuator is the presence of force observer, pressure controller and the valve plant within the FMU which makes the dynamics more complex but allows a much better tracking and control of the braking performance. Therefore, if these three components are replaced with a time constant within the FMU, it would represent an ideal controller (or a Basic Actuator in this case).

The results shown below pertain to a simulation setup with the advanced actuator-controller FMU included at each wheel end of the complete vehicle which is being tested on road surfaces with different coefficients of friction. The FMU wraps the model of the advanced actuator which includes the slip controller, force observer, pressure controller and the advanced valve plant. Again, the slip targets are described in the simulations as a constant input to the FMU. For this case, the values is set to 12% and 10% on the front and the rear wheel-ends respectively. These slip targets are shown in the plots for slip with a dashed line (in 'red'). The vehicle accelerates to a maximum speed of 70 km/h before applying a brake pedal wherein the pedal is engaged from 0 (no engagement) to 1 (full engagement) within 0.2 seconds which generates a brake pressure demand of approximately 8.5 bar.

It should also be noted that there are 4 different gain values that influences the response of the FMU to the given input variables. [16]

1. ' k ': important for stabilizing the loop.
2. ' δ ': important for determining the smoothness of the sliding mode torque request.
3. ' ϕ ': helps in providing higher torque at higher slip errors.
4. ' b ': makes the controller more robust but increases the air consumption.

From the plot of the front wheel end (as shown in Figure 4.7.a and 4.7.b), it becomes quite apparent that the current setup with the FMU integrated in the loop, the results seem to be plausible until the vehicle reaches a low speed point. The initial

two-thirds of the manoeuvre i.e. between 0 and 3 seconds, the plots indicate that for the vehicle undergoing braking from a vehicle speed of 70 kph, the wheel speed is lower than the vehicle longitudinal speed which theoretically amounts to a negative longitudinal slip; which is also indicated in the plot for longitudinal slip just below it. The oscillations in the longitudinal slip curve seem to be averaged near the target of 12% with certain acceptable deviations. Even the force observer shows relatively low variation in oscillations during this period. The next one-third of the manoeuvre, i.e. between 3 seconds and 4 seconds, is where there is a considerable increase in the amount of oscillations which are visible both in the wheel speed-vehicle speed plots as well as plots representing the longitudinal slip and the slip target (in Figures 4.7.a and 4.9.a).

In this part of the manoeuvre, the wheel speed can be seen going much higher than vehicle speed curve indicating that the delays in longitudinal tyre forces generated increase to an extent and stays in the positive direction for a long time. The high amplitude oscillations can also be seen in the slip curves due to which the slip moves on to positive side of the curve. This can be attributed to the fact that the slip target set has not been appropriately tracked. This can also be observed in the third subplot in Figure 4.7.a which compares the F_x generated between the tire and the road in TruckMaker (Referred to as ' F_x from TruckMaker' (curve in 'Red') or the 'Real F_x ') which is the actual F_x and the F_x estimated by the Force Observer within FMU (referred to as ' F_x from Observer' (curve in 'Blue')). The variation in the subplot of F_x shows that observer is able to estimate the required F_x close to the 'Real F_x ' from TruckMaker until the point where the vehicle reaches the low speed manoeuvre part wherein the force observer's estimation gets deviated from the actual F_x from TruckMaker setup. This can be attributed to the numerical oscillations being generated by the FMU.

If observed closely for the subplot showing the results from the force observer, for e.g., in the Figure 4.7, it can be observed that variation of F_x should be similar to the variation of the longitudinal slip (shown in the curve exactly above the curves for F_x). Certain cases with the current setup do not show a match between the two. The reason for this may be attributed to the fact that the tire model being used in TruckMaker is transient due to which additional dynamics get involved and hence F_x 's variation does not match exactly with that of s_x 's. But this transient nature of the tire model in TruckMaker needs to be investigated further to come to a conclusion about this.

The third subplot in each of the figures shown in this section shows the variation of longitudinal force F_x at the tire contact patch. If one of the cases, for e.g. the high- μ case, is considered (represented by Figure 4.7), and if F_x of either of the front wheel ends are compared with corresponding F_x of the rear wheel ends, it can be observed that F_x of the front is one-tenth of the F_x of the rear. As mentioned earlier, this might be a bit concerning specifically for the high- μ case since the front axle load is 2.5 times the rear (this can be observed from vehicle parameters in Table 4.1). Therefore, the F_x results for the high- μ case needs to be looked into further.

Assuming this to be the case, the difference can be explained by the fact that F_x is

dependent on the normal load F_z . It is known that the value of parameter D in the magic formula controls the peak of the braking force which, in turn, is dependent on the value of friction coefficient μ_x and the normal load F_z ; given by the relation $D_x = \mu_x F_z$. It should be noted that μ_x also depends on the value of F_z . Other curve-fit parameters used in the Magic Formula, such as B_x , E_x and D_x are also dependent on F_z . It is also known that during braking on a high- μ surface, there is a considerable amount of load transfer; meaning that $F_{z,rear} \ll F_{z,front}$. For a high- μ case, this can be observed from the Figure A.5. In the plot, it can be observed that $F_{z,front} \approx 30kN$ whereas $F_{z,rear} \approx 3kN$. This means that the magnitude of load transfer between the front and the rear is approximately one-tenth. If the linear range of the tire is considered, it can be said that this correlation between the front and the rear normal loads leads to similar correlation between the braking force values between the front and the rear.

The same line of reasoning can be applied to justify the difference in the values of F_x between the front and the rear wheels ends in every friction scenario for both the basic and advanced actuator simulation cases.

The braking distance results achieved with the FMU have been noted in Table 4.3.

Longitudinal Speed	Friction	Braking Distance
v_x [kph]	μ [-]	[m]
70	0.8	37.96
70	0.3	111.20
70	0.1	373.56
70	0.5/0.8	48.42
70	0.3/0.8	61.98
70	0.1/0.8	89.86

Table 4.3: Braking Distance Results with Advanced Actuator FMU

From Table 4.3, it can be observed that even though the advanced actuator is much more sophisticated than the basic actuator, it produces comparatively higher braking distances than the basic actuator with the current setup. The difference in braking distances between the two, with the current setups, can be attributed to two reasons:

- Higher braking distance implies that the deceleration is lower; meaning lower F_x . This lower value of F_x can be either due to inadequate slip tracking or due to the fact that the slip tracking is good but the slip target set is far from the peak slip value. This means that the braking distance also depends on the performance of the slip controller along with its dependence on the value of F_x .
- Higher oscillations towards the low speed end of the braking manoeuvre also contributes to some extent for the lower braking distances. But this needs to be evaluated further.

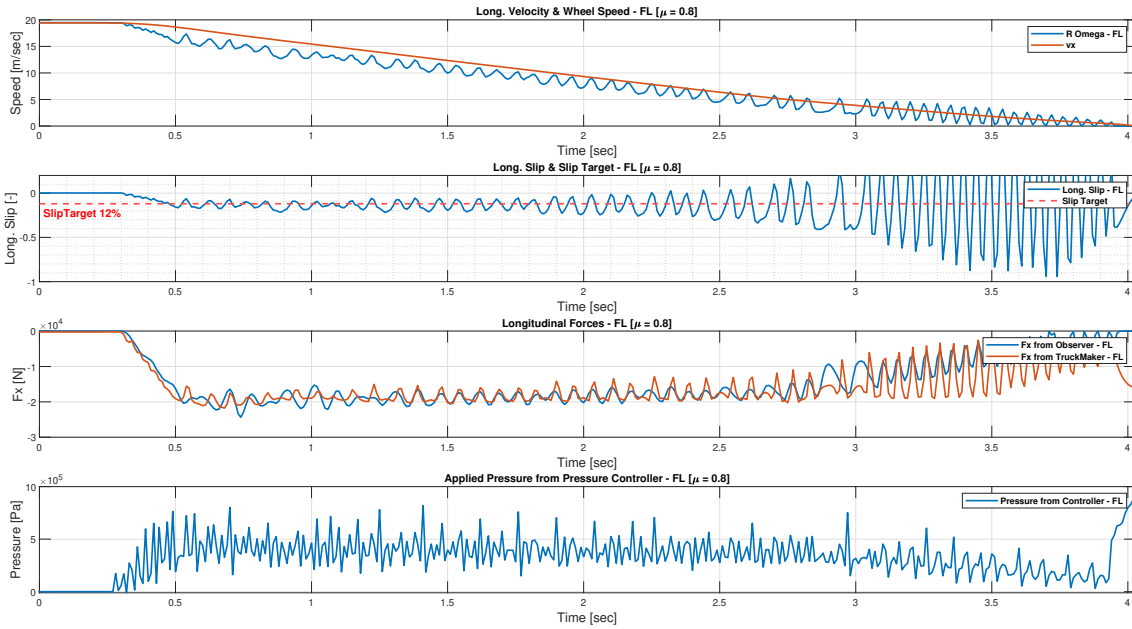
4.3.2 Results with Actual Reference Models

Figures 4.10, 4.11 and 4.12 represent the scenario when the same vehicle model setup is co-simulated with actual brake reference models in Simulink instead of the FMU. This is done so as to compare the results obtained from the FMU and the actual control reference models. When comparing 4.10.a and 4.7.a, it can be observed that the behaviours are significantly different in the low speed part of the manoeuvre. The high frequency oscillations observed in the case of results with the FMU in the low speed end of the manoeuvre (shown in Fig. 4.7.a), are absent in the case of actual reference models which may be pointing to the fact that there might be comparatively less disturbances induced within the force observer for it to estimate the values of longitudinal force that are close to the 'Real F_x ' obtained from TruckMaker. Therefore, there are less oscillations observed in the slip variation plot (i.e. the second subplot in each wheel end) which shows that the signals coming out from the actual reference model's controller contain less disturbances as compared to the signals from the FMU. From this we can conclude that at the low speed part of the braking manoeuvre, there were some numerical disturbances or noises induced in the case of the simulation with the FMU in the loop when compared to the actual models since everything else remained the same in terms of test scenarios, vehicle model, tire model, etc. Thus, these numerical oscillations in the case of the FMU are a result of co-simulation of the FMU with TruckMaker models.

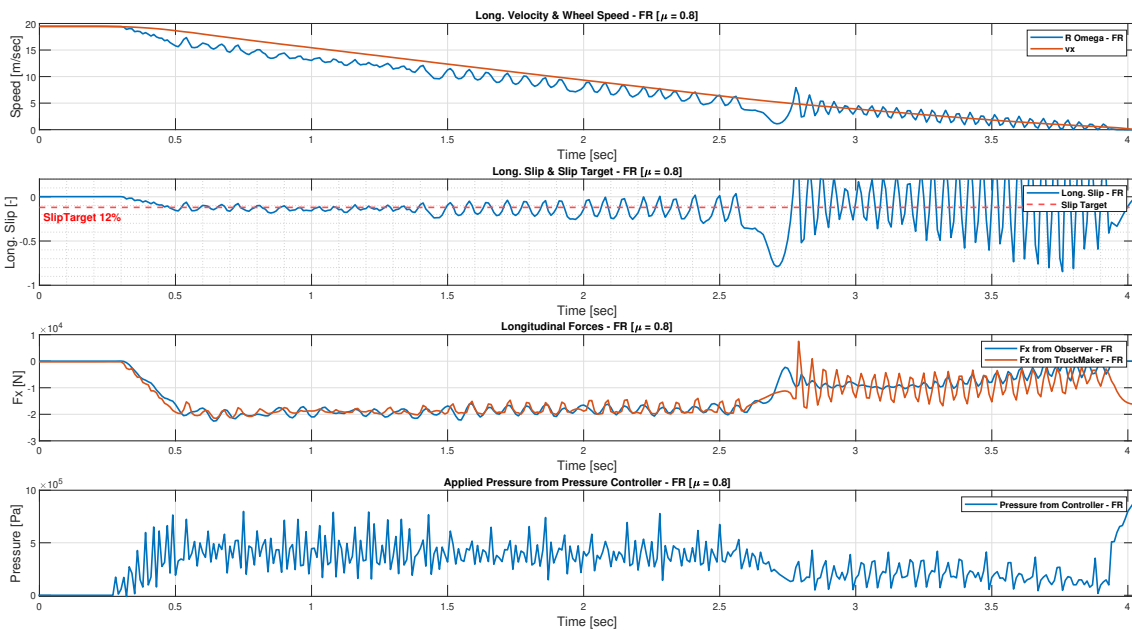
It should be noted that the brake distances were not available for the actual reference models, at present, to make a comparison with the braking distances achieved with the FMU.

The sharp spikes in the results for F_x observed within the subplot in Figure 4.11 is something that needs to be analysed more in order to understand the variation.

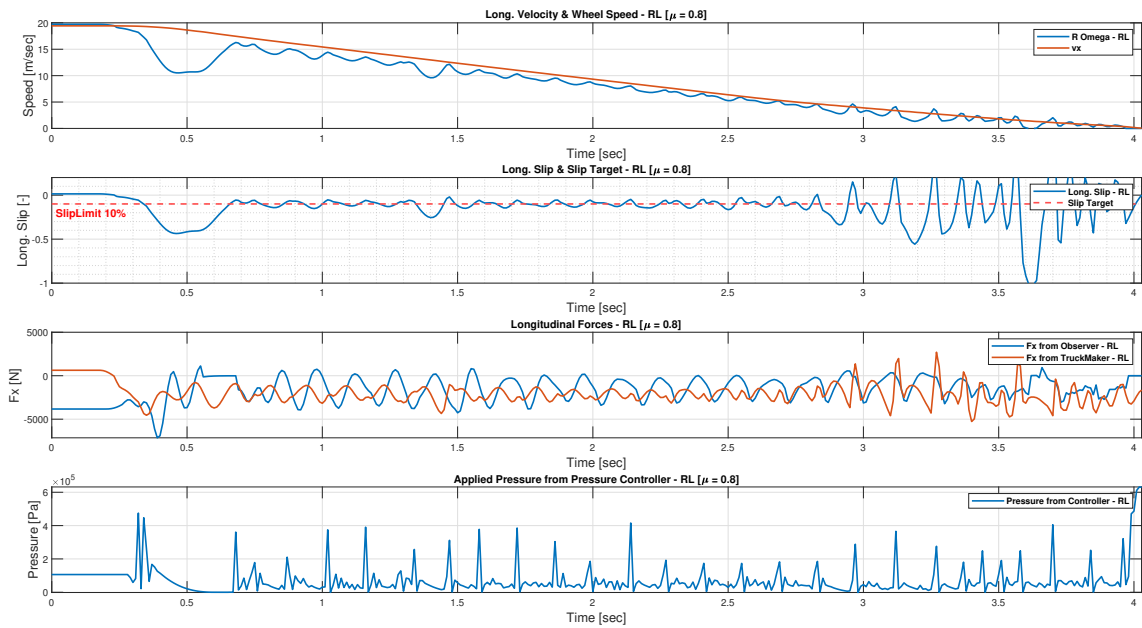
4. Results and Discussions



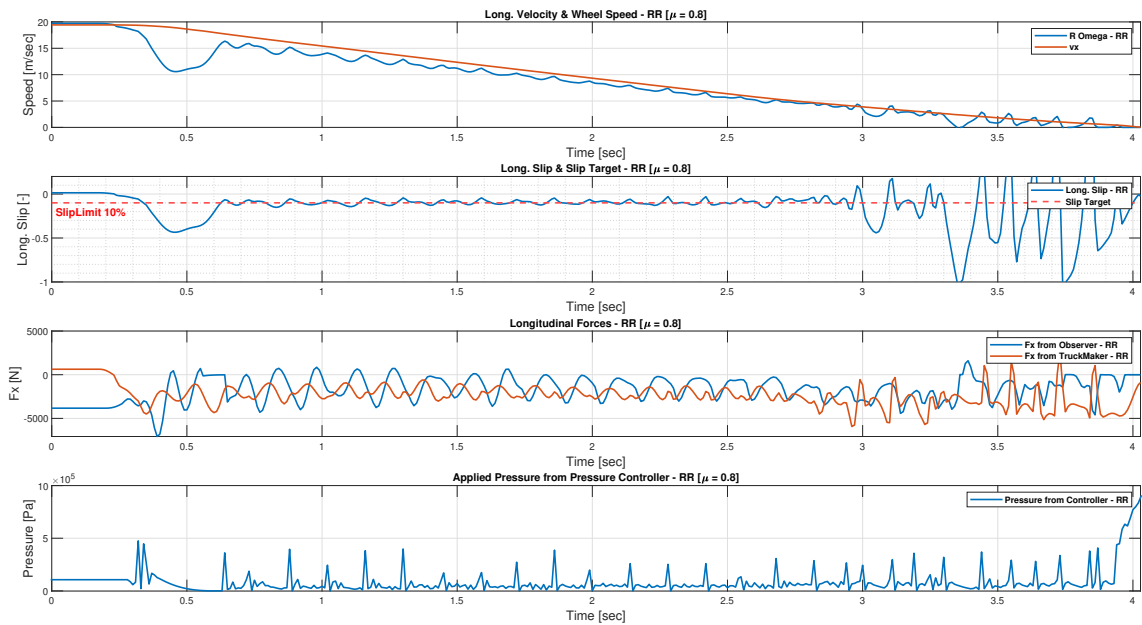
4.7.a. Front Left



4.7.b. Front Right



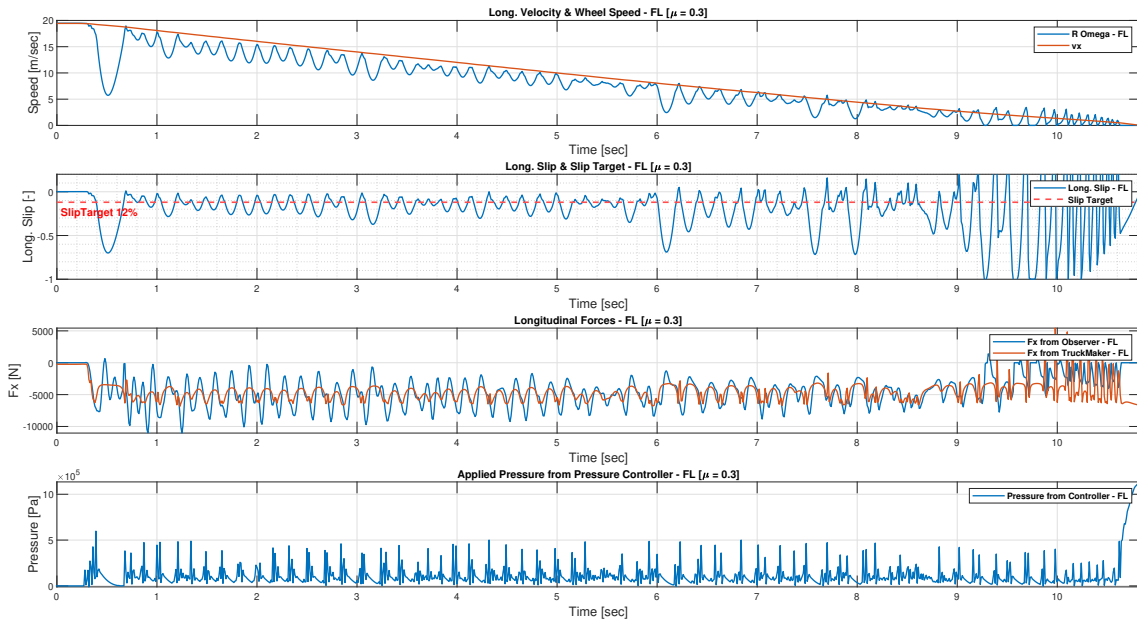
4.7.c. Rear Left



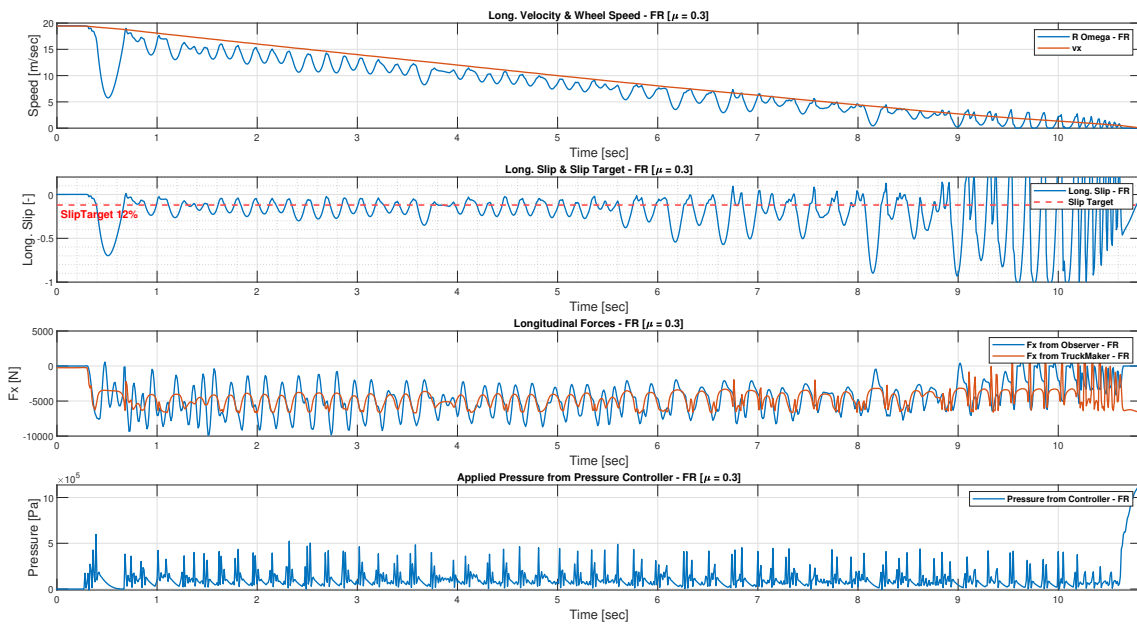
4.7.d. Rear Right

Figure 4.7. Results with Advanced Actuator (FMU) - Speed Variation, Long. Slip Variation and Long. Force Variation for a High μ Surface ($\mu = 0.8$), Slip Target - 12% Front and 10% Rear with the FMU

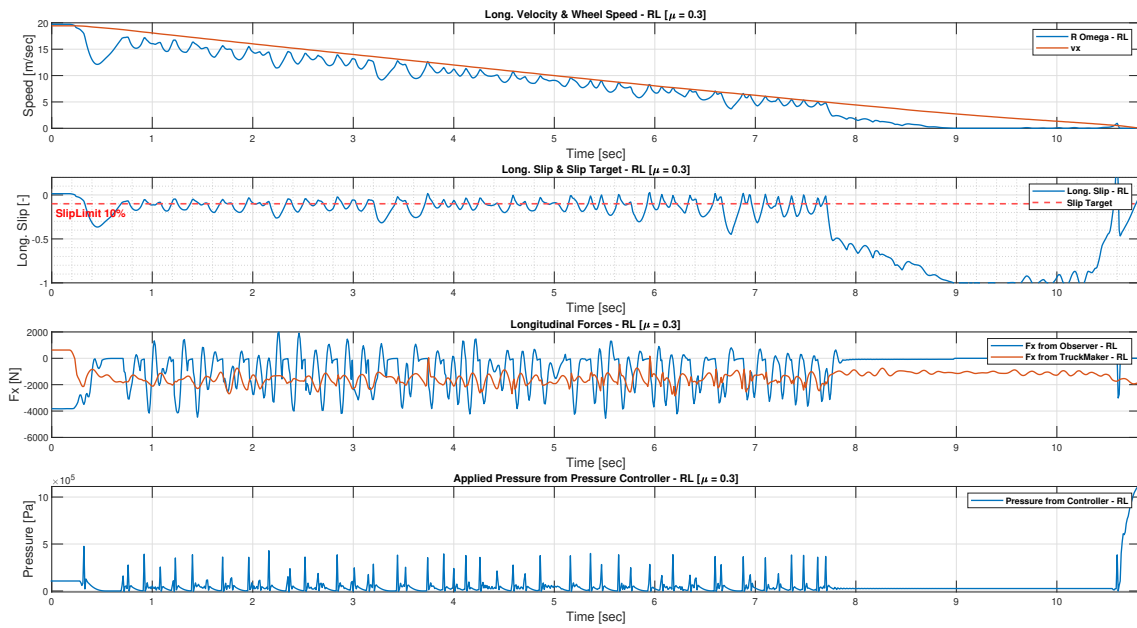
4. Results and Discussions



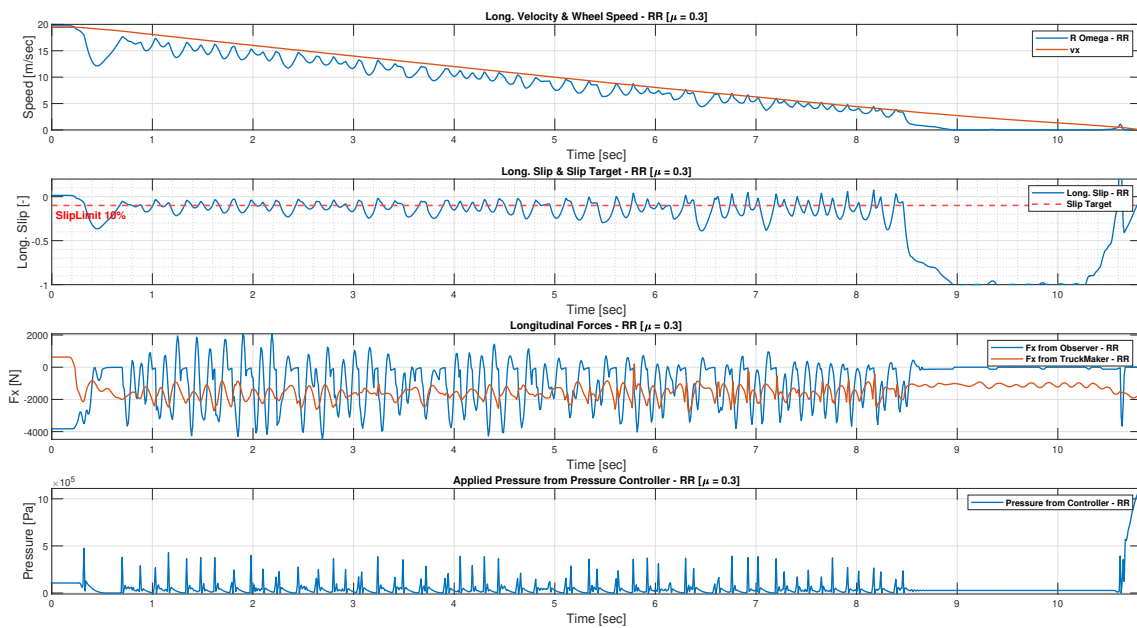
4.8.a. Front Left



4.8.b. Front Right



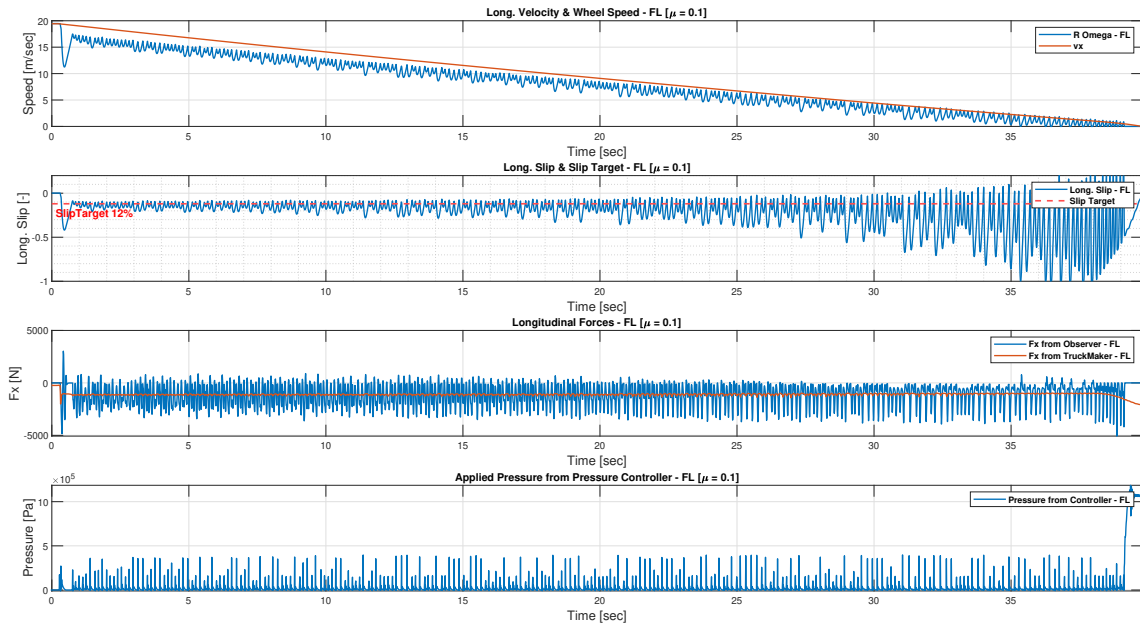
4.8.c. Rear Left



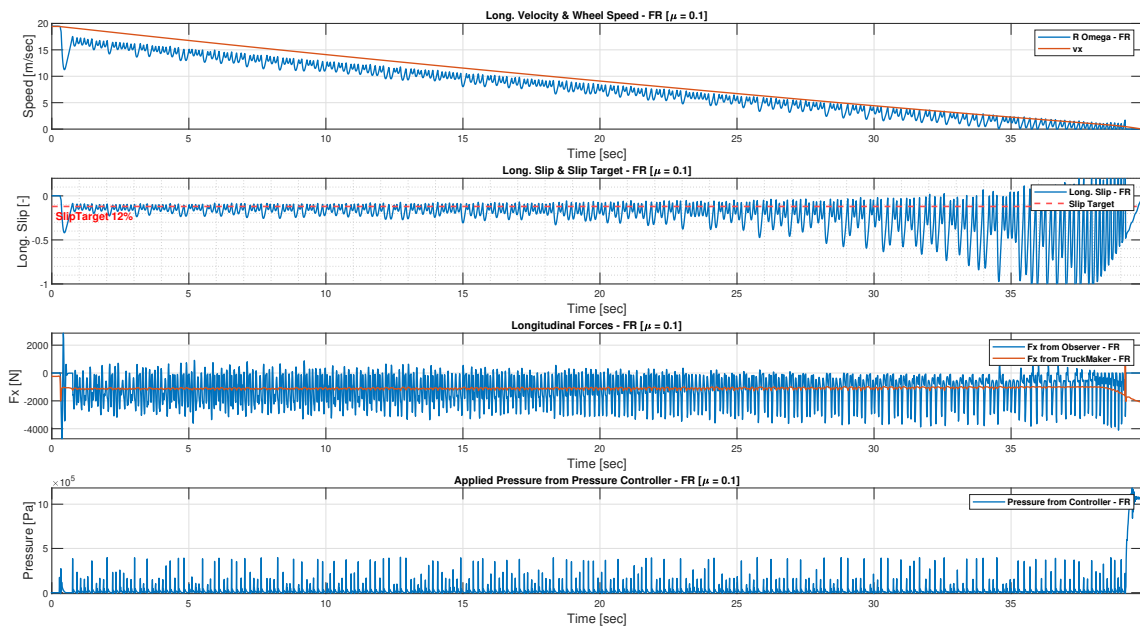
4.8.d. Rear Right

Figure 4.8. Results with Advanced Actuator (FMU) - Speed Variation, Long Slip Variation and Long. Force Variation for a Mid μ Surface ($\mu = 0.3$), Slip Target - 12% Front and 10% Rear

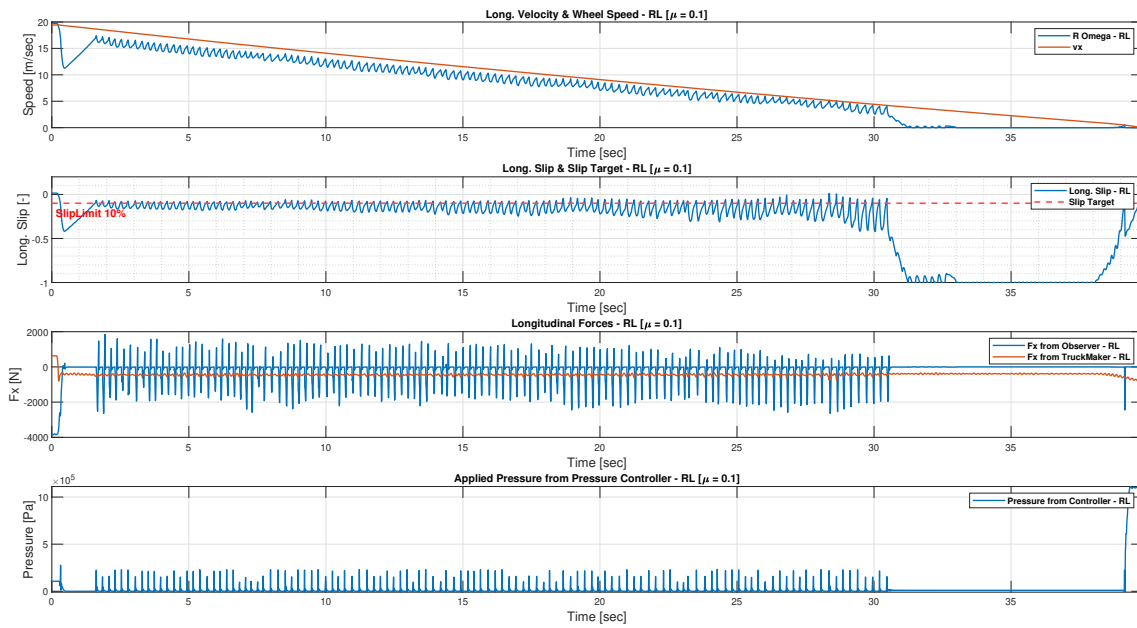
4. Results and Discussions



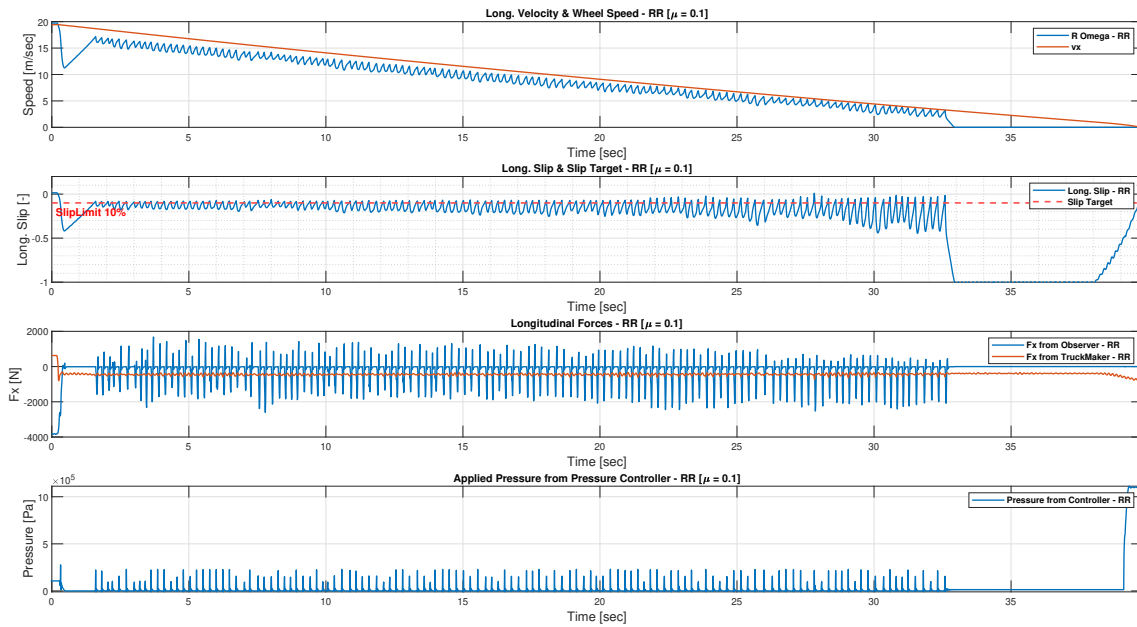
4.9.a. Front Left



4.9.b. Front Right



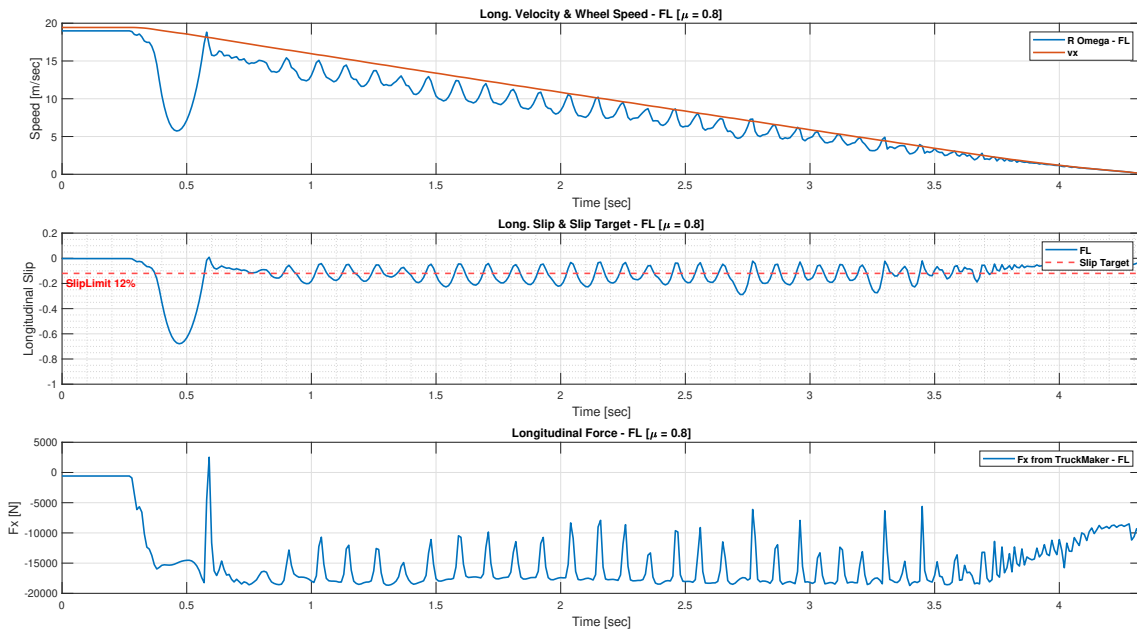
4.9.c. Rear Left



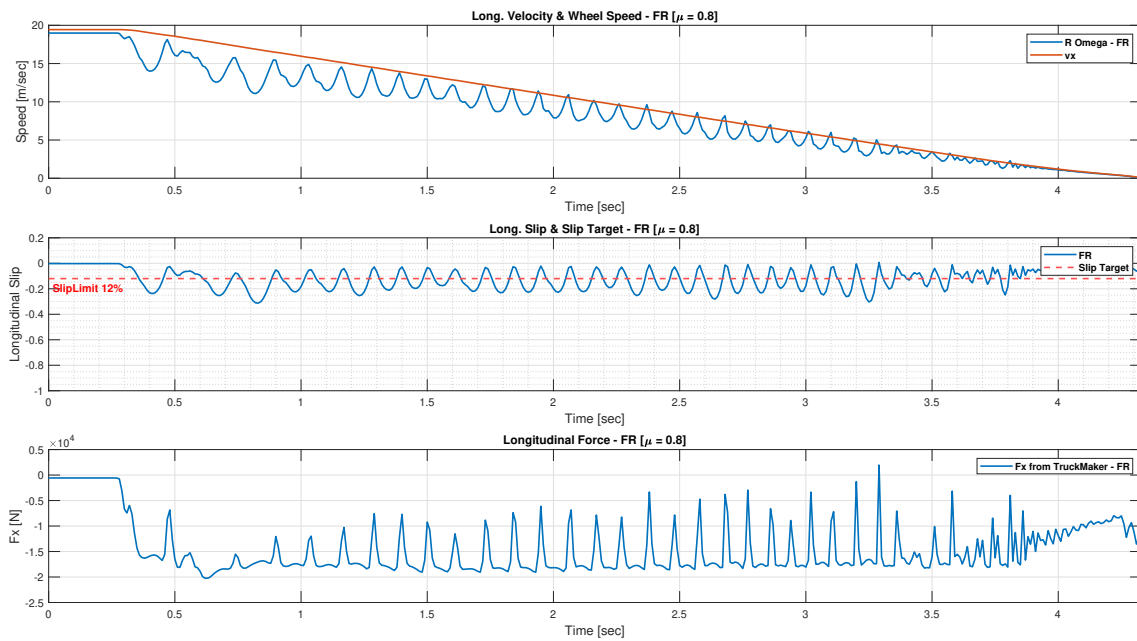
4.9.d. Rear Right

Figure 4.9. Results with Advanced Actuator (FMU) - Speed Variation, Long. Slip Variation and Long. Force Variation for a Low μ Surface ($\mu = 0.1$), Slip Target - 12% Front and 10% Rear with the FMU

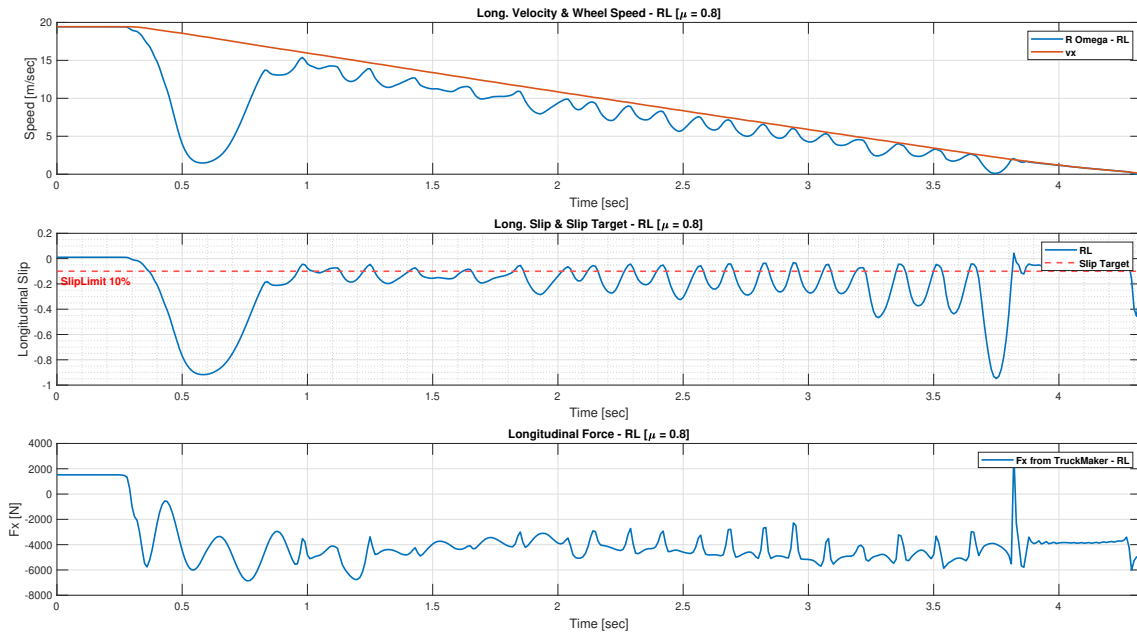
4. Results and Discussions



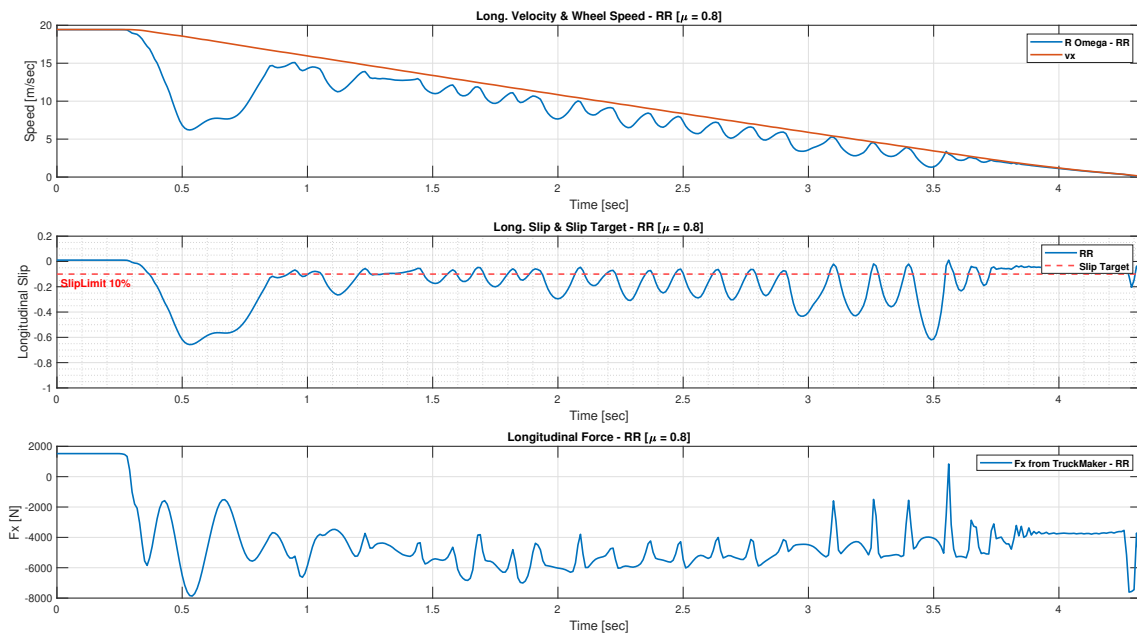
4.10.a. Front Left



4.10.b. Front Right



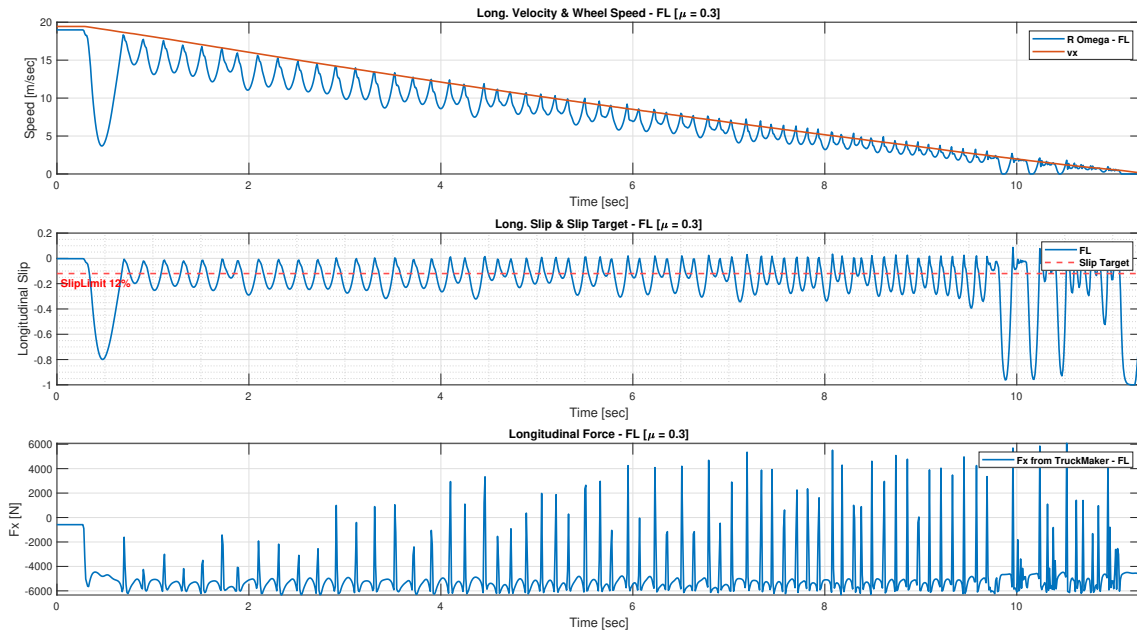
4.10.c. Rear Left



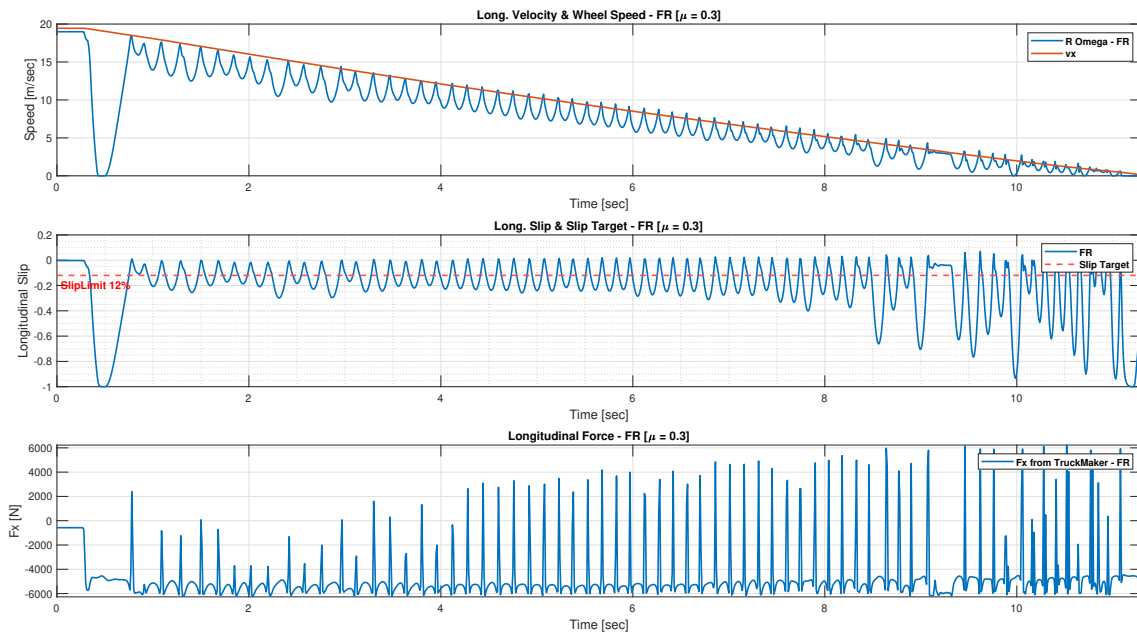
4.10.d. Rear Right

Figure 4.10. Results with Actual Models - Speed Variation, Long. Slip Variation and Long. Force Variation for a High μ Surface ($\mu = 0.8$), Slip Target - 12% Front and 10% Rear with Actual Models

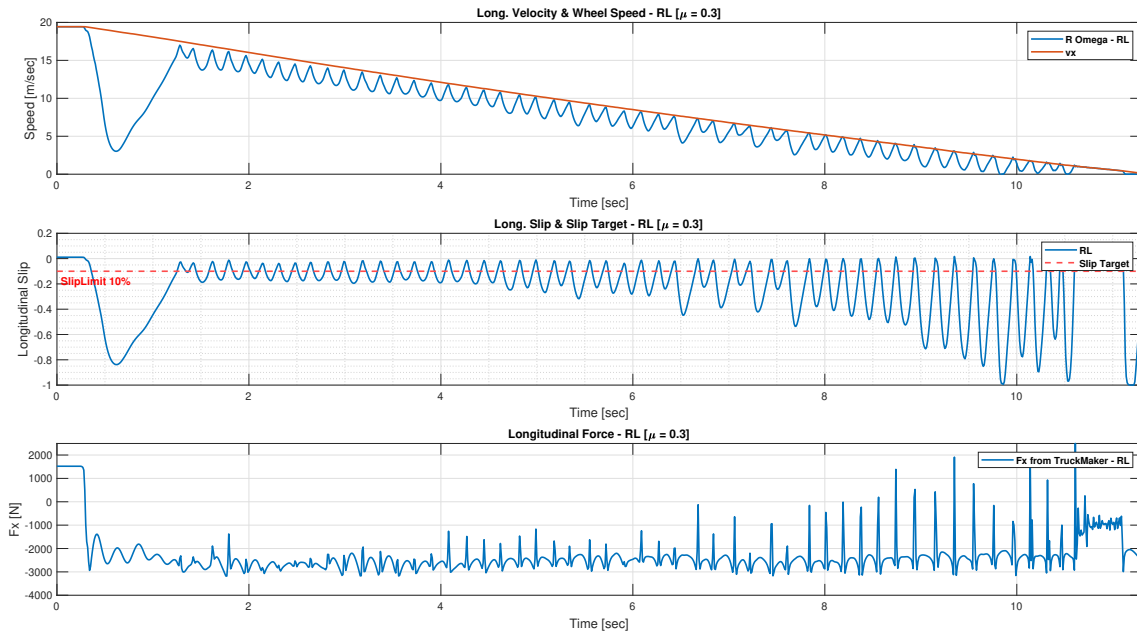
4. Results and Discussions



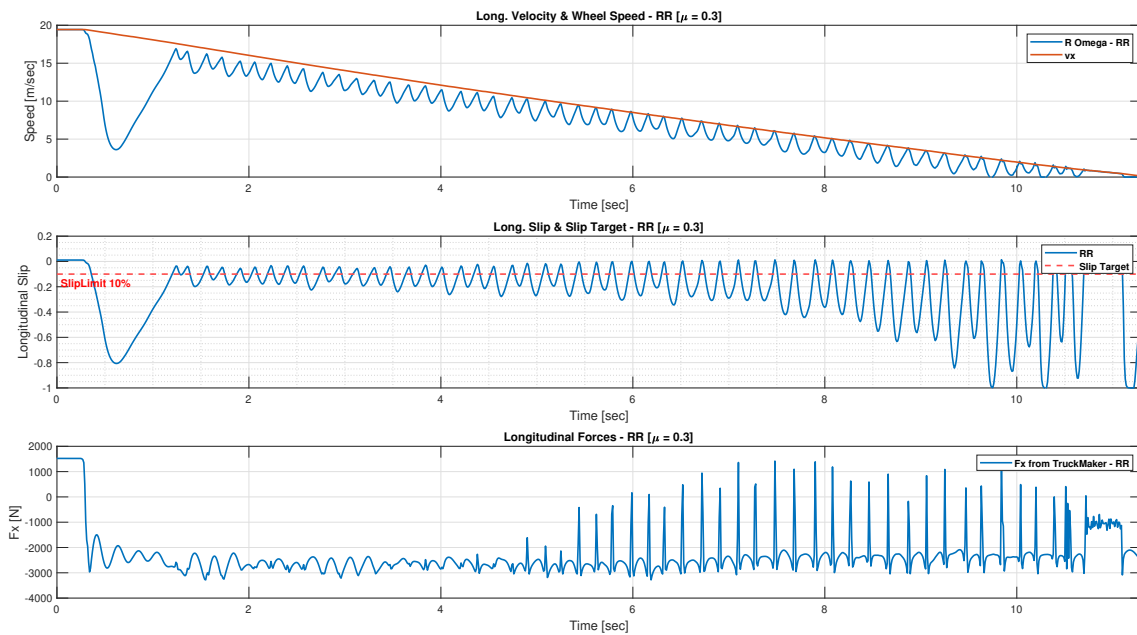
4.11.a. Front Left



4.11.b. Front Right



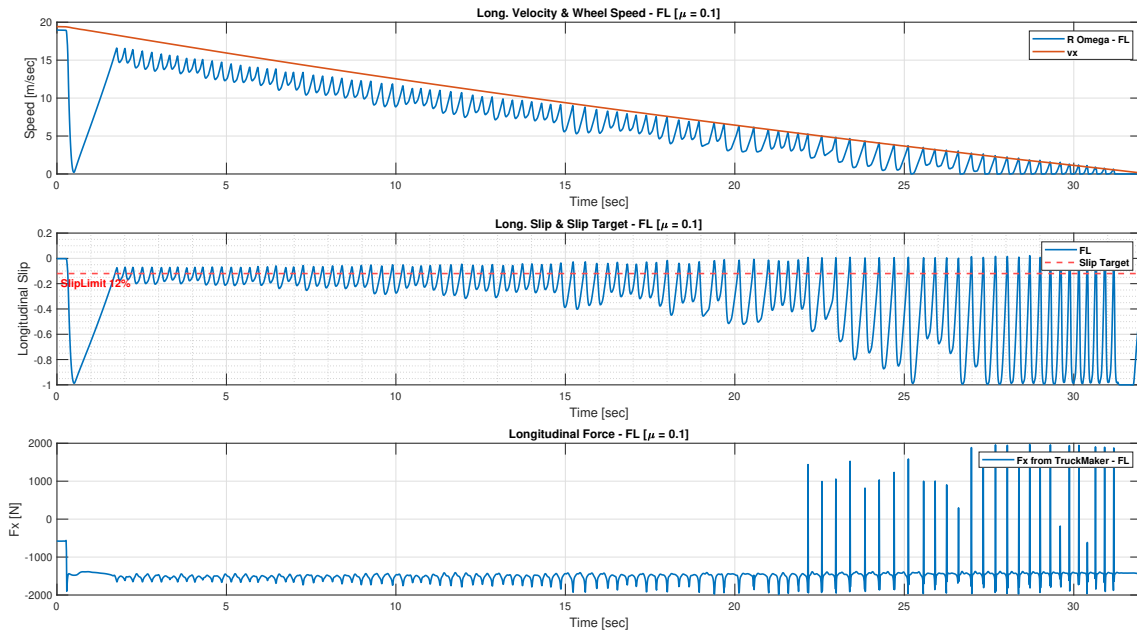
4.11.c. Rear Left



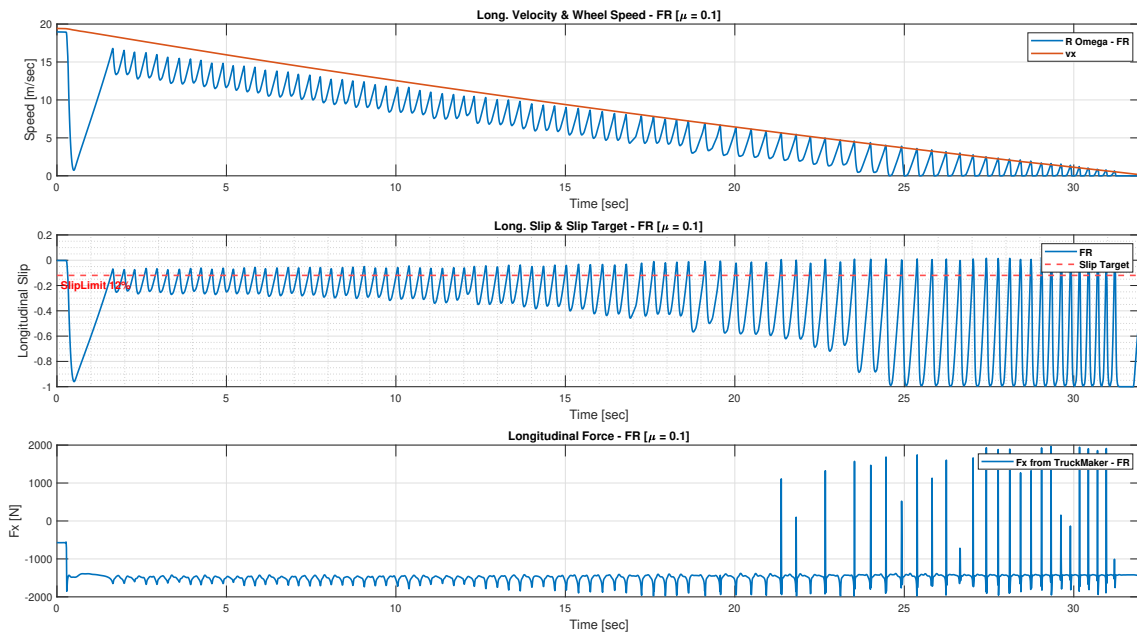
4.11.d. Rear Right

Figure 4.11. Results with Actual Models - Speed Variation, Long. Slip Variation and Long. Force Variation for a Mid μ Surface ($\mu = 0.3$), Slip Target - 12% Front and 10% Rear with Actual Models

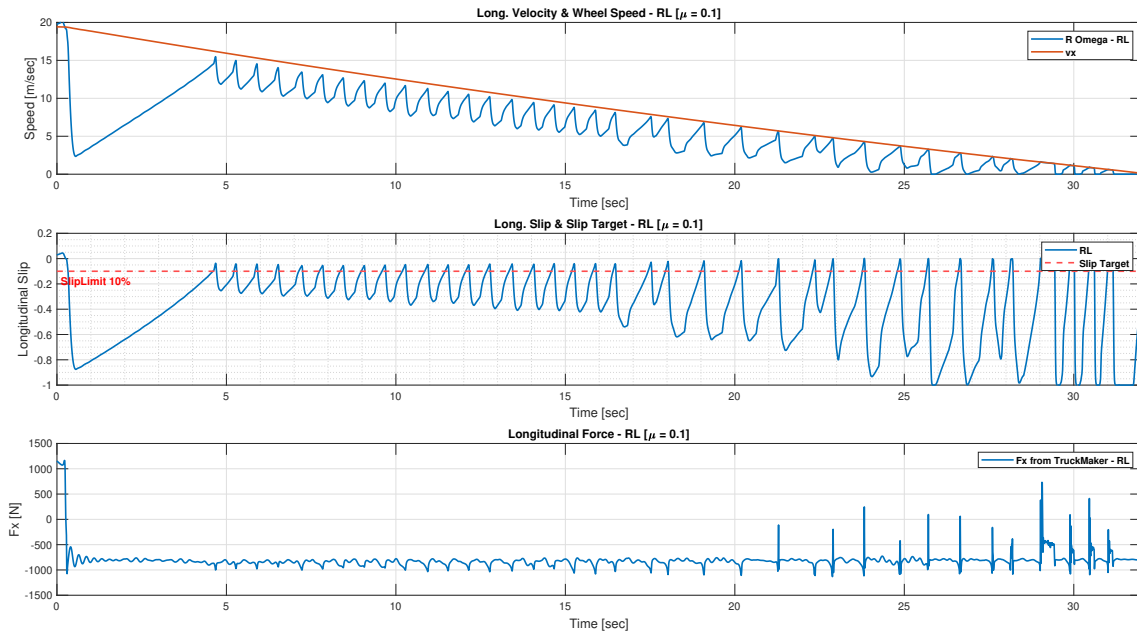
4. Results and Discussions



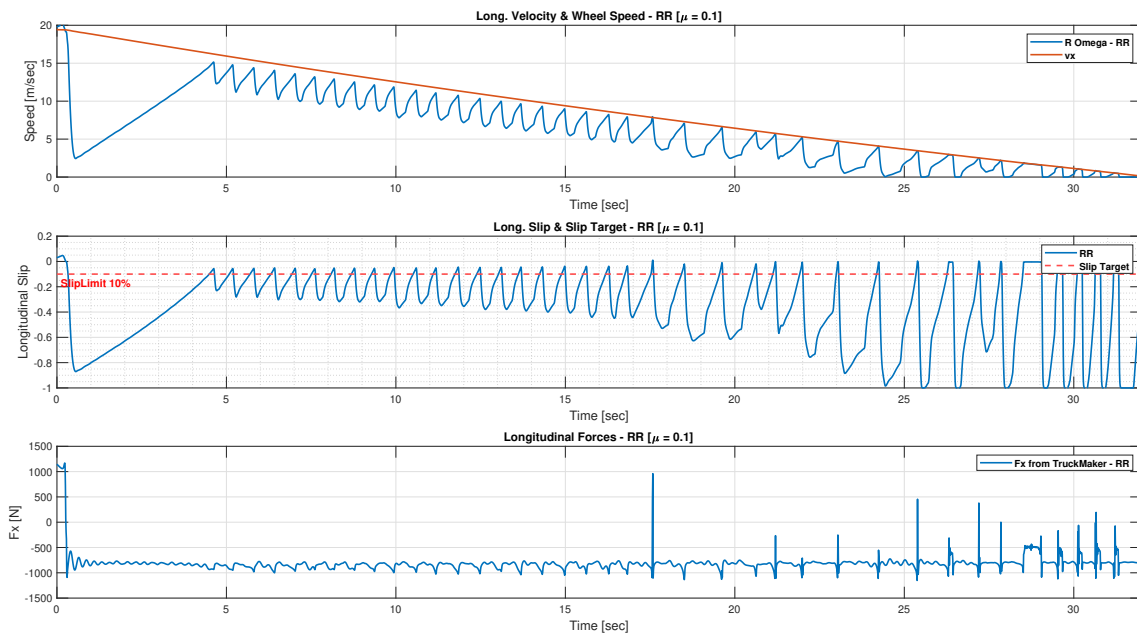
4.12.a. Front Left



4.12.b. Front Right



4.12.c. Rear Left



4.12.d. Rear Right

Figure 4.12. Results with Actual Models - Speed Variation, Long. Slip Variation and Long. Force Variation for a Low μ Surface ($\mu = 0.1$), Slip Target - 12% Front and 10% Rear with Actual Models

5

Conclusion

As the aim of the thesis suggests, a method has been developed for the development of brake control system for heavy vehicles. The main take from this thesis are as follows

- With the completion of this thesis, most of the deliverables have been achieved. A reference truck model has been developed equipped with both basic and advanced actuation system. One manoeuvre with different conditions have also been defined for the simulation.
- As mentioned in the deliverables, results from both basic and advanced actuation systems were obtained and analyzed.
- Tools and methods have been formulated for the development of control systems for brake systems. This method can be used for further development of brake control systems by implementing different braking systems on the trucks and also on the trailer.
- There were no pre-existing Simulink example models for neither basic nor advanced brake controllers for trailers. This was realized after initial simulations were performed with the trailer attached. Importing the brake control models on the trailer brakes was not feasible within this project.
- The basic actuator model provides good results in terms of braking distances but it should be noted here, that there have been assumptions made such as, in the simulations here, brake torque request signal is ideal and does not contain any disturbances. This ideal signal is then used to obtain clamping force. The braking distance values obtained from Basic Actuator for a high μ case may be considered comparable to the one obtained experimentally in [7]. Other assumptions may be stated with respect to knowing the velocity when vehicle is under deep slip during braking. Also, in reality, there might also be disturbances in the wheel speed signal that might make the signal have less resolution.
- The results obtained from the advanced actuator models shows that further development of the simulation with the FMU is required. Specifically issues with the oscillations need to be resolved. The results deviate from reality but that may be due to the fact that the torque provided as input may not be good enough for close tracking of F_x generated by TruckMaker by the force observer.
- It should also be noted here, in order to carry out a realistic comparison between the braking distances obtained in the basic and advanced actuators, the systems being compared should be equal and robust. Also, the Basic Actuator is shown to work here as an ideal actuator i.e. the actuator here has

5. Conclusion

infinite bandwidth and that the value of time constant being used has a small effect.

These are the conclusions we can make after completing this thesis. This thesis provided a great opportunity for diving deeper into the brake system of heavy vehicles and how it affects the braking distances of a heavy vehicle.

6

Future Work

There are provisions for the future work as a result of this Master thesis project

- The implementations of basic actuation system and advanced actuation system in the trailers would help to make make it more realistic. Also, addition of payload to both trailer and truck would give more realistic results.
- Further develop the implementation of the FMU in the simulation model to resolve issues with oscillations and slip values remove the high amplitude oscillation and also the negative slip values thereby generating better results for the same.
- More types of manoeuvres like braking in a curved road along with the trailer attached can be added to the development of the method.
- Results from different braking systems can be compared and analysis can be done for the scope of improvement of the brake systems.

Bibliography

- [1] Jacobson et al, Vehicle Dynamics Compendium, Chalmers University of Technology, 2018, <https://research.chalmers.se/publication/505928>,
- [2] MSc Thesis Proposal in Vehicle Dynamics: Virtual Verification of Complete Vehicle Requirements for Heavy Vehicles for the Development of Brake Systems, Chalmers University of Technology, 2019.
- [3] Ledeneva, Yulia and García Hernández, René Arnulfo & Gelbukh, Alexander. (2008). Automatic Estimation of Parameters of Complex Fuzzy Control Systems. 10.5772/6268.
- [4] Nada Scientific, Air Brake System Trainer for Trucks with ABS/ASR on wall panel. https://nadascientific.com/automotive_education/air-braking-system-for-trucks-with-abs-asr-stand-with-wheels.html
- [5] Prof. Dr.-Ing. Konrad Reif et al, Automotive Handbook, Sept 2014, fig. 15, pp no. 949.
- [6] Miller, J., Henderson,L. & Cebon, D. Designing and Testing an Advanced Pneumatic Braking System for Heavy Vehicles. *Proceedings of IMechE Part C: J Mechanical Engineering Science 2013*
- [7] Henderson, L. & Cebon, D. Full scale testing of a novel slip control braking system for heavy vehicles. *Proceedings of IMechE Part D: J Automobile Engineering 2015*
- [8] Miller, J. & Cebon, D. Modelling and performance of a pneumatic brake actuator. *Proceedings of IMechE Part C: J Mechanical Engineering Science 2011*
- [9] Henderson,L., Cebon, D., & Laine, L. Brake System Design for Future Heavy Goods Vehicles.*HVTT14*
- [10] Henderson, L. Improving Emergency Braking Performance of Heavy Goods Vehicles. Ph.D, Cambridge University Department of Engineering, 2013.
- [11] Miller, J. Advanced Braking System for Heavy Vehicles. Ph.D, Cambridge University Department of Engineering, 2010.
- [12] Fox, J., Roberts, R., Baier-Welt, C., Ho, L. et al., Modeling and Control of a Single Motor Electronic Wedge Brake. SAE Technical Paper 2007-01-0866, 2007

- [13] <https://paultan.org/2007/03/15/siemens-electronic-wedge-brake-ewb/>
- [14] Basselink, I.J.M; An improved Magic Formula/Swift tyre model that can handle inflation pressure changes
- [15] Kienhöfer, F.W., Cebon, D. An Investigation of ABS Strategies for Articulated Vehicles. Cambridge University, Engineering Department *Proceedings of 8th International Symposium on Heavy Vehicles Weights and Dimensions*
- [16] Marzbanrad, A., Bruzelius, F., Jacobson, B., Drenth, E. Enhanced Sliding Mode Wheel Slip Controller For Heavy Goods Vehicles.
- [17] <https://fmi-standard.org/>
- [18] Automatic Estimation of Parameters of Complex Fuzzy Control Systems - Scientific Figure on ResearchGate.
- [19] https://en.wikipedia.org/wiki/Time_constant
- [20] IPG TruckMaker Reference Manual
- [21] Prof. Dr.-Ing. Konrad Reif et al, Automotive Handbook, Sept 2014,pp no. 974.
- [22] IPG TruckMaker Reference Manual
- [23] <https://www.favcars.com/volvo-fh-540-4x2-2012-wallpapers-155023.htm>

A

Appendix

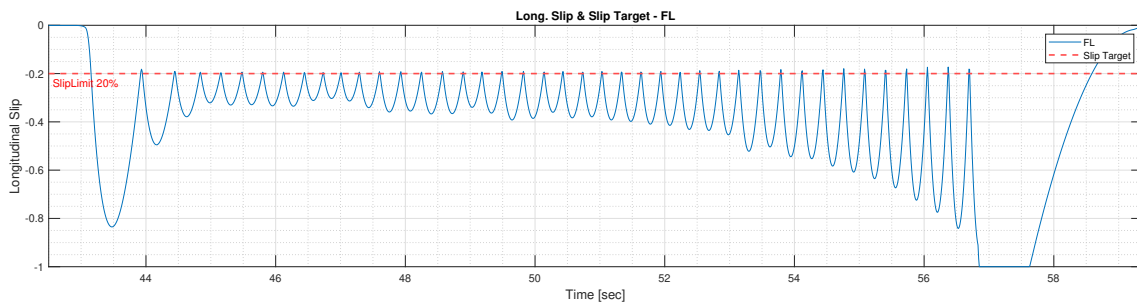
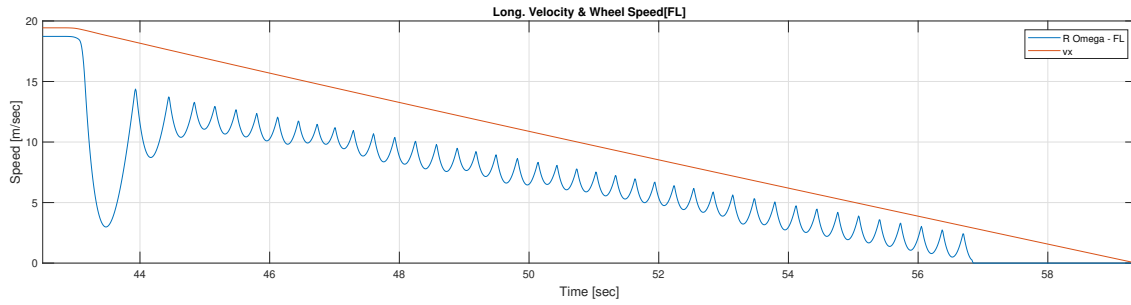
This chapter contains additional simulation results performed with the Basic Actuator and Advanced Actuator. But here, the results are plotted with a different time constant than the one described in the subsection 4.2.1.

A.1 Results with Basic Actuator

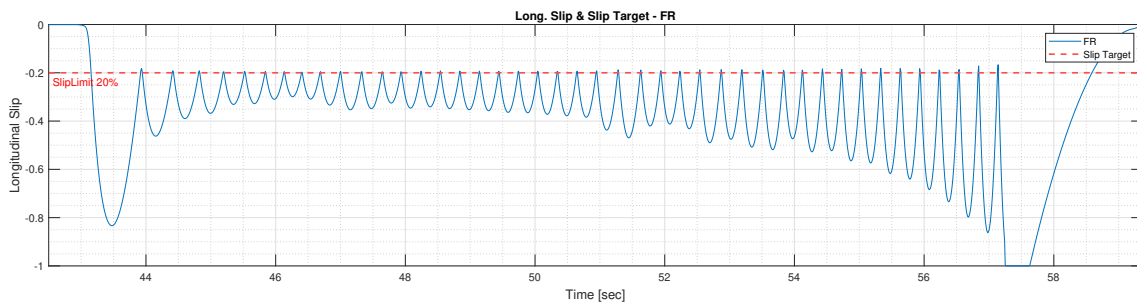
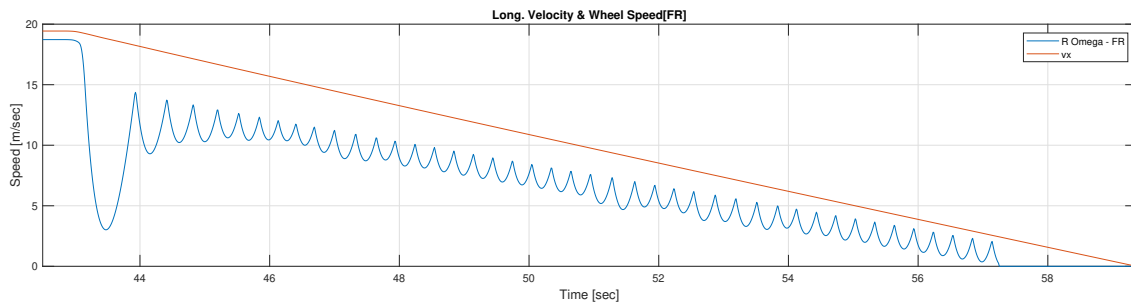
A.1.1 Straight Line Braking - Constant μ Surface

All the simulation parameters remain the same as described in Section 4.2.1. The only change is with respect to the time constant being used here. Here, a reduced time constant is used during the simulations and then compared with the results obtained with a time constant of 350ms for a friction surface of 0.1.

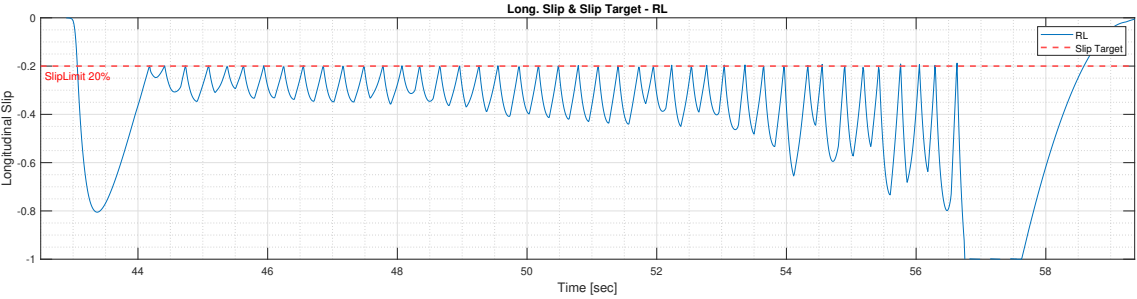
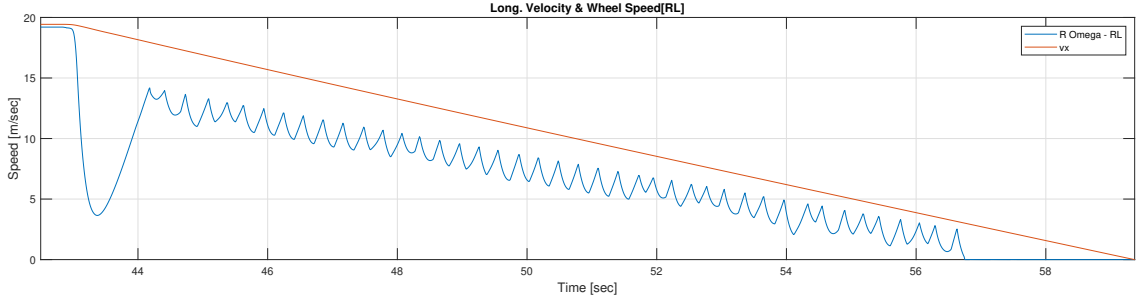
A. Appendix



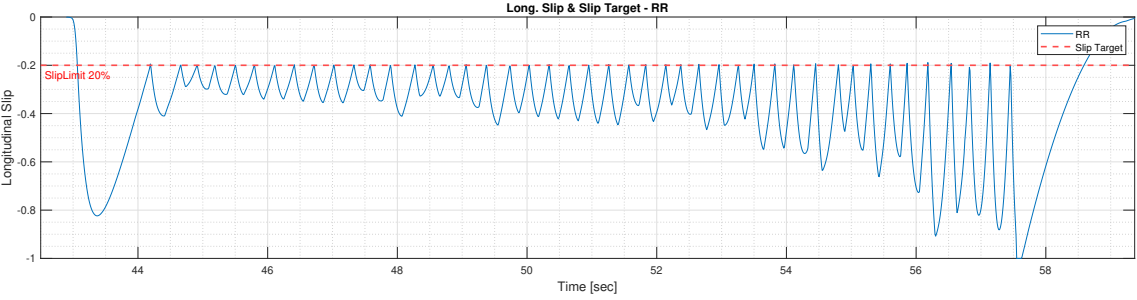
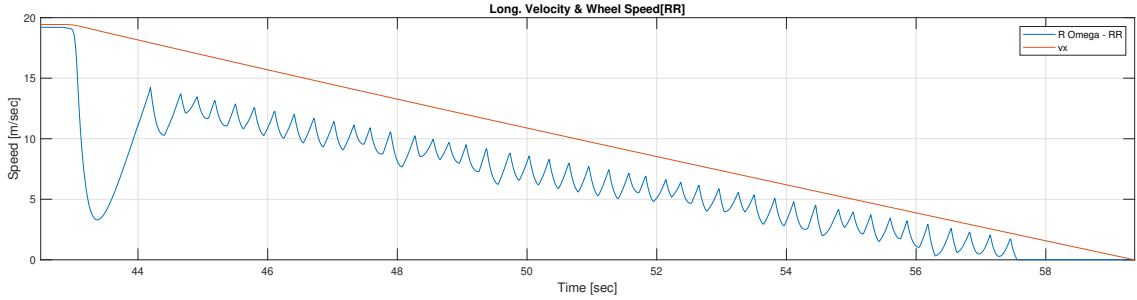
A.1.a. Front Left



A.1.b. Front Right



A.1.c. Rear Left



A.1.d. Rear Right

Figure A.1. Vehicle Speed, Wheel Speed and Longitudinal Slip Variation for a Low μ Surface ($\mu = 0.1$), Time Constant = 150ms and Slip Target of 20%

A.1.2 Straight Line Braking - Split- μ Surface

This subsection contains additional results required to support the statements made in the Results Section for simulations on a Split- μ surface.

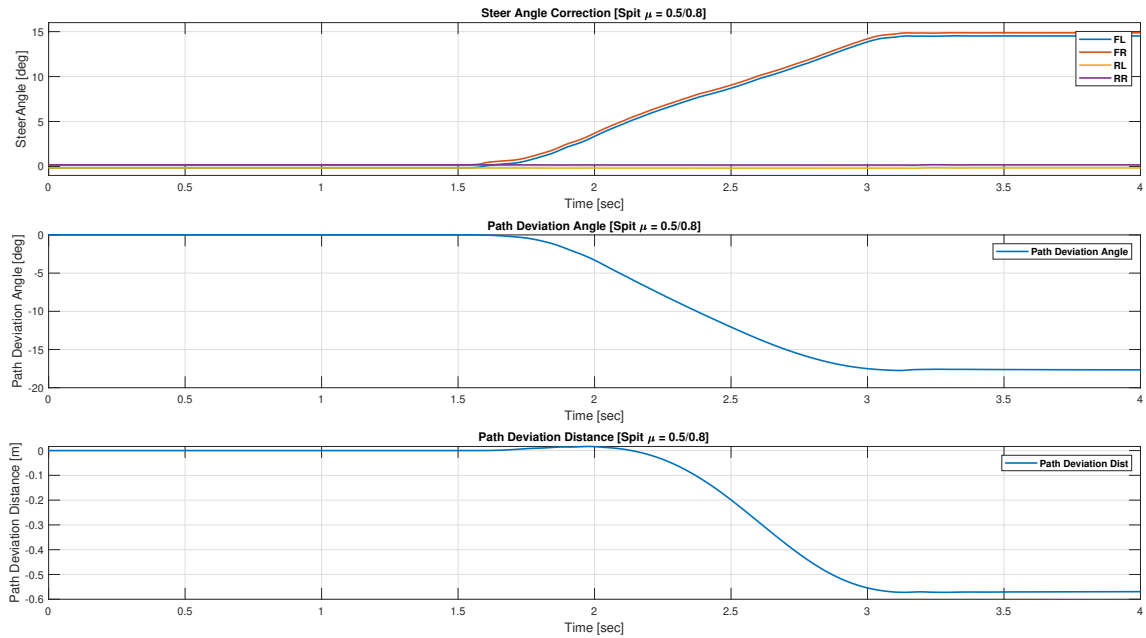


Figure A.2. Results with Basic Actuator - Steer Angle Correction and Path Deviation for a Split- μ Surface of 0.5(Left)/0.8(Right), Time Constant = 350ms

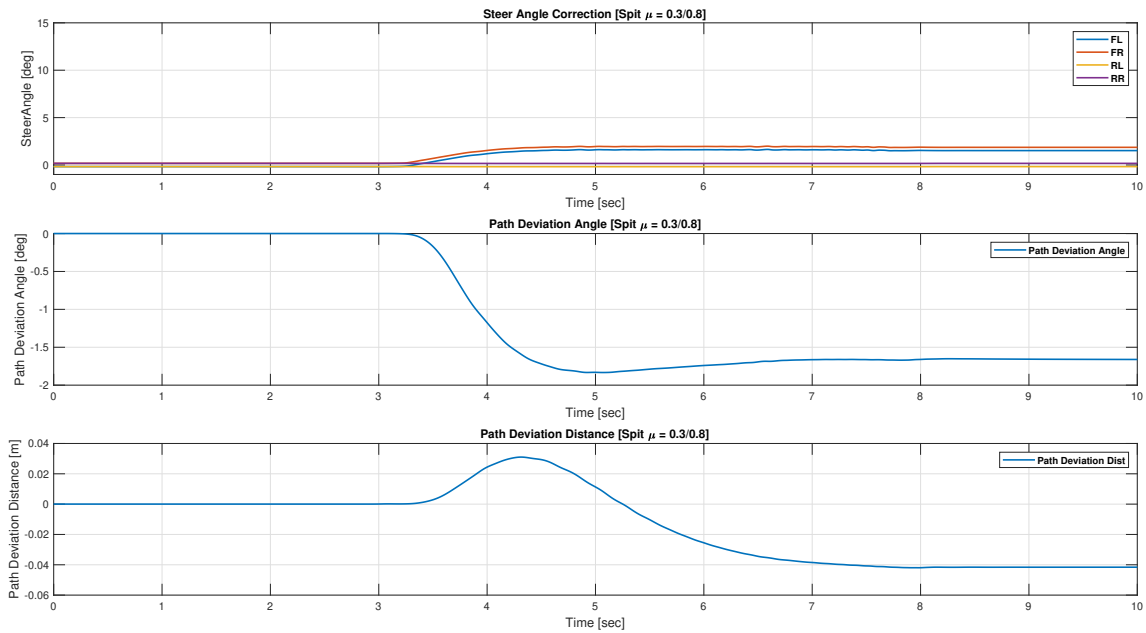


Figure A.3. Results with Basic Actuator - Steer Angle Correction and Path Deviation for a Split- μ Surface of 0.3(Left)/0.8(Right), Time Constant = 350ms

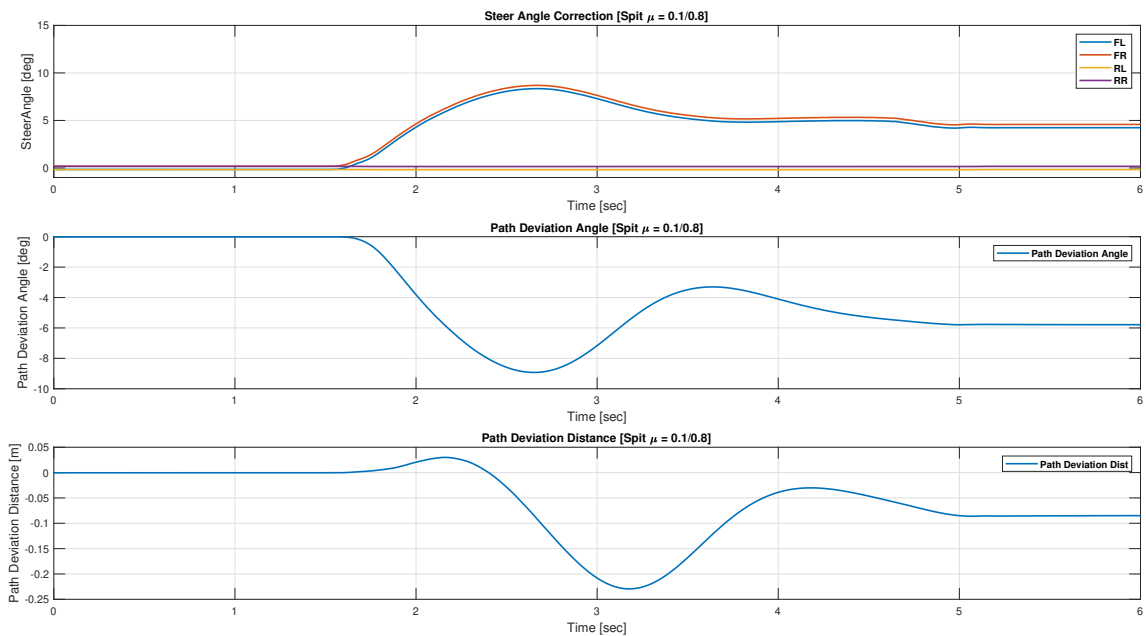


Figure A.4. Results with Basic Actuator - Steer Angle Correction and Path Deviation for a Split- μ Surface of 0.1(Left)/0.8(Right), Time Constant = 350ms

A.2 Results with Advanced Actuator

A.2.1 Straight Line Braking - Constant- μ Surface

This part contains additional results with respect to the simulations performed in Section 4.3. All the parameters of the simulation remain the same as described in this section.

The results shown here are with respect to the vertical force acting at the tire contact patch.

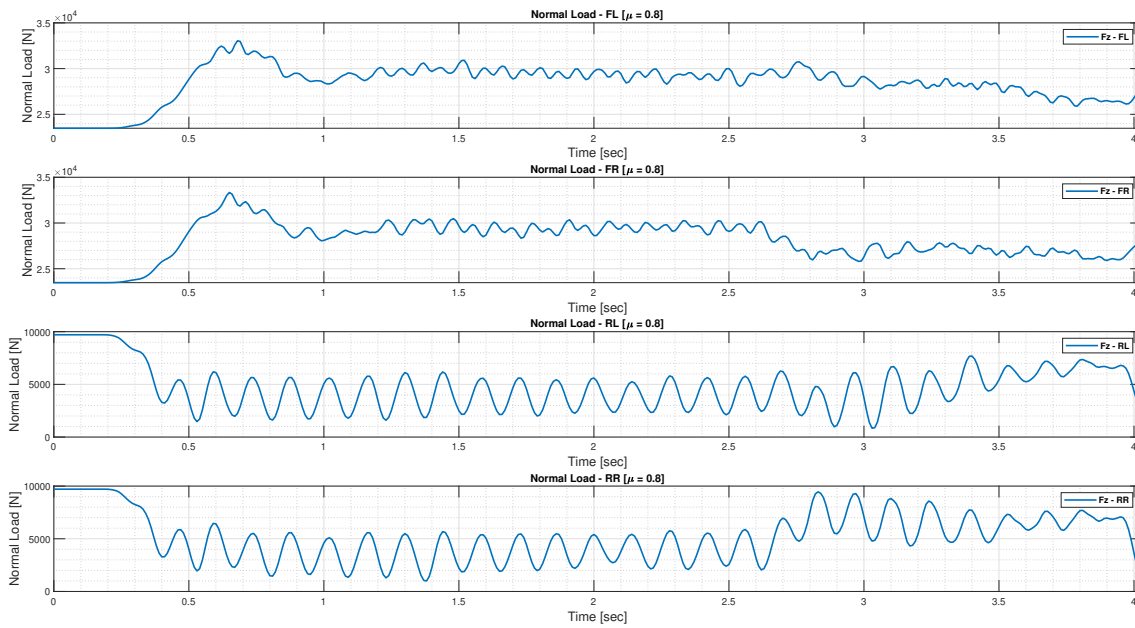


Figure A.5. Results with Advanced Actuator (FMU) - Vertical Force Variation on all 4 wheel ends for a High μ Surface ($\mu = 0.8$), Slip Target - 12% Front and 10% Rear with the FMU

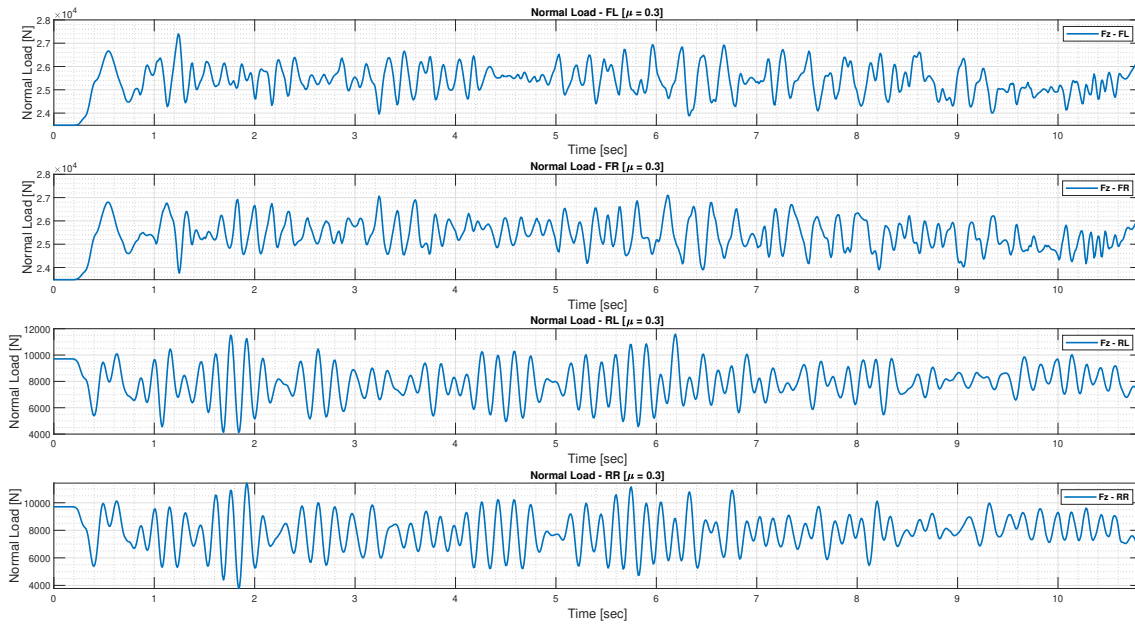


Figure A.6. Results with Advanced Actuator (FMU) - Vertical Force Variation on all 4 wheel ends for a Mid μ Surface ($\mu = 0.3$), Slip Target - 12% Front and 10% Rear with the FMU

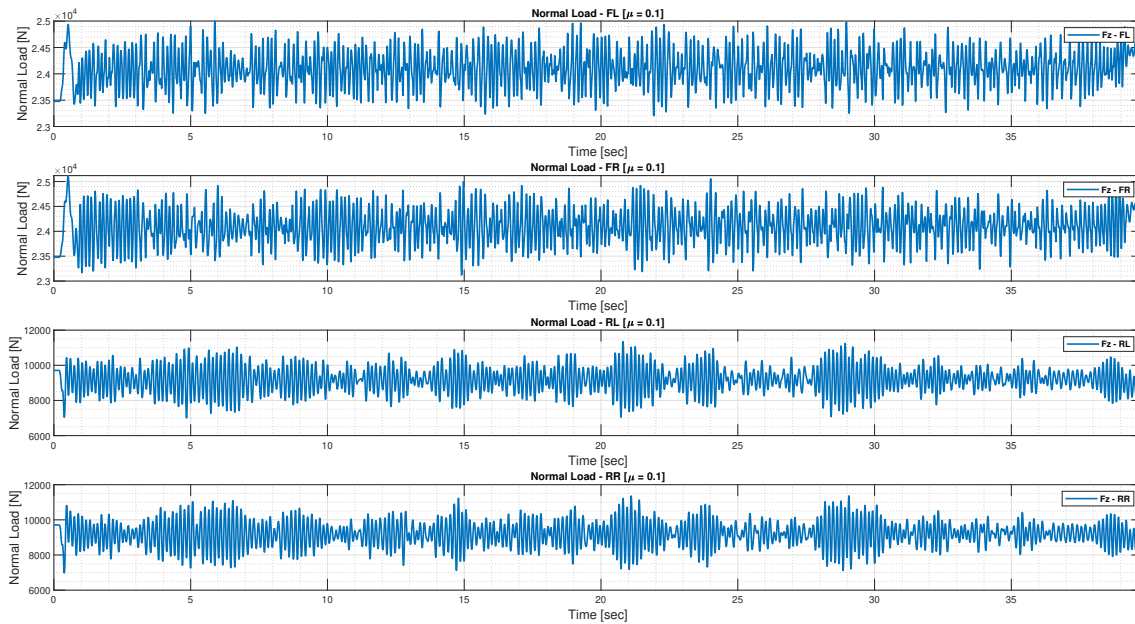


Figure A.7. Results with Advanced Actuator (FMU) - Vertical Force Variation on all 4 wheel ends for a Low μ Surface ($\mu = 0.1$), Slip Target - 12% Front and 10% Rear with the FMU